TESIS DE LA UNIVERSIDAD DE ZARAGOZA
2021
116

Eduardo Royo Amondarain

Non-perturbative physics in lattice gauge theories

Director/es
Azcoiti Pérez, Vicente
Follana Adín, Eduardo

ISSN 2254-7606

Prensas de la Universidad
Universidad Zaragoza

ISSN 2254-7606

Universidad Zaragoza
1542

Tesis Doctoral

NON-PERTURBATIVE PHYSICS IN LATTICE GAUGE THEORIES

Autor

Eduardo Royo Amondarain

Director/es

Azcoiti Pérez, Vicente
Follana Adín, Eduardo

UNIVERSIDAD DE ZARAGOZA
Escuela de Doctorado

Programa de Doctorado en Física

2021

Universidad Zaragoza

Non-perturbative physics in lattice gauge theories

Doctoral dissertation of

Eduardo Royo Amondarain

Supervised by

Vicente Azcoiti Pérez

Eduardo Follana Adín

UNIVERSIDAD DE ZARAGOZA

Departamento de Física Teórica

&

Centro de Astropartículas y Física de Altas Energías

2020

Departamento de Física Teórica
Universidad Zaragoza

Aknowledgements
Agradecimientos

Llevar a buen puerto el trabajo que aquí se presenta, y que ha sido origen de no pocos desvelos, habría sido imposible de no contar con el apoyo de muchas personas. Dada la dificultad de nombrar a todas ellas en tan pocas líneas, querría empezar por dar las gracias de forma general a quien, desde su propio ámbito y en mayor o menor medida, haya contribuido en esta empresa. Sin perjuicio de lo anterior, y rogando se disculpe cualquier omisión que pueda producirse a continuación, en lo que sigue quisiera destacar algunos nombres que considero especialmente relevantes.

En lo académico, resulta ineludible reconocer la labor del Profesorado con el que he tenido la oportunidad de coincidir en las diferentes etapas del Sistema Educativo. Buenos ejemplos serían mi profesora de Lengua en 1º de la E.S.O. o mi tutor durante ese mismo curso, de Dibujo, sin olvidar la profesora que, en 2º de la E.S.O., me involucró en la Olimpiada Matemática. Del mismo modo, ya durante la etapa universitaria, pude disfrutar de un gran elenco de docentes que supieron transmitir su pasión por esta disciplina, con mención especial para el Departamento de Física Teórica, cuyas asignaturas siempre dejaban con ganas de seguir indagando en la materia. El agradecimiento al Departamento es doble, de hecho, pues su acogida y acompañamiento a lo largo de estos años han sido dignas de elogio. Ha sido para mí un auténtico honor habitar, siquiera temporalmente, los pasillos de Teórica, en los que siempre me han hecho sentir como en casa.

A caballo entre lo académico y lo personal, tengo que dar las gracias a mis directores, Vicente y Eduardo, cuya guía por los no-siempre-claros caminos del doctorado ha sido encomiable. De ellos he podido aprender mucho, pero por si esto fuera poco, su contribución trasciende ampliamente lo profesional. Además de ser buenos colegas, en el sentido más formal del término, también han demostrado ser buenos amigos. En este mismo sentido, no podré agradecer lo suficiente la excelente acogida de Giuseppe durante mis estancias en L'Aquila. Muy difícilmente se puede dar en la vida con una persona de mayor calidad humana. No quiero olvidarme tampoco de otros compañeros ocasionales de viaje, como Alex o Matteo, ni por

supuesto de mi compañero de fatigas y despacho, Filiberto.

Ya en el terreno personal, gracias a todas las amistades que han estado ahí en tantos momentos. A mis compañeros del Stadium Casablanca, con los que durante muchos años he podido disfrutar del balonmano. A los del Instituto y a los de la carrera, con mención especial al eje *reformista-populista*. A las Colonas, reino animal incluido, que solíamos ser de Catán—y que cada vez somos más. Y, por supuesto, gracias a mi familia. Gracias a Menchu, Musta, Nora y Avi, que siempre me han hecho sentir como uno más. Gracias a Arrate, Jesús, Alejandro y Gato, porque decir que siempre me habéis apoyado incondicionalmente sería quedarse corto. Habéis sido el mejor apoyo que un hijo o un hermano puede tener. Gracias también, Robin, por sacarme a pasear todos los días, pues no hay mejor manera de darle una vuelta a un problema rebelde.

Finalmente y por encima de todo, gracias a Cecilia y a Yasmina, sobre cuyo trabajo de cuidados descansa el grueso de esta tesis. Ambas habéis sido condición sine qua non para que este trabajo haya podido salir adelante, tanto como lo sois para mí. Va por vosotras.

Este trabajo ha sido financiado por el Ministerio de Economía y Competitividad a través de la ayuda predoctoral para la formación de doctores BES-2013-063567. De igual modo, cabe mencionar los proyectos del Ministerio de Economía y Competitividad/Fondo Europeo de Desarrollo Regional FPA2012-35453 y FPA2015-65745-P, y de la Diputación General de Aragón/Fondo Social Europeo 2015-E24/2.

Contents

Introduction

A few decades have passed since quantum chromodynamics (QCD) was established as the theory describing strong interactions. It is broadly accepted as one of the most successful theories in modern physics, and it has been extensively tested, both from the theoretical and the experimental perspectives.

At high energies, QCD is asymptotically free, which means that its fundamental constituents, *quarks* and *gluons*, interact with a strength that decreases as the energy scale reaches higher values. In this regime, it is feasible to use perturbation theory to resolve short distance interactions. When studying high energy cross sections, both short and long distance interactions have to be taken into account. However, with the help of factorization theorems [1], it is possible to combine perturbative QCD with some non-perturbative input, from empirical or theoretical sources, and obtain predictions that can be confronted with experiment. Indeed, this program has been carried out by a wide community of scientists, working in hundreds of Universities, laboratories and often organized in large international collaborations, including several particle colliders around the world. The significant amount of evidence gathered has allowed QCD to become a reliable component of the Standard Model of particle physics. Moreover, perturbative QCD is nowadays a very active field of research, since facilities such as the Large Hadron Collider provide new experimental data every year [2], and a great theoretical effort must be done in order to calculate the first terms of the corresponding expansions.

On the other hand, for not-so-high energies, the strong interaction cannot be reduced to a converging series of Feynman diagrams. In fact, one of the characteristic properties of QCD is the so-called color-confinement. This means that quarks are always (excluding high density regimes) in bound states, called hadrons, which are color-neutral. In this purely non-perturbative regime, there are few techniques that can analyze the theory successfully. Probably the most well-established of them is *lattice QCD*. Since the foundational work of Wilson in 1974 [3], the success of the lattice approach has been growing consistently over time. Whereas during the first years performing the necessary calculations to extract meaningful results from QCD seemed remote, the progressive refinement of the algorithms

and the exponential increase of computer power available worldwide turned over the situation. Many milestones have already been reached: precise simulations including the effects of virtual quark loops [4], the determination of the light hadron spectrum with fully controlled systematics [5] or, more recently, the computation of the isospin splittings—mass difference between neutron and proton, and other hadronic channels—with great agreement with the experimental data, even exceeding its precision in some cases [6]. All of these are good examples of the success of the method.

For the above reasons, QCD is believed to be the correct theory describing strong interactions, both for high and low energies, and lattice QCD is recognized by the community as a trustworthy ab initio approach that has an *useful interaction with experiment*, paraphrasing Wilson [7]. It is tempting to think that, with the current evolution of computing power, it is just a matter of time for the lattice approach to address, and eventually solve, every non-perturbative problem that still awaits an answer. Of course things are not so easy, and even if for a subset of problems it would be enough to have more powerful machines, there are some fundamental topics that still constitute open questions. At least two problems share this status: the behavior of matter at finite baryonic density—including its temperature-density phase diagram—and the studies involving topological effects in QCD. Although, as we will see, there have been numerous attempts, the advances in both topics have been scarce. The main difficulty behind the modest progress achieved in both areas is the same: the action of the theory is complex, and there is no known reformulation that can avoid the appearance of a severe sign problem (SSP).

The SSP can be defined as the problem of numerically evaluating the integral of a highly oscillatory function, depending on a large number of variables. It belongs to the *NP-complete* class of problems [8], meaning that finding an algorithm that overcomes the SSP in polynomial time would be equivalent to prove that P=NP, one of the seven *Millennium Problems* posed by the Clay Mathematics Institute. In other words, if such an algorithm exists, it would solve *all* NP problems in polynomial time. But, up to this day, the P vs NP dilemma remains without answer, and consequently there is no general solution to the SSP that allows the usual Monte Carlo techniques to work. Thus, efforts in trying to overcome this major difficulty concentrate in the elaboration of different methods, tailored to the specifics of the problem at hand. Such is the case of QCD with an imaginary part in the action, which shows up when chemical potential ($\mu > 0$) or topological (θ) terms are present.

In order to advance in the understanding of complex action QCD, several proposals have been developed over the last few decades. Complex Langevin dynamics [9–11], the approaches developed by Azcoiti et al [12, 13] and, more recently,

Lefschetz thimbles [14–16] and the density-of-states method [17–19], are relevant examples of some of these attempts. In general, these strategies have allowed to study a considerable number of toy models and, in some cases, have obtained some interesting results for QCD with finite chemical potential. However, almost no progress has been made with θ QCD, due to either the different fundamental limitations these methods suffer of, or the practical difficulties that their implementations involve.

In this context, the main part of this thesis has been devoted to study models which suffer from a SSP, such as the two-dimensional Ising model within an imaginary magnetic field or the massive 1-flavor Schwinger model with a θ term. In the first case, we study the well-known model by means of analytical techniques, exploring a region of the parameter space—real temperature and purely imaginary magnetic field—somewhat unattended by the literature, possibly due to the difficulty of applying either analytical or numerical techniques. According to the few works that explore this system [20, 21], a rich phase structure should be expected. Our work pretends to test the validity of one of the methods of Azcoiti et al [13,21] in this scenario, and, as long as it can provide an insight into a critical region that suffers from a SSP—which had hampered the attainment of a numerical solution—we hope that it can serve as a benchmark for methods aspiring to overcome the SSP in any lattice gauge theory.

With the aim of engaging with QCD-like systems with a θ term, and in this way develop further the methods dealing with the SSP, we have studied the massive 1-flavor Schwinger model with a θ term, which corresponds to QED in $1+1$ dimensions. As we shall see, it shares a large number of features with QCD, including confinement and, in a way, asymptotic freedom, being in fact broadly used as its toy model. Moreover, defining the topological charge on the lattice is almost trivial in this model, in contrast with any of the usual definitions of this observable in lattice QCD, which are much more involved. This fact has allowed us to explore the model with a feasible computational cost, obtaining results that are compatible with Coleman's analytical prediction [22] and, more importantly, testing the method developed in [13] in a gauge theory with fermions, which constitutes an important step in the way to its application in full QCD.

As a byproduct of the previous line of work, and driven by the necessity of optimizing further our previous algorithms, we have also analysed the 2-flavor version of the Schwinger model. In this case, we have bypassed the computation of the full fermionic determinant by following an approach based on the use of pseudofermions [23].

Beyond the study of systems afflicted by a SSP, another topic within lattice QCD has been treated during the development of this thesis: the running coupling α_S. The dependence of $\alpha_S(q^2)$ with the momentum transfer q, which encodes the

underlying interactions of quarks and gluons in the QCD framework, constitutes a very active field of research, that includes a large variety of approaches [24]. The interest that this matter generates is divided between the behavior of the coupling in the infrared region—where nowadays there is no consensus about $\alpha_S(q^2 \to 0)$ tending to zero, *freezing* or even diverging—and at large momenta, where perturbative QCD can be applied and both experimental and theoretical methods try to provide the most accurate approximation. In this context, lattice-based strategies have been capable of delivering results both in the infrared region and in the high energy regime, where in fact they provide the most precise determination of $\alpha_S(M_Z)$ [2]. Our work can be framed precisely into these approaches that come from lattice QCD, and it relies upon a ghost-gluon vertex computation, as in [25–27].

This thesis is orgnized as follows. In Chapter 1 we review the fundamentals of some of the topics presented in this introduction, including a brief historical review of the lattice approach. A motivation for the inclusion of a θ term in the QCD action is developed in Chapter 2, together with a brief review of the existing approaches to this problem. Chapter 3, based on the work presented in [28], is dedicated to the Ising model within an imaginary magnetic field. Hereafter we address the study of the massive Schwinger model with a θ term. The 1-flavor results, relying on the work presented in [29], are reported in Chapter 4, whereas the 2-flavor case is treated with a pseudofermions approach in Chapter 5. Finally, Chapter 6 covers the computation of $\alpha_s(q^2)$ via the ghost-gluon vertex. Lastly, our conclusions are summarized in the homonymous chapter and technical details concerning the computation of the cumulant expansion performed in Chapter 3 are given in Appendix A.

Introducción

Varias décadas han pasado desde que la cromodinámica cuántica (QCD, por sus siglas en inglés) se estableció como la teoría que describe las interacciones fuertes. Es ampliamente aceptada como una de las teorías más exitosas de la física moderna y ha sido puesta a prueba de forma exhaustiva, tanto desde el punto de vista teórico como del experimental.

A altas energías, QCD es asintóticamente libre, lo que significa que sus constituyentes fundamentales, *quarks* y *gluones*, interaccionan con una intensidad que decrece conforme la energía alcanza escalas más altas. En esta situación, resulta factible aplicar la teoría de perturbaciones para resolver las interacciones a corta distancia. Al estudiar secciones eficaces en procesos de altas energías, es necesario tener en cuenta las interacciones producidas tanto a corta como a larga distancia. Sin embargo, con la ayuda de los teoremas de factorización [1], es posible combinar QCD perturbativa con cierto *input* no perturbativo, proveniente de fuentes empíricas o teóricas, y obtener así predicciones que pueden ser confrontadas experimentalmente. De hecho, este programa ha sido llevado a cabo por una amplia comunidad de científicos y científicas, trabajando en cientos de Universidades, laboratorios y habitualmente organizados en grandes colaboraciones internacionales, incluyendo varios aceleradores de partículas. La importante cantidad de evidencias recogidas en este proceso ha permitido a QCD convertirse en un componente muy fiable del actual Modelo Estándar de física de partículas. Además, QCD perturbativa es hoy en día un campo de investigación muy activo, toda vez que centros como el Gran Colisionador de Hadrones proveen de nuevos datos experimentales cada año [2], y debe invertirse un gran esfuerzo teórico en el cálculo de los primeros términos de las expansiones correspondientes.

Por otro lado, para escalas de energía no tan elevadas, la interacción fuerte no puede ser reducida a una serie convergente de diagramas de Feynman. De hecho, una de sus propiedades características es el llamado confinamiento de color. Esto significa que los quarks se encuentran siempre (excluyendo régimenes de alta densidad) en estados ligados, llamados hadrones, que son neutrales respecto del color. En esta situación puramente no perturbativa, hay pocas técnicas que puedan analizar la teoría con éxito. Probablemente la que mejor establecida está es QCD

en el retículo, denominada comunmente *lattice* QCD. Desde el trabajo fundacional de Wilson en 1974 [3], el éxito del método ha ido creciendo con el tiempo. Si bien durante los primeros años realizar los cálculos necesarios para extraer resultados significativos de QCD parecía muy lejano, el progresivo refinamiento de los algoritmos junto con el crecimiento exponencial de la capacidad computacional mundial dio la vuelta a la situación. Muchos hitos han sido ya alcanzados: simulaciones precisas incluyendo los efectos de loops de quarks virtuales [4], la determinación del espectro de hadrones ligeros con errores sistemáticos totalmente controlados [5] o, más recientemente, la computación de los *splittings* de isospín (esto es, de las diferencias de masa entre neutrón y protón, u otros canales hadrónicos) con gran acuerdo con los datos experimentales, incluso excediendo su precisión en algunos casos [6]. Todos ellos son buenos ejemplos del éxito de este enfoque.

Por los motivos citados, QCD es considerada como la teoría que describe correctamente la interacción fuerte, tanto para altas como para bajas energías, y *lattice* QCD es reconocido por la comunidad como un método *ab initio* fiable que tiene una *interacción útil con lo experimental*, parafraseando a Wilson [7]. Es tentador pensar que, con la evolución actual de la potencia de cálculo, sería simplemente cuestión de tiempo que el enfoque de la *lattice* enfrentase y resolviese cada uno de los problemas no perturbativos que todavía esperan una solución. Por supuesto, las cosas no son tan sencillas, e incluso cuando para un subconjunto de problemas bastaría con contar con equipos más potentes, existen temas fundamentales que hoy en día constituyen preguntas abiertas. Al menos dos problemas comparten este estatus: el comportamiento de la materia a densidad bariónica finita—incluyendo su diagrama de fases de temperatura-densidad—y los estudios que involucran efectos topológicos en QCD. Aunque, como veremos, los intentos han sido numerosos, los avances en ambos campos han sido escasos. La principal dificultad detrás de este modesto progreso en ambas áreas es la misma: la acción de la teoría es compleja, y no existe reformulación conocida que pueda evitar la aparición de un problema de signo severo (SSP, por sus siglas en inglés).

El SSP puede ser definido como el problema de evaluar numéricamente la integral de una función muy oscilatoria, que además depende de un gran número de variables. Pertenece a la clase de problemas *NP-completos* [8], lo que significa que encontrar un algoritmo que superase el SSP en tiempo polinómico equivaldría a probar que P=NP, uno de los siete *Problemas del milenio* propuestos por el *Clay Mathematics Institute*. En otras palabras, si un algoritmo así existiese, resolvería *todos* los problemas de clase NP en tiempo polinómico. Pero, hasta el día de hoy, el dilema P vs NP continúa sin respuesta, y consecuentemente no existe solución general para el SSP que permita la aplicación de las técnicas de Montecarlo usuales. Así pues, los esfuerzos dedicados a intentar superar esta dificultad se concentran en la elaboración de diferentes métodos, adaptados a las

particularidades del problema en cuestión. Este es el caso de QCD con componente imaginaria en la acción, que aparece cuando están presentes los términos correspondientes al potencial químico ($\mu > 0$) o a efectos topológicos ($\theta \neq 0$).

Con el objetivo de avanzar en la comprensión de QCD con acción compleja, varias propuestas se han desarrollado a lo largo de las últimas décadas. La dinámica de Langevin compleja [9–11], los métodos desarrollados por Azcoiti et al [12, 13] y, más recientemente, los *dedales* de Lefschetz [14–16] y el método de la densidad de estados [17–19], son ejemplos relevantes de algunos de estos intentos. En general, estas estrategias han permitido estudiar un número considerable de *toy models* y, en algunos casos, han obtenido resultados interesantes para QCD con potencial químico finito. Sin embargo, en el caso de θ QCD no se ha podido obtener casi ningún progreso, debido bien a las diferentes limitaciones fundamentales de las que los métodos citados adolecen, bien por las dificultades prácticas que sus respectivas implementaciones implican.

En este contexto, la parte principal de esta tesis se ha dedicado al estudio de modelos que sufren de un SSP, como el modelo de Ising bidimiensional con campo magnético puramente imaginario, o el modelo de Schwinger masivo con un único *flavor* y un término θ. En el primer caso, estudiamos el conocido modelo por medio de técnicas analíticas, explorando una región del espacio de parámetros (temperatura real y campo magnético imaginario) algo desatendida en la literatura, posiblemente debido a la dificultad de aplicar técnicas tanto analíticas como numéricas. De acuerdo con los pocos trabajos que exploran este sistema [20, 21], se espera una estructura de fases con cierta riqueza. Nuesto trabajo pretende probar la validez de uno de los métodos de Azcoiti et al [13, 21] en este escenario y, dado que puede arrojar algo de luz en una región crítica que sufre de un SSP (que ha obstaculizado la consecución de una solución numérica) esperamos que pueda servir como referencia para otros métodos que aspiren a superar el problema del signo en cualquier teoría gauge en el retículo.

Con el objetivo de enfrentar sistemas similares a QCD con un término θ, y de este modo desarrollar los métodos que lidian con el SSP, hemos estudiado el modelo de Schwinger masivo con un *flavor* y término θ, que se corresponde con QED en dimensión $1 + 1$. Como veremos, comparte un gran número de propiedades con QCD, incluyendo el confinamiento y, en cierto modo, la libertad asintótica, por lo que de hecho es ampliamente usado como su *toy model*. Además, definir la carga topológica en este modelo es casi trivial, en contraste con cualquiera de las definiciones usuales para este observable en QCD, que resultan mucho más intrincadas. Este hecho nos ha permitido explorar el modelo con un coste computacional factible, obteniendo resultados compatibles con la predicción analítica de Coleman [22] y, lo que es más importante, poninedo a prueba el método desarrollado en [13] en una teoría gauge con fermiones, lo que constituye un paso

importante en el camino a su aplicación en QCD.

Como derivado de la línea de trabajo anterior, y empujados por la necesidad de una mayor optimización de los algoritmos anteriores, también hemos analizado la versión de 2 *flavors* del modelo de Schwinger. En este caso, se ha evitado el cálculo completo del determinante fermiónico siguiendo un enfoque basado en la técnica de los pseudofermiones [23].

Más allá del estudio de sistemas afectados por un problema de signo, otro tema, incluido dentro de *lattice QCD*, se ha tratado en esta tesis: el *running coupling* α_S. La dependencia de $\alpha_S(q^2)$ con el momento transferido q, que codifica las interacciones subyacentes de quarks y gluones en el marco de QCD, constituye un campo de investigación muy activo, que incluye una gran variedad de metodologías [24]. El interés que esta materia genera se divide entre el comportamiento de este acoplamiento en la región infrarroja, donde hoy en día no existe consenso sobre si $\alpha_S(q^2 \to 0)$ tiende a cero, se *congela* o incluso diverge, y a momentos altos, donde QCD perturbativa puede ser aplicada y métodos tanto teóricos como experimentales intentan proveer la aproximación más precisa. En este contexto, las estrategias basadas en el retículo han sido capaces de ofrecer resultados para ambos casos, consiguiendo de hecho la determinación más precisa para $\alpha_S(M_Z)$ [2]. Nuestro trabajo puede ubicarse precisamente entre los enfoques que vienen de la *lattice*, y se apoya en un cálculo del vértice ghost-gluon, como en [25–27].

Esta tesis se organiza como sigue. En el Capítulo 1 repasamos lo fundamental de algunos de los temas presentados en esta introducción, incluyendo un breve resumen histórico sobre el origen de *lattice* QCD. Una motivación para la inclusión del término θ en la acción de QCD se desarrolla en el Capítulo 2, junto con un breve repaso de de los enfoques existentes para este problema. El Capítulo 3, basado en el trabajo presentado en [28], se dedica al modelo de Ising en un campo magnético puramente imaginario. A continuación enfrentamos el estudio del modelo de Schwinger masivo con término θ. Los resultados para el caso de un único *flavor*, presentados en [29], se ofrecen en el Capítulo 4, mientras que el caso de 2 *flavors* se trata con un método basado en pseudofermiones en el Capítulo 5. Finalmente, el Capítulo 6 cubre la computación de $\alpha_s(q^2)$ mediante el vértice ghost-gluon. Para acabar, nuestras conclusiones se resumen en el capítulo homónomio, y algunos detalles técnicos, que conciernen al cómputo de la expansión de cumulantes realizada en el Capítulo 3, se discuten en el Apéndice A.

Chapter 1

The lattice approach

In this chapter we cover the essential points of the lattice approach to QCD, including a brief historical review of its birth and evolution over the past few decades. The main aspects of the formalism are explained, discussing the strenghs and limitations of Monte Carlo methods when studying lattice gauge theories. Finally, some considerations about the type of errors associated with this methodology are discussed, recalling how we can control them and, eventually, in which way we can provide a precise estimation of a given observable.

1.1 The dawn of color

The appearance of quarks and gluons as the fundamental constituents of baryons and mesons is relatively recent. In order to give the necessary context, it is desirable to go back to the middle of the last century. The discovery of the pion through cosmic ray experiments in 1947 [30], which was soon followed by those of the first strange particles, the kaon and the Λ, marked the beginning of a tendency that continued during the 50s, by means of different experiments involving particle colliders. This experimental fact, i.e., the discovery of a large number of new particles and resonances that were somehow related, claimed for an explanation in terms of a reduced set of degrees of freedom. It was in 1961 when Murray Gell-Mann (who had previously introduced the strangeness as a quantum number, conserved by both electromagnetic and strong interactions) provided a successful explanation of the so-called *particle zoo*, in his famous *The Eightfold Way* [31]. By extending the $SU(2)$ isospin symmetry, Gell-Mann proposed a $SU(3)$ *flavor* symmetry, broken by mass differences, that was capable to organize all the observed hadronic states. Moreover, this symmetry predicted the existence of the Ω^- baryon, a particle that was observed three years later, with a mass that matched accurately the value anticipated by the model [32]. Precisely Gell-Mann in 1964, and independently

Zweig [33], proposed that both mesons and baryons were composed of more fundamental constituents (called quarks by the mentor, and *aces* by his pupil) which hold fractional electric charge.

At this point, some questions still remained to complete the quark puzzle. Particularly relevant was the fact that the Ω^- particle, composed of three s quarks in its ground state, should have a symmetric wave function. This was in contradiction with Pauli exclusion principle, which required an antisymmetric wave function under the exchange of two quarks, which were assumed to be fermions of spin 1/2. Another concern involved the decay amplitudes predicted by the quark model, which differed from the values measured in electron-positron colliders. Both issues were addressed by Gell-Mann, Fritzsch and Bardeen, who during 1971 and 1972 introduced a new exact $SU(3)$ symmetry for the quarks, named *color* [34–36], which was exactly conserved. Color was soon interpreted as a gauge symmetry and a field theory was constructed by Gell-Mann, Fritzsch and Leutwyler [37] and independently by Gross and Wilczek [38] in 1973, who emphasized (as Politzer in [39]) one of the characteristic properties of the new theoretical artifact: asymptotic freedom. Later, Fritzsch and Gell-Mann would finally give the theory its modern name: Quantum Chromodynamics.

In order to complete the picture of QCD, another phenomenon had to be explained: why experiments only measure color singlets, i.e., baryons and mesons are free of any color charge, and individual quarks are not present in nature as free particles. To explain this confinement of quarks and gluons into hadrons, Wilson demonstrated in 1974 how lattice gauge theories confine charged states in the strong coupling limit [3]. This work set the basis for the qualitative understanding of color confinement—and in this way closes the early period in which QCD was constructed—but its influence over the theory would transcend by far this objective, since the regularization developed by Wilson opened a whole new field within high energy physics. With respect to confinement itself, it should be noted that, although there exist broad numerical evidence of its validity, today a rigorous mathematical proof is still lacking.

1.2 A discretized spacetime

The formulation of Quantum Chromodynamics as the dynamical theory of the strong interaction, together with the understanding of asymptotic freedom and confinement, is without doubt one of the key milestones reached during the past century. Even so, and due to the strongly coupled nature of the theory, the predictive power of QCD was severely limited during its first steps. Specially at low energies, perturbative methods—developed with great success for processes involving Quantum Electrodynamics—were of no use, making observables such as the

hadron spectrum unreachable.

In this context, Wilson introduced—in which is considered to be the foundational work of the lattice approach [3]—a novel non-perturbative regularization of QCD. The essential ideas of the procedure, applicable to any gauge theory, have endured up to the present day, and are relatively simple. Starting from Feynman's path integral formalism, spacetime is discretized in a four-dimensional (Euclidean) hypercube. All objects are now defined in the *sites* of the hypercube, or the *links* joining them. This procedure is done in such a way that gauge symmetry is exactly preserved. Although Lorentz (or Euclidean) invariance is lost for any finite lattice spacing a, Wilson argued that this obstacle could be overcome by means of a renormalization-group approach, possible if there exists a critical point at some value of the gauge-coupling of the theory.

At this point, and even if lattice QCD had elucidated the confinement phenomenon, it was unclear how the approach could be exploited in order to calculate relevant physical observables. The turning point came by the end of the decade, when a procedure widely used at the time in Statistical Mechanics was introduced into the realm of Field Theory. In 1978, Wilson [40] proposed to apply Monte Carlo methods, namely a Metropolis algorithm, to lattice gauge theories, in order to elucidate numerically the confinement phenomenon. With a detailed prescription of how observables should be measured in such a framework, he also pointed out that the first calculations were already ongoing for the $SU(2)$ gauge theory. The first numerical results, that demonstrated the potential of the new technique, came by Creutz, Jacobs and Rebbi in 1979 [41], who performed a simulation of the gauge $Z(2)$ model in four dimensions, observing a first-order transition that supported the confinement hypothesis by countering a previous conjecture due to Migdal [42]. In the same year, Wilson [43] presented another renormalization-group approach to the $SU(2)$ gauge theory, importing block-spin techniques from Statistical Mechanics. Already in 1980, Creutz [44] provided further evidence of both confinement and asymptotic freedom in the $SU(2)$ gauge theory, ensuring in this way the possibility of taking the continuum limit by holding constant a physical observable like the string tension.

These novel ideas crystallized in several works over the years to follow, including the pioneering computations of the rho meson mass for a discrete approximation of the $SU(2)$ theory, by Weingarten [45], or the calculation of several hadron masses due to Hamber and Parisi [46], performed already with $SU(3)$ as the gauge group. In both cases, the limits imposed by computational resources were alleviated by the use of the so-called *quenched approximation*, which neglects entirely the effect of virtual quark loops—with the associated addition of uncontrolled errors. The inclusion of *full dynamical* fermions, i.e., taking into account both gluon and quark dynamics, was achieved first in 1983 by Azcoiti and Nakamura [47], who, leaning

on the pseudofermions method proposed by Fucito et al [23], computed the mass splitting of the rho and omega mesons for the icosahedral approximation of $SU(2)$ as the gauge group. A similar computation, also relying in the pseudofermionic approach, was made by Hamber in 1985 [48], already using $SU(3)$ as the gauge symmetry group.

These early studies, even when they were made with very modest computational power by today standards, and with a number of sources of uncontrolled systematic errors—especially significant for those made within the quenched approximation—were successful in proving the feasibility of the lattice approach. During the subsequent decades, computing resources kept growing steadily. In parallel, new algorithmic and theoretical advances were developed, which ultimately made possible breakthroughs such as the computation of the light hadron spectrum from first principles [5] or, more recently, the determination of the isospin mass splittings [6]. At present time, there exist many research groups actively working in this area; state-of-the-art results can be reviewed annually in the proceedings of the International Symposium on Lattice Field Theory.

For more details about the historical development of the lattice approach, including a more technical discussion on the issue, we refer the interested reader to the extensive review of Fodor and Hoelbling [49].

1.3 The formalism

At this point, and before discussing some of the caveats of the lattice approach, it seems desirable to sketch at least the basic premises of the method. In any case, for a more exhaustive introduction to the topic, we recommend the interested reader the lecture notes of Davies [50] or the more recent book by Gattringer and Lang [51], which in fact has served as a reference for some of the topics presented in this section.

1.3.1 A finite path integral

The starting point of the approach is the path integral formalism [52,53], which, for a given quantum field theory, allows to write its partition function as a functional integral

$$\mathcal{Z} = \int \mathcal{D}\Phi e^{-S[\Phi]}, \tag{1.1}$$

where S is the euclidean action of the theory—even being considered at imaginary time, physical information can be recovered as long as the theory fulfills a set of axioms [54,55]—and the integration is meant to be performed over *all possible configurations* of the fields of the theory, denoted generically by Φ. If we particularize

for QCD, the fields to be considered are quarks ψ, antiquarks $\bar{\psi}$ and gluons A_μ, and (1.1) can be formulated schematically as

$$\mathcal{Z}_{\rm QCD} = \int \mathcal{D}\psi\mathcal{D}\bar{\psi}\mathcal{D}A_\mu e^{-S_{\rm QCD}[\psi,\bar{\psi},A_\mu]}, \tag{1.2}$$

with vacuum expectation values of operators $\mathcal{O}(\psi,\bar{\psi},A_\mu)$ being given by

$$\langle\mathcal{O}\rangle = \frac{1}{\mathcal{Z}_{\rm QCD}}\int \mathcal{D}\psi\mathcal{D}\bar{\psi}\mathcal{D}A_\mu \mathcal{O}(\psi,\bar{\psi},\mathcal{A}_\mu)e^{-S_{\rm QCD}[\psi,\bar{\psi},A_\mu]}. \tag{1.3}$$

The precise meaning of the integration symbol present in (1.2) and (1.3) is a subtle mathematical issue; at this point the theory would be ill-defined and a regularization is mandatory in order to extract any physical information and avoid divergences. To this end, there are several possibilities that lean on perturbative expansions in the coupling, such as Pauli-Villars (or dimensional) regularization [56], which have been widely used both in QED and QCD. The prescription of Wilson that was introduced earlier [3], is however the only fully non-perturbative regularization known, allowing to study quantum field theories from first principles, especially QCD beyond short-distance interactions, where confinement—together with the highly non-trivial structure of the QCD vacuum—poses an insurmountable obstacle to perturbative-based approaches.

Thereby, going ahead with QCD, we discretize the continuum four-dimensional euclidean space-time in an hypercubic grid with constant lattice spacing a; this parameter will be the regulator of the theory, in which limit $a \to 0$ its original version is recovered. Moreover, we restrict the full spacetime to a simple 4-d box of finite extent, limiting in this way the spatial volume and the imaginary-time evolution of the system. By doing so, the number of variables to consider becomes finite and the original problem can begin to be pictured as computationally treatable. If we return to (1.2), the fields $\psi(x)$ and $\bar{\psi}(x)$ now take values only for $x = a(n_1, n_2, n_3, n_4)$, where n_i are integers satisfying $0 \leq n_i a < L_i$, L_i being the spatial (temporal) extent of the 4-d box in each dimension.

With respect to the gluon field $A_\mu(x)$, it is convenient to postpone briefly its definition on the lattice. First, we should note that the action of the theory, $S_{\rm QCD}$ in (1.2), is the spacetime integral of the following euclidean[1] lagrangian density,

$$\mathcal{L}_{\rm QCD} = \bar{\psi}\left(i\gamma_\mu D_\mu + m\right)\psi + \frac{1}{2g^2}\,{\rm Tr}\,(F_{\mu\nu}F_{\mu\nu}), \tag{1.4}$$

[1]The ordinary real-time version of $\mathcal{L}_{\rm QCD}$, i.e., with Minkowski spacetime metric, is just $\bar{\psi}\left(i\gamma_\mu D^\mu - m\right)\psi - {\rm Tr}\,(F_{\mu\nu}F^{\mu\nu})/2g^2$. Note that we are using a rather compact notation, where only spacetime indexes are explicit, while those corresponding to color, spin and flavor are kept implicit. A more detailed notation could label quark (and antiquark) field components by $\psi^f_{\alpha,c}$, since ψ is a 3-color vector, a 4-Dirac spinor and a n_f-flavor vector. In the same way, m is a diagonal matrix in flavor space, containing each one of the quark masses.

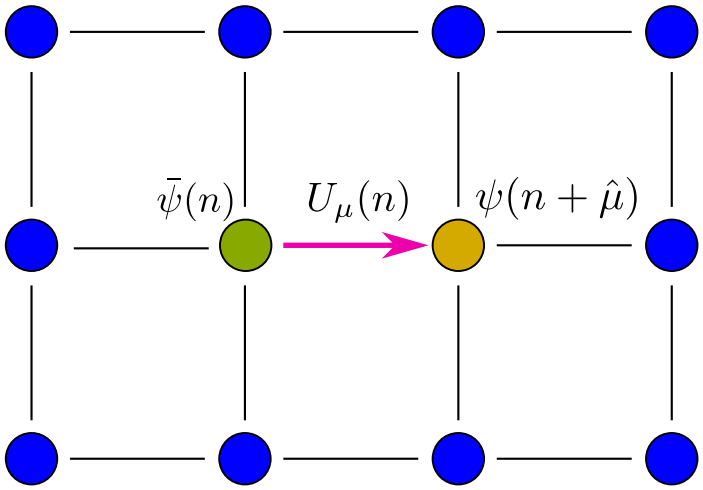

Figure 1.1: A bidimensional section of a four dimensional lattice. Quark and antiquark fields are defined at the sites of the grid, whereas links lie between them, connecting nearest neighbors. The ordered product of the three elements pictured—an antiquark, a link and a quark—is gauge invariant.

where $D^\mu = \partial^\mu - iA^\mu$ is the covariant derivative and $F_{\mu\nu}$ is the gluon field tensor, which depends only on the gluon field[2] A_μ and its derivatives. In the lattice, S_{QCD} becomes simply the sum over lattice sites of a discretized version of $\mathcal{L}_{\text{QCD}}$. Since the derivative terms present in the continuum lagrangian—which involve both quark and gluon fields—can be discretized in multiple ways via finite differences, there is no unique prescription for the lattice expression of the action, S_{latt}. In fact, a careful modification of this lattice action can be used to alleviate discretization errors in a systematic way [57,58]. In any case, and in order to introduce the gluon field $A_\mu(x)$ in the lattice, it is convenient to proceed as in the continuum, requiring gauge symmetry to be preserved in the discretized action S_{latt}. To this end, we focus on the quark and antiquark fields, which transform in the continuum as

$$\psi(x) \to G(x)\psi(x), \tag{1.5}$$

$$\bar{\psi}(x) \to \bar{\psi}(x)G^\dagger(x), \tag{1.6}$$

where $G(x)$ is an arbitrary element of the gauge group, $SU(3)$ in QCD, and depends on the coordinate x, since the action is required to be invariant under local—rather

[2] Although it is not required for the following discussion, it is worth noting that the gluon field A_μ—in contrast with its analogous in QED, the photon field—can be understood as a vector field with eight color components, each of them corresponding to one element of the basis of the SU(3) algebra (which are usually chosen to be proportional to the Gell-Mann matrices λ_a). Alternatively, it is customary to talk about eight different gluon fields, since each of the components of A_μ can be pictured as a gauge field on its own.

than global—transformations. It is straightforward to extend this expressions to the lattice by restricting its domain to the lattice *sites*, i.e., to $x = a(n_1, n_2, n_3, n_4)$. By doing so, local quark-antiquark products present in (1.4) retain their gauge invariance when considered in S_{latt}. Instead, the discretization of the term involving the derivatives of the quark fields $\partial^\mu \psi(x)$, even in its simplest form, give rise to bi-local terms $\bar{\psi}(x)\psi(y)$, which would transform naively as

$$\bar{\psi}(x)\psi(y) \to \bar{\psi}(x)G^\dagger(x)G(y)\psi(y). \tag{1.7}$$

In order to preserve the required symmetry, a gauge field $U_\mu(n)$ connecting every couple of neighboring sites $(n, n+\hat{\mu})$ is introduced. Each of the gauge variables $U_\mu(n)$, usually called *links*, is a member of the gauge group—$SU(3)$ for QCD—and it will represent in what follows the gluonic degrees of freedom. It is formally a parallel transporter, related with its continuum counterpart $A_\mu(x)$ by

$$U_\mu(n) = \mathcal{P} e^{i \int_n^{n+\hat{\mu}} A_\mu(x) dx}, \tag{1.8}$$

where $\mathcal{P}$ indicates that the integral is to be made along the path ordered product of $A_\mu(x)$. Under a gauge transformation, $U_\mu(n)$ changes as

$$U_\mu(n) \to G(n)U_\mu(n)G^\dagger(n+\hat{\mu}). \tag{1.9}$$

From (1.5) and (1.9) it follows that products of the form

$$\bar{\psi}(n)U_\mu(n)\psi(n+\hat{\mu}), \tag{1.10}$$

which connect neighboring quark and antiquark fields with the corresponding link variable, as in Figure 1.1, are gauge invariant. In fact, it is possible to go further and consider all possible gauge-invariant combinations composed by products of gauge and fermion fields. A straightforward consequence of (1.9) is that ordered products of link variables along a given path, connecting sites x and y, transform as if they were a single link connecting precisely x with y. In order to make this product of consecutive links gauge invariant, two possibilities arise: add a quark-antiquark pair (placed at the end and the beginning of the path) or consider a closed path and take the trace in color space; both alternatives are pictured in Figure 1.2.

Having defined quark, antiquark and gluon fields on the lattice, we can now give a precise meaning to the regularized version of the integration measure $\mathcal{D}\psi\mathcal{D}\bar{\psi}\mathcal{D}A_\mu$, which in the expressions of the partition function (1.2) and the expectation value of an observable (1.3) was simply formulated as the *sum over all possible configurations*. In its discretized version, all fields are only defined over a finite number of

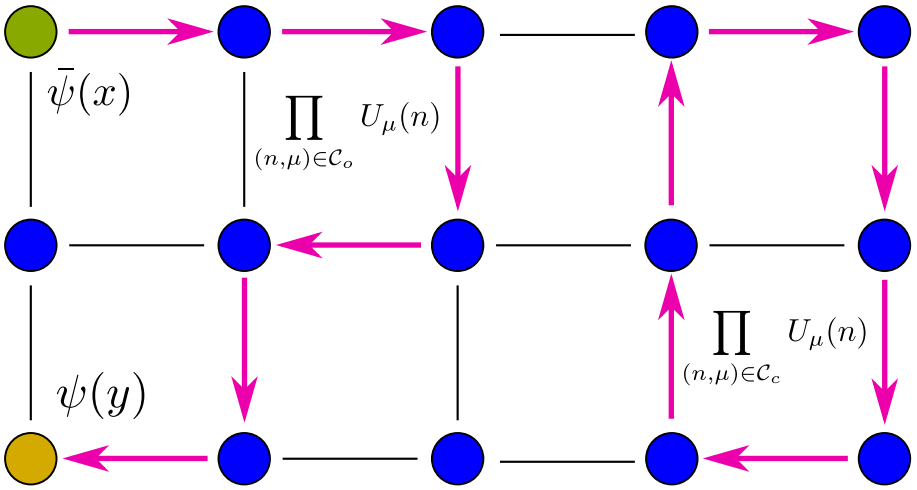

Figure 1.2: Two types of gauge-invariant quantities can be constructed on the lattice: it suffices to consider any path, open or closed, and take the ordered product of the links involved. In the first case, antiquark and quark fields should be appended to the ends of the path; for a loop is enough to take the color trace.

points. This allows to rewrite the integration measure as a product of differentials, formulating the following lattice version of $\mathcal{Z}_{\text{QCD}}$:

$$\mathcal{Z}_{\text{latt}} = \int \prod_{n,\mu} dU_\mu(n) \int \prod_n d\psi(n) d\bar{\psi}(n) e^{-S_{\text{latt}}[\psi(n),\bar{\psi}(n),U_\mu(n)]}. \tag{1.11}$$

As the integration over the variables $U_\mu(n)$, elements of $SU(3)$, is required to be gauge invariant, it is to be performed according to the corresponding Haar measure—uniquely defined up to a multiplicative constant. On the other hand, the fermionic quantities $\psi(n)$ and $\bar{\psi}(n)$ are anticommuting numbers, and thereby they are to be evaluated according to the Grassmann (or Berezin) rules of integration. In fact, these rules allow a considerable simplification of the previous expression, for which is necessary to consider in a general way the form of S_{latt}. For this purpose, it suffices to realize that every lattice action is the sum over all sites of a given discretization of the lagrangian density $\mathcal{L}_{\text{QCD}}$ (1.4), and as a consequence it is possible to split the discretized action into a fermionic term S_f, bilinear in antiquark and quark fields, and a purely gluonic term S_g, namely

$$S_{\text{latt}}(U,\psi,\bar{\psi}) = \bar{\psi} M(U) \psi + S_g(U), \tag{1.12}$$

where $M(U)$, the *fermionic matrix*, encodes the discretization of the covariant derivative—thus depending on the gauge fields—and includes the fermion mass

term. With this input, the fermionic degrees of freedom in the partition function (1.11) can be integrated out analytically, arriving at

$$\mathcal{Z}_{\text{latt}} = \int \mathcal{D}U e^{-[S_g(U) - \log\det M(U)]}, \tag{1.13}$$

where $\mathcal{D}U$ stands for an abbreviation of the product of Haar measures $dU_\mu(n)$ of (1.11). As a word of caution, it should be noted that in some relevant scenarios, such as finite density QCD, the logarithmic term involving the fermionic determinant can be a complex[3] number. In any case, the same procedure can be applied to the expectation value of an observable containing a product of a quark and an antiquark; the continuum expression (1.3) then becomes

$$\langle \psi^{f_2}_{c_2}(y)\bar{\psi}^{f_1}_{c_1}(x)\rangle_{\text{latt}} = \frac{1}{\mathcal{Z}_{\text{latt}}} \int \prod_{n,\mu} dU_\mu(n) \left[M^{-1}\right]^{c_2 c_1}_{f_2 f_1}(y,x) e^{-[S_g - \log\det M]}, \tag{1.14}$$

where c_i and f_i label the color and flavor components of the field, respectively. The above formula can be generalized also to higher order products, understanding that a given observable has to be replaced by the corresponding Wick contraction.

Before discussing the actual form of S_g and M, i.e., of the lattice action, it is important to note several properties that follow from the last expressions. First, the partition function $\mathcal{Z}_{\text{latt}}$ depends on fermions only through the determinant of M. Moreover, this property is shared by the expectation value of any observable composed solely by gauge fields. Neglecting the effect of the determinant, $\det M = 1$, simplifies notoriously the numerical computation of these kind of objects, at the cost of ignoring the effects of virtual quark loops and thus introducing a source of uncontrollable systematic error. Such procedure, as we noted in Section 1.2, was profusely used in the early stages of lattice QCD, and it led to considerable successful results in areas such as light hadron spectroscopy, where the masses of several particles could be determined by different collaborations with sufficient statistical precision, observing systematic deviations with respect to the experimental measures within the 10% level [59–62]. However, the *quenched* approximation—as it is commonly referred to—is far from adequate when considering other scenarios, including topological effects, finite density QCD or even hadron spectroscopy when a few percent precision level is required. Moreover, in the case of some species such as the η' meson, the inclusion of the fermionic determinant is mandatory to avoid dramatic discrepancies with experiment.[4] Finally, when considering observables composed by quark fields, an additional dependence appears, via the inverse

[3] The finite density case, giving rise to a complex action, suffers from a sign problem when a numerical evaluation of the path integral is to be performed. In Chapter 2, another complex action system will be reviewed, namely QCD with a topological term in the action.

[4] In the quenched approximation, the masses of the pseudoscalar meson η' and the pion π^0

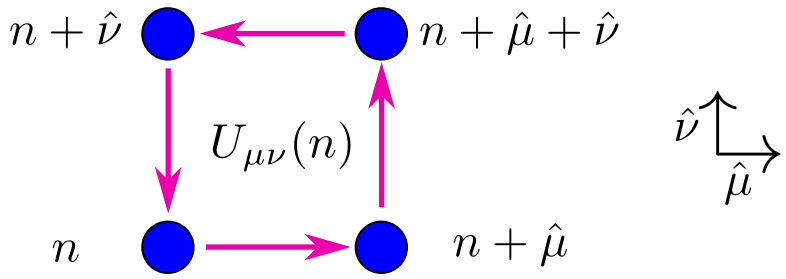

Figure 1.3: The most elementary gauge loop is called plaquette variable. Its trace is a gauge invariant quantity, and in the continuum limit $a \to 0$ it reduces to $F_{\mu\nu}(n)$ squared, i.e., the gluonic part of the QCD action.

fermion matrix, as in (1.14). In any case, the flip side of the analytical integration of Grassmann variables is the introduction of the fermionic determinant—a highly non-local object that severely increases the need of computing resources.

1.3.2 Gluon dynamics

In order to construct the lattice action components, S_g and M, it is required that the gauge invariance of the continuum formulation remains preserved. As pictured in Figure 1.2, when constructing lattice observables as products of gauge and quark fields—or linear combinations of them—only two kind of gauge-invariant quantities appear: gauge loops and quark-antiquark pairs connected by a gauge path. As a consequence, S_{latt} is to be constructed by these type of terms. In addition to that, it must have the proper limit when the lattice spacing a vanishes, although this does not determine a unique action—the discretization of boson and fermion derivative terms in S_{QCD} introduces many degrees of freedom. In other words, different lattice actions must share the limit

$$S_{\text{latt}} \xrightarrow{a\to 0} S_{\text{QCD}}, \tag{1.15}$$

even if they can have different subleading terms.

At this point, a legitimate question—that the cautious reader is probably already wondering—is if this freedom in choosing among an infinite number of actions will not spoil the continuum limit. In other words, all possible actions S_{latt}

are degenerate, while experimentally the former is much heavier. As explained by the Witten-Veneziano mechanism [63,64], the chiral $U(1)$ anomaly of QCD contributes significantly to the η' mass, preventing the particle to be an approximate Goldstone boson. Furthermore, the theorized η'-π^0 splitting requires the existence of fermionic species: this is the reason why fermion dynamics needs to be taken into account. In fact, lattice numerical studies confirm the WV picture [65] and give good estimates for the η' mass, as in [66], where u, d and s quarks are included into the computations.

conform a space in which just one point (namely S_{QCD}, which corresponds to $a = 0$) encodes the proper physics. Thus, we need at least to compute the limit $a \to 0$ along a given trajectory. But, even if we succeed in this labor, how could we assure that the limit does in fact exist? If the presence of an alternative path, leading to a *different* action, could not be discarded, our work would be in vain. The answer to this concern is given by Renormalization Group theory: the continuum limit in any lattice model is to be taken in a critical point of the system, where correlation length diverges and only a few parameters—such as symmetries, dimension and critical exponents—determine the universality class of the model. In the case of QCD, asymptotic freedom grants the existence of the required critical point; thereby, the continuum limit can be taken quite confidently, albeit there exist other subtleties that have to be dealt with. For now, and in order to preserve some discourse coherence, we left a more detailed answer to this issue for an upcoming section.

In any case, it is worth to mention that the freedom in choosing an action has its positive side. As we mentioned before, this leeway has been profusely used during the last decades, with objectives such as to ameliorate discretization errors—this is known as the Symanzik improvement program [57, 58]—or to preserve certain symmetries on the lattice formulation. At the present time, there exist a number of gauge and fermionic actions that are part of the standard lore of the lattice community. In what follows, we go over the most elementary of them—discussing first the gluonic term, since the introduction of fermions involves a number of subtleties.

In order to address the construction of the gauge component of the lattice action, S_g, it is advisable to identify one of the gauge-invariant objects presented earlier, namely the smallest possible loop, which is composed by the product of four consecutive links forming a square,

$$U_{\mu\nu}(n) := U_\mu(n) U_\nu(n+\mu) U_\mu^\dagger(n+\nu) U_\nu^\dagger(n), \tag{1.16}$$

as in Figure 1.3. It is conventionally called *plaquette*, and its color trace is, as discussed earlier, a gauge-invariant quantity. More importantly, the sum of all plaquettes give rise to a pure gluonic term in the action, which can be proven to have the correct continuum limit if S_g is formulated in the following terms

$$S_g = \beta \sum_{n,\mu,\nu} \left[1 - \frac{1}{3} \operatorname{Re} \operatorname{Tr} U_{\mu\nu}(n) \right], \tag{1.17}$$

with $\beta = 6/g_{\mathrm{latt}}^2$; the coupling g_{latt} is simply the unrenormalized or *bare* version of the coupling g present in $\mathcal{Z}_{\mathrm{QCD}}$. This term is known as the Wilson gauge action, and has discretization errors of order $\mathcal{O}(a^2)$. Although there exist more involved

prescriptions that minimize further the order of the errors, the original proposal of Wilson provides a good balance between the precision achieved and the complexity of its definition. In any case, improved gauge actions are built by adding higher order terms to (1.17), involving loops larger than the plaquette that are suppressed by powers of a. This type of gluonic actions are state-of-the-art in modern lattice computations.

1.3.3 Interlude: chiral symmetry in the continuum

Just before addressing the construction of the fermionic matrix M, we found necessary to make at least a shallow review of the role of chiral symmetry in QCD, as its formulation on the lattice has deep and direct implications in how dynamical fermions can enter into the lattice action.

In its continuum formulation, the action of QCD for N_f flavors is given by the spacetime integral of the lagrangian (1.4). Focusing on the fermionic part and keeping a compact notation, where ψ and $\bar{\psi}$ fields are understood to be N_f-vectors in flavor space, we have

$$\mathcal{S}_{\text{QCD-F}} = \int d^4x \, \bar{\psi} \left(i\gamma_\mu D_\mu + m \right) \psi. \tag{1.18}$$

For the particular case of zero fermion mass, i.e., if all the components of the diagonal matrix m vanish, there exist two sets of transformations that leave the above action invariant. The first family is composed by the so-called *vector transformations*, given by

$$\psi \to e^{i\alpha \mathbb{1}} \psi \qquad \bar{\psi} \to \bar{\psi} e^{-i\alpha \mathbb{1}}, \tag{1.19}$$

$$\psi \to e^{i\alpha T_i} \psi \qquad \bar{\psi} \to \bar{\psi} e^{-i\alpha T_i}, \tag{1.20}$$

where the T_i matrices are the generators of the flavor group, $SU(N_f)$, and so, the index i runs from 1 to $N_f^2 - 1$. When considering altogether (1.19) and (1.20), the group extends to $U(N_f)$. The other family of transformations can be constructed by including a γ_5 matrix in the previous ones, and thus they are given by

$$\psi \to e^{i\alpha\gamma_5 \mathbb{1}} \psi \qquad \bar{\psi} \to \bar{\psi} e^{-i\alpha\gamma_5 \mathbb{1}}, \tag{1.21}$$

$$\psi \to e^{i\alpha\gamma_5 T_i} \psi \qquad \bar{\psi} \to \bar{\psi} e^{-i\alpha\gamma_5 T_i}. \tag{1.22}$$

This last set receives the name of *axial transformations*. When considered together with vector transformations, they receive the name of chiral transformations; in the same way, the massless limit—in which they preserve S_{QCD}—is called *chiral limit*. To differentiate the two sectors that compose chiral symmetry, it is customary to label them with a V or a A subscript. In this way, the full chiral group is given by

$$SU(N_f)_V \times SU(N_f)_A \times U(1)_V \times U(1)_A. \tag{1.23}$$

It is important to note that axial transformations are symmetries of the massless action, but this symmetry is explicitly broken for finite mass quarks. On the contrary, vector transformations (1.20) preserve the action also in the degenerate mass case—i.e., N_f species of equal non-zero mass—conforming the well-known isospin symmetry. Furthermore, (1.19) is always a symmetry of the action, which implies baryon number conservation.

Equally relevant is the so-called axial anomaly. Although $U(1)_A$ is a symmetry of the massless action, it is explicitly broken in the fully quantized theory. This reduces the full expression (1.23) to the following symmetry group:

$$SU(N_f)_V \times SU(N_f)_A \times U(1)_V. \tag{1.24}$$

This group is usually expressed in slightly different terms. To this aim, it suffices to recall that chiral symmetry splits both the quark fields and the action into two separate pieces, commonly named left- and right-handed. Defining the projectors P_L and P_R as

$$P_L = \frac{\mathbb{1} - \gamma_5}{2} \qquad P_R = \frac{\mathbb{1} + \gamma_5}{2}, \tag{1.25}$$

it is possible to partition the full flavor space, since introducing the projected quark and antiquark fields

$$\psi_{L,R} \equiv P_{L,R}\psi \qquad \bar{\psi}_{L,R} \equiv \bar{\psi}P_{R,L}, \tag{1.26}$$

allows to express the quark (antiquark) field as the sum of ψ_L and ψ_R, separating in this way the action into several components:

$$S_{\text{QCD-F}} = \int d^4x \left\{ \bar{\psi}_L \left(i\gamma_\mu D_\mu\right) \psi_L + \bar{\psi}_R \left(i\gamma_\mu D_\mu\right) \psi_R + \left(\bar{\psi}_L m \psi_R + \bar{\psi}_R m \psi_L\right) \right\}. \tag{1.27}$$

From the above expression it trivially follows that, in the chiral limit, only the first two components survive. Remarkably, they are completely decoupled in this limit, interacting only through the mass terms in the above formula. For this reasons, the chiral symmetry group (1.24) is often reformulated in terms of its left- and right-handed degrees of freedom, i.e., as

$$SU(N_f)_L \times SU(N_f)_R \times U(1)_V. \tag{1.28}$$

In any case, when considering quarks of finite but degenerate mass, the axial sector symmetry is broken explicitly—just the $SU(N_f)$ part, since the one corresponding to $U(1)_A$ was already broken by the anomaly—and the above group gets reduced to its vector sector $U(N_f)_V$, or following the structure of (1.24)

$$SU(N_f)_V \times U(1)_V. \tag{1.29}$$

Eventually, if one considers N_f flavors with different masses, the above symmetry gets reduced to the tensor product of N_f copies of $U(1)_V$.

Before closing this interlude, we want to stress a couple of issues concerning chiral symmetry. The first one is that chiral symmetry—or more precisely, its axial sector—is **spontaneously broken** in QCD at zero temperature. Let us consider the action with just two flavors: *up* and *down*. Since these quarks have a very small mass compared to the QCD scale, its explicit symmetry breaking, corresponding to the shift between (1.28) and (1.29) for $N_f = 2$, should give rise to experimental effects. In particular, some particles—as, e.g., parity partners—should have almost-degenerate masses. However, this expected symmetry does not match the observations; mass differences due to the explicit breaking of the QCD action are significantly smaller than the experimental measures. The origin of these discrepancies is, precisely, that the global symmetry (1.28) is spontaneously broken, since the vacuum of the theory is not invariant under the corresponding transformations. In other words, although the action is *almost* preserving chiral symmetry, the ground state of the system is not.

The second point to discuss is just a corollary of the previous argument: since there is a continuous symmetry being spontaneously broken, **Goldstone's theorem** predict the appearance of several massless bosons. This is in fact the case, since if we consider just quarks u and d, we should expect three light bosons—since the symmetry is slightly explicitly broken—which can be identified with the three pions π^0, $\pi^\pm$. Including also the *strange* quark s, would account for eight bosons, which can also be identified with the four kaons $K^0, \bar{K}^0, K^\pm$ and the η meson, which sums up to the three pions. Note that if we overlook the anomaly, in the last case 9 light mesons should appear, and the η' particle should be also considered within this picture. It is precisely the anomaly what allows to explain the $\eta' - \pi^0$ mass difference, as was stressed in the previous subsection.

With these considerations, we can now proceed to talk of fermions in the lattice, with a last word of caution that summarizes the previous argument. The lightest particles of the QCD spectrum gain their low masses thanks to the spontaneous breaking of chiral symmetry. If we were to tweak the theory and remove the chiral invariance from the action, the explicit breaking of this symmetry would prevent these particles from being pseudo Goldstone bosons, and consequently their masses would be expected to increase.

1.3.4 Dynamical fermions: doubling and chiral symmetry

In order to implement full QCD in the lattice, we need to choose an action S_{latt} which, as in (1.12), can be decomposed into two components. First, a purely gluonic term S_g, for which a viable candidate has already been reviewed in subsection 1.3.2. In second place, a term involving quark and antiquark fields is needed. Now

that the basics of chiral symmetry in continuum QCD have been discussed, we can face the task of constructing this fermionic term, completing in this way the lattice action. Thereby, in this subsection we will analyze the difficulties in proposing a proper lattice version of the fermionic matrix M, which defines how quarks and antiquarks interact.

While the construction of the Wilson gauge action (1.17) was not very troublesome, the situation changes substantially when trying to proceed with the fermionic part of the action in a similar way. The simplest approach to discretize the continuum term consists in replacing the first order derivatives in $\mathcal{L}_{\text{QCD}}$ by a standard symmetric difference. In this way, the continuum fermionic term $\bar{\psi}\left(i\gamma_\mu D_\mu + m\right)\psi$ becomes

$$\frac{1}{2a}\bar{\psi}(n)\left[i\gamma_\mu\left(U_\mu(n)\psi(n+\hat{\mu}) - U_\mu^\dagger(n-\hat{\mu})\psi(n-\hat{\mu})\right) + m\right]\psi(n), \tag{1.30}$$

which is indeed gauge-invariant, as bilocal products of quark-antiquark fields are connected by the corresponding link variables. Unfortunately, this procedure introduces the so-called *doublers*: for each of these *naive* fermions included in the lattice action, 16 copies appear in the continuum limit, 15 of them being unphysical. In order to fix this situation, an alternative is to use *Wilson fermions*, which add an extra term to the naive formulation. Its aim is to assign a divergent mass, of order $\mathcal{O}(a^{-1})$, to each of the unwanted doublers, decoupling them from the theory in the continuum limit. This mechanism is sufficient to fix the continuum limit of the action, however, the axial sector of chiral symmetry gets explicitly broken in the lattice by the extra term—not only the anomalous part $U(1)_A$, which in fact should be broken, but the whole group $U(N_f)_A$. In continuum QCD, as it was discussed in the previous subsection, chiral symmetry plays a central role, since its non-anomalous sector is spontaneously broken, producing approximate Goldstone bosons. With an explicitly broken chiral symmetry, this mechanism is not possible anymore: particles such as pions, kaons or the η, which conform the so-called meson octet, acquire masses well above its original values. This behavior hinders actual simulations from reaching the physical point. In fact, during decades of lattice numerical works, the achieved mass of the pion—a very relevant quantity, being the lightest hadron in the spectrum—has been very far from its physical value, which makes necessary to perform extrapolations to the physical point.

The previous discussion rises a natural question: is it possible to find a fermion formulation that, whithout introducing unphysical multiplicities, preserves chiral symmetry? For a long time, it was believed that, unfortunately, it was not. In fact, far from being a technical complication, the doublers issue has its root in the chiral anomaly of QCD. In the naive lattice formulation of (1.30) the anomaly disappears, canceled exactly by the extra doublers. Adding the Wilson term, which decouples the extra particles, can be interpreted as introducing a lattice version of

the anomaly by hand—with one undesirable effect: it also breaks the non-anomalus part of the symmetry, spoiling the spontaneous breaking mechanism. In fact, as was proven in 1981 by Karsten and Smit [67], this is a general result: either the axial anomaly is canceled by the presence of extra fermions, or it is introduced in the lattice by a term that, necessarily, explicitly breaks chiral symmetry, including its non-anomalous sector. In the same way, a contemporary result due to Nielsen and Ninomiya—the so-called no-go theorem—states that it is not possible to construct a lattice formulation of QCD that has at the same time absence of doublers, chiral symmetry, and locality [68, 69]. Furthermore, there also exists a scheme-independent version of this result, with slightly different conditions [70], that makes the impossibility of regularizing a theory with chiral fermions a rather profound question, not exclusive of the lattice approach. As a consequence, a choice must be made between preserving chiral symmetry *in its continuum form* or avoiding unwanted degrees of freedom; every fermion formulation on the lattice suffers from one pathology or the other.

But, even though the above results are correct, a workaround fortunately exists. Almost 40 years ago, Ginsparg and Wilson realized that a remnant of chiral symmetry could be identified within the lattice formulation, in such a way that the axial anomaly is still properly preserved and, at the same time, no unphysical degrees of freedom are introduced [71]. While the continuum form of chiral symmetry—i.e., the preservation of the transformation sets (1.19) to (1.22)—requires the massles Dirac operator to anticommute with γ_5, the *remnant* symmetry proposed in [71] verifies a broader restriction, namely

$$D\gamma_5 + \gamma_5 D = aD\gamma_5 D, \tag{1.31}$$

where $D \equiv i\gamma_\mu D_\mu$ stands for the massless Dirac operator. This condition is in fact different from its continuum counterpart for every finite lattice spacing a, although they converge in the $a \to 0$ limit. In this sense, (1.31) can be interpreted as an extension of the continuum definition, with a singular advantage: it is able to evade the Nielsen-Ninomiya no-go theorem, since only the continuum form of chiral symmetry—with a vanishing right-hand side in (1.31)—is affected by it [72]. Moreover, a modified chiral rotation can be defined in the lattice, in such a way that the gauge fields transform essentially as its continuum versions, preserving relevant results as, i.e., the index theorem [73]. However, the solution given in [71] was not constructive, in the sense that a particular form of D could not be found at that moment; it would took almost two decades to find a practical implementation of these ideas.

Within the above scenario, other alternatives would be explored over the years to come. In fact, a number of these strategies were developed and nowadays are part of the current lore of the field. They can be classified in groups according to

how they deal with the doubling problem. Some approaches choose to give up chiral symmetry; this is the case of Wilson fermions. In this category are also included *clover* fermions, a Symanzik improved version of Wilson fermions that removes $\mathcal{O}(a)$ discretization errors [74], and *twisted mass* fermions, which consider pairs of mass degenerate Wilson fermions together with an isospin mass splitting term [75]. An alternative approach consists in preserving chiral symmetry, while assuming some of the doublers degeneracy. Here the prime example are Kogut-Susskind or *staggered* fermions [76]. This variant is constructed from the naive formulation, but distributes the usual Dirac 4-spinor components over neighboring sites, in such a way that the doublers degeneracy gets reduced from 16 to 4 species. Moreover, for some observables it is possible to remove the residual degrees of freedom by taking the fourth root of the fermion determinant—a procedure commonly referred to as *rooting*, originally proposed by Marinari, Parisi and Rebbi, in the context of the massive Schwinger model [77]. Although its validity was at first controversial, both numerical evidence [78] and theoretical arguments [79] support that this technique leads to the correct theory as long as continuum and chiral limits are taken precisely in this order. As with Wilson fermions, there also exist Symanzik improved versions of the staggered action; two of them, widely used by the lattice community, are the Asqtad action [80]—for a-squared tadpole improved—and the HISQ action [81]—for highly improved staggered quarks. In Chapter 4 we make use of staggered quarks, while on Chapter 6 the analyzed configurations were generated with the HISQ action.

For the sake of completeness—even if it is less related with the work developed in this thesis—there is still another class of fermions that deserves at least a mention: the particular solutions of the Ginsparg-Wilson equation (1.31). They preserve chiral symmetry without the doublers pathology, so in this sense they are the *best* possible fermions, and they should be preferred when compared to other alternatives. However, all their implementations suffer from the same illness—they are by far the most expensive fermions in computational terms. As a consequence, its use is reserved to situations where chiral symmetry is needed with considerable precision. There exist two different solutions that are broadly used: they are called overlap [82–84] and domain-wall [85, 86] fermions. In the first case, the fermionic matrix is constructed by operating with a Wilson-like matrix—the result being a costly non-sparse matrix. For domain-wall fermions, an extra fifth dimension of infinite extent is needed to preserve chiral symmetry. Since in practice this is implemented as an additional dimension in a finite lattice, a mild violation of the symmetry still remains, although it can be controlled.

1.3.5 Monte Carlo: ensembles and observables

Summing up all the previous considerations, we have now a fully regularized version of QCD. Thereby, the original expressions for the partition function (1.2) and the vacuum expectation value (1.3) of a given observable acquire now a well-defined mathematical meaning.

If we now want to consider, e.g., a purely gluonic observable $\mathcal{O}(U)$, we should compute the following integral:

$$\langle \mathcal{O} \rangle = \frac{\int \mathcal{D}U \mathcal{O}(U) e^{-S_{\text{latt}}(U)}}{\int \text{ffl}athcal DU e^{-S_{\text{latt}}(U)}}. \tag{1.32}$$

The above integration measure $\mathcal{D}U$ is composed by the product of as many individual Haar measures as links are in the given lattice, which amount to $V \equiv \prod_i L_i$ times the dimension of the lattice. So, for almost any size that we can think of, (1.32) contains a highly multidimensional integral, with a vast configuration space that, even for small lattices, can not be fully explored by any computational means. There exist however a class of numerical approaches, commonly referred to as Monte Carlo methods, that are capable of properly sampling these kind of spaces—to apply them to the lattice regularization was, in fact, one of the key proposals of Wilson [40].

In order to compute the expectation value of (1.32), a first Monte Carlo approach could consist in generating a random sample of link configurations, i.e., a collection or ensemble of gauge fields U^i, each one containing the information of each individual link $U_\mu(n)$ in the lattice. Then, $\langle \mathcal{O} \rangle$ could be computed as a weighted average over the previous ensemble, with weight $e^{-S_{\text{latt}}(U)}$. In a similar fashion, statistical errors could be computed by standard techniques. However, this approach is too naive for the problem at hand, since the exponential factor in (1.32) highly suppresses a great majority of the configuration space elements; in other words, only a small subset of the whole space contributes significantly, and a naive random sampling of the space would miss the area of interest. In order to fix this issue, *importance sampling* is to be applied: again, an ensemble of configurations U^i is generated, but they should be selected with probability $e^{-S_{\text{latt}}(U^i)}$. Then, provided a well-distributed ensemble of N elements is available, an estimator for the expectation value of a given observable can be straightforwardly computed as

$$\bar{\mathcal{O}} = \frac{1}{N} \sum_i^N \mathcal{O}(U^i). \tag{1.33}$$

The original problem is now shifted to the generation of the U^i collection. This can be achieved by starting from a given initial configuration, say U^1, and following a Markov chain process, in which the selection of the next configuration is regulated

by a probability that depends only on the immediate previous state. The idea is that, even if one starts far from the meaningful configurations, the Markov process should drive the system to an equilibrium state, in which the distribution $e^{-S_{\text{latt}}(U^i)}$ is reproduced. To guarantee that, the transition probabilities from each U^i to any other U^j need to be adequately defined. It is sufficient (but not necessary) to require the *detailed balance condition* to be fulfilled, so if we label the transition probability of the chain as $p(U^i|U^j)$,

$$p(U^i|U^j)e^{-S_{\text{latt}}(U^j)} = p(U^j|U^i)e^{-S_{\text{latt}}(U^i)} \tag{1.34}$$

would be required for every i and j. In this case, if the system is also ergodic—meaning every configuration is accessible from any other in a finite number of steps—it is guaranteed that, with independence of the initial configuration chosen, the Markov process will reach equilibrium and, consequently, a well-distributed ensemble will be generated.

Then, to elaborate a particular algorithm that follows the described Markov process consists then in specifying how the next element of the chain is selected, and which transition probabilities connect the configuration space. With respect to the latter point, most of the algorithms used by the lattice community verify the detailed balance condition. Maybe the most elementary of them is Metropolis algorithm, which accepts a change between U^i and U^j with probability $\max\{1, e^{-\Delta S_{\text{latt}}}\}$. This is exactly the approach followed in Chapter 3. More involved alternatives include the heatbath algorithm [44], which often includes some overrelaxation steps [87–89]. Furthermore, for the more general case in which fermions are included into the action, one of the most widely used algorithms is the Hybrid Monte Carlo [90, 91], which at each update combines a microcanonical evolution with a final metropolis step to accept or reject the proposed change.

In any case, the stochastic nature of Monte Carlo methods introduce some uncertainty into the computed observables, in the form of statistical errors associated to the corresponding estimators. Nevertheless, these can be dealt with without much difficulty, just by taking into account two fundamentals. First, that the generated ensemble has to be *thermalized*, meaning that sufficient iterations need to be spent to reach the equilibrium distribution of the Markov chain. This can be achieved by monitoring a set of observables that allow to determine when the Markov evolution is stationary. Secondly, and even more important, is the inherent *correlation* of the configurations generated by the update process—generally a local algorithm that needs a high number of iterations to produce a *new* configuration far from the original. In this case, the use of standard error analysis tools, such as jacknife binning, or even the direct computation of autocorrelation times for each observable, allows to estimate in a reliable way the statistical errors of any computed observable.

1.4 Reaching the continuum and sources of error

Up to this point, we have covered how continuum QCD can be regularized into a spacetime lattice where, taking advantage of Monte Carlo methods, it is possible to estimate vacuum expectation values of given observables. The computed observables will depend in general on the dimensions of the lattice and on the bare values of the gauge coupling β and the N_f masses of the fermion species involved. Although knowing these values can be enough for some applications, in most calculations the objective is to obtain a physically measurable quantity that can be eventually contrasted with experiment. This is not the case of the present thesis, since the work being presented is not directly concerned about the last part of a general lattice calculation; however, in order to give a general perspective of what a complete computation would require, and for the sake of completeness, hereafter we proceed with a brief overview of the issues involving the last steps of the lattice approach.

Obtaining a physical prediction from bare lattice results requires a somewhat involved limit procedure; not only the lattice spacing a should vanish—this would be the continuum limit—but also the bare couplings should go to their physical values. In other words, the *physical point* needs to be reached; if not, the simulated theory would be describing an alternative scenario, one with, e.g., different hadron masses. In fact, the couplings of the theory are not directly observable (since confinement prevents quark fields to manifest outside a color-singlet, the mass of the quark is not an observable and depends on the renormalization scheme). In place, other observables, such as hadron masses ratios—which of course depend on the aforementioned parameters—are to be computed in the lattice, so they can be compared with the experimental values. Thus, in order to compute a given quantity, it is necessary to keep track of several additional observables, one for each of the free parameters—or flavor species—that are included into the calculation. Morover, it should be noted that the lattice spacing a is not a free parameter of the lattice theory, but another quantity that needs to be measured within the lattice.

The above scenario can be summarized as follows: we need to take the continuum limit, $a \to 0$, *while* driving a set of physically measurable quantities to their experimentally determined values. Moreover, since doing the computations on a lattice of infinite extent is out of reach, the procedure is to be performed on a 4D box of finite physical size.[5] In order to take the $a \to 0$ limit, it is required to repeat the computations at different lattice sizes, keeping the physical size of the box constant. In this way, lattices with different values for the lattice spacing a—and consequently for the number of nodes N—are computed, while the volume of the

[5] In fact, repeating the calculations in several box sizes allows to extrapolate the results to the thermodynamic limit.

box a^4N is kept constant. It should be recalled that while N is a free parameter, a is an observable that needs to be measured (depending not only on the gauge coupling but also on the inclusion of fermionic species). So, as a first consequence, keeping the physical volume constant is not a completely trivial issue.

The same problematic that appears when trying to fix the volume of the 4D box applies to every physical observable that is intended to be kept constant (or driven to a suitable value, obtained from experimental sources). To achieve this, essentially two options are possible: either the free parameters are tuned in an iterative process—one lattice at a time up to the physical point—or the computations are repeated for several values of these parameters, and then interpolated to the desired point. A less ideal variation of the latter is to reach the physical point by means of an extrapolation. This was in fact the rule during several decades of lattice numerical computations, since the different types of fermion discretizations (reviewed in Section 1.3.4) have many difficulties in reaching a sufficiently low mass for the pion.[6]

As a final remark, it is important to stress that any full computation on the lattice should include a careful analysis of all sources of errors. First, statistical errors are introduced by the Monte Carlo evaluation process. These are however relatively easy to deal with, since they can be estimated by standard methods and, even more importantly, can be systematically reduced by increasing the computation time. A more challenging obstacle is in estimating the different issues leading to systematic errors, specially when a high precision is desired—and previously unnoticed systematic errors can become big enough to be taken into account. A non-exhaustive but common record of the different sources of systematics considered would include the errors associated with the tuning or interpolation to the physical point and the continuum limit process. Usually less severe are those related with the thermodynamic limit—finite volume effects—or with the exclusion from the action of electromagnetic effects, which, given that the quarks are electrically charged particles, should be accounted for. In general, any approximation assumed should account for its corresponding error—as, e.g., the case of some lattice fermion types which consider u and d quark bare masses as degenerate, and thus are required to account for the corresponding isospin breaking effects.

[6] Although Ginsparg-Wilson fermions preserve chiral symmetry, they suffer from a large computational overhead that spoils their advantage with respect to other fermion types, when reaching a physical pion mass is considered.

Chapter 2

Topology in QCD

In the previous chapter we have covered the essential points of the lattice approach to QCD, which is in fact applicable to other gauge theories, mutatis mutandis. Having reviewed the basics in a general way, our aim in the present chapter is to set the focus on a particular aspect of QCD, providing the necessary context to introduce and motivate upcoming chapters.

As was outlined at the beginning of this thesis, the lattice approach has proven to be a reliable tool for the study of non-perturbative phenomena, and accounts for a high number of successes. Even so, there exist some problems that still constitute wide open questions, a major example being theories which have a complex action. In this situation, the sign problem appears, forbidding standard importance sampling techniques and forcing to look for alternative workarounds. Within QCD, this is the case when finite density or the inclusion of a topological term in the action are considered. In fact, our interest will be drawn by the latter topic, which is commonly referred to as θ QCD.

Thereby, in this chapter we recall the fundamentals concerning topological effects in QCD, including a brief discussion on the strong CP problem and one of its more popular solutions: the axion. Subsequently, we mention some of the approaches that deal with complex action systems, including the methods of Azcoiti et al [12, 13].

2.1 A topological term in the action

When, during the description of the lattice formalism, the action of QCD was introduced, no appearance of a complex term or a topological object was present. Additionally, it was stressed that there are $N_f + 1$ free parameters in the theory, namely the gauge coupling and the fermion masses. Actually, in the Lagrangian density (1.4) there is a deliberate, and usual, omission: that of the θ or topological

term, which in Euclidean spacetime corresponds to

$$\mathcal{L}_\theta = -i\theta \frac{g^2}{64\pi^2} \epsilon_{\mu\nu\rho\sigma} F^a_{\mu\nu} F^a_{\rho\sigma}, \tag{2.1}$$

where, as in (1.4), $F_{\mu\nu}$ is the gluon field tensor, and the a index label color space. Before going any further, we found worthy to discuss the nature and implications of the above term by following a discourse close to the actual historical development. In this way, we expect both to recall the main theoretical points and to motivate the upcoming contents of this thesis.

2.1.1 From the axial anomaly to the strong CP problem

The Lagrangian density of QCD—and also its spacetime integral, the action—with N_f flavors of massless quarks, is invariant under the group of chiral transformations, as defined in Section 1.3.3. In particular, its axial subgroup

$$U(N_f)_A = SU(N_f)_A \times U(1)_A \tag{2.2}$$

holds only as a global symmetry in the massless fermion case, being explicitly broken otherwise. Since the actual masses of up and down quarks—and, to a lesser extent, of the strange quark—are small when compared with the QCD scale, some signal of this approximate symmetry should be observable. However, as was pointed out in the previous chapter, axial symmetry is spontaneously broken, leading to the appearance of N_f^2 pseudo Goldstone bosons. Considering up, down and strange quarks,[1] Goldstone theorem would predict nine massless bosons, which in fact could be identified, according to their inherited quantum numbers, with the three pions $\pi^0, \pi^\pm$, the four kaons $K^0, \bar{K}^0, K^\pm$ and the η and η' mesons. Moreover, each of these particles should have a relatively small and similar mass, since the deviations from an ideal massless Goldstone would be justified only by the non-zero, but again small, quark masses. However, the experimental mass of the η' is significantly higher than that of any of its eight companions, which discards this particle from being a pseudo Goldstone. This $\pi^0 - \eta'$ splitting, or equivalently, $\eta - \eta'$ splitting, was in fact a puzzling question in the early development of QCD; the solution of this paradox was to come by the axial $U(1)_A$ anomaly of the theory.

Although the anomaly mechanism was discovered by Adler [92] and Bell and Jackiw [93] in 1969, and thus it was known before the formulation of QCD, it was believed to have no physical effects in this theory. In fact, Weinberg addressed this

[1] One can also include only two flavors and consider up and down quarks, in which case the spontaneous breaking of $U(2)_A$ would naively imply 4 Goldstone bosons. These could be identified with the three pions and the η, according to their quantum numbers. In any case, the experimental mass differences lead to analogous conclusions.

question in 1975, suggesting that a way out of the so-called $U(1)$ *problem* could be achieved if the $U(1)_A$ symmetry was not conserved, although he dismissed the anomaly as the source of this breaking [94]. The argument was a natural one, since even if the conservation law of the axial current includes a term due to the anomaly,

$$\partial_\mu(i\bar{\psi}^a\gamma_\mu\gamma_5\psi^a) = -i\frac{g^2}{32\pi^2}\epsilon_{\mu\nu\rho\sigma}F^a_{\mu\nu}F^a_{\rho\sigma}, \tag{2.3}$$

it can be shown that it is equivalent to a total derivative, and as a consequence it seems reasonable to expect the Lagrangian of the theory to be unaffected by it. By 1976, 't Hooft—leaning on a previous work of Belavin et al [95] which found topological solutions in 4D Yang-Mills theories—realized that the anomaly term in (2.3) could be identified with instanton configurations that have non-vanishing effects on the action, eventually leading to a finite contribution to the η' mass [96]. A different approach, based on the $1/N$ expansion, was soon developed by Witten and Veneziano, providing solid theoretical foundations to the mechanism by which the η' meson acquire its mass from the anomaly [63, 64]. In summary, what occurs is that axial $U(1)_A$ symmetry is explicitly broken by the anomaly, and as a consequence no Goldstone boson is produced; in other words, the mass of the η' is not protected, in contrast with the masses of the meson octet.

The aforementioned works gave a consistent solution to the $U(1)$ problem. In fact, they were supported by later lattice computations that numerically confirmed the Witten-Veneziano picture [65, 66]. However, the realization that instanton solutions have an actual contribution to the dynamics introduced another problem in QCD. A term proportional to the anomaly (2.3) needs to be accounted for in the Lagrangian density, coupled to an additional free parameter, the vacuum angle θ. The expression (2.1) for $\mathcal{L}_\theta$ is commonly written as

$$\mathcal{L}_\theta = -i\theta q(x), \tag{2.4}$$

where $q(x)$ is the topological charge density. Its spacetime integral,

$$Q = \int d^4x\, q(x) = \int d^4x \frac{g^2}{64\pi^2}\epsilon_{\mu\nu\rho\sigma}F^a_{\mu\nu}F^a_{\rho\sigma}, \tag{2.5}$$

is the topological charge. It has the characteristic property of being an integer number, classifying gauge fields A_μ into different sectors that cannot be connected by a sequence of infinitesimal gauge transformations. A first consequence of this is that the vacuum state of the theory cannot be constructed as a perturbation of a classical state; it has instead a fully non-perturbative nature [97]. In fact, in a theory with massive fermions, θ labels an infinite number of non-equivalent vacua, which are degenerate only in the massless case. The true vacuum is then

a superposition across different topological sectors, and the partition function of QCD can be written within the lattice regularization as

$$\mathcal{Z}_{\text{latt}} = \sum_{Q} e^{i\theta Q} \mathcal{Z}(Q), \tag{2.6}$$

where $\mathcal{Z}(Q)$ is the original partition function, considered at a fixed value of the topological charge Q.

Moreover, concerning global symmetries, the topological charge is invariant under charge conjugation, but not under parity or time reversal transformations; as an immediate consequence, including $\mathcal{L}_\theta$ in the QCD Lagrangian density spoils the conservation of CP symmetry. This fact is quite troublesome, since there exist stringent experimental constraints to any violation of CP in QCD processes, the most relevant of them being the empirical upper bounds to the neutron electric dipole moment, which ultimately restrict the θ vacuum angle to a value smaller than 10^{-11}. This need of fine tuning a free parameter constitutes the so-called strong CP problem. In fact, the situation gets even worse if one considers the full SM theory—i.e., QCD with several quark flavors that are also affected by electroweak interactions—since the θ parameter coming from QCD gets shifted by the complex phase of the Yukawa mass matrix. Thus, the total angle θ, which should have physically measurable effects, is given by the sum of two components,

$$\theta = \theta_{\text{QCD}} + \text{Arg}\det M, \tag{2.7}$$

that emanate from quite different theoretical sources. In order to describe our world, both parts should cancel out to a high level of precision.

Although at present the strong CP problem is still unsolved, different proposals have been developed in order to explain it. Hereafter we go over the most popular candidate, the Peccei-Quinn mechanism.

2.1.2 The Peccei-Quinn mechanism and the axion

A possible way out of the strong CP problem would be the existence of a massless fermion in the theory, namely that the mass of the up quark would vanish. This scenario would render the different θ vacua equivalent, or in other words, θ would become an *unphysical* parameter. However, current experimental knowledge discards this possibility with an outstanding margin of confidence [2], and other mechanisms need to be searched for.

An altenative path is given by the so-called anthropic solution. It suffices to consider that we live in a world where the θ parameter is just a very small number; at least, smaller than 10^{-11}. After all, there exist other examples of SM parameters that are orders of magnitude apart, such us the bare masses of the quarks, where up

and top masses are separated by five orders of magnitude, roughly. However, the solution of the $U(1)$ problem requires a much more precise cancellation, specially taking into account that there are two independent parameters in (2.7) that need to be adjusted to this end.

Although it is not possible to absolutely discard the anthropic argument, the truth is that this solution is not perceived as sufficiently satisfactory. Instead, the strong CP problem has been interpreted since its appearance—and it still is—as a sign of new physics beyond the Standard Model. A first mechanism dealing with this question, and remarkably the most popular, was given by Peccei and Quinn in 1977, who proposed that QCD could hold an additional $U(1)$ global symmetry that could drive dynamically the θ angle to zero [98]. Soon after, Weinberg [99], and independently Wilczek [100], realized that the spontaneous breaking of the postulated $U(1)_{\mathrm{PQ}}$ symmetry gives rise to a light pseudo Goldstone boson, namely a neutral pseudoscalar that was called *axion*. This new particle can be pictured as a prediction of the Standard Model, in a way similar to the Higgs boson. In fact, much interest is dedicated to the search of this particle, either by studying different axion alternatives and its measurable implications or by exploring its vast mass-coupling parameter space—a real challenge, since both parameters can vary over many orders of magnitude. Nevertheless, several kinds of experiments are currently devoted to this search, in part due to the fact that, in addition of solving the strong CP problem, the axion constitutes a very promising candidate to the cold dark matter of the Universe.

In any case, the properties of the axion, and those of other postulated axion-like particles, are rich enough to touch on many areas of fundamental physics, such as cosmology or string theory; for a thorough discussion on this extense topic, we refer the reader to a recent review by Irastorza and Redondo [101]. For what concerns this thesis, it suffices to stress that the topological objects of QCD—e.g., the topological susceptibility or the topological charge dependence on θ—have a direct impact on axion physics, and so their computation within the lattice framework is strongly motivated.

2.2 The sign problem in complex action QCD

As was outlined in the previous section, QCD has topological non-trivial solutions, classically known as instantons, that need to be taken into account in order to properly describe its physics. In fact, this situation is valid not just for QCD, but for any 4D $SU(N)$ gauge theory. In terms of the path integral formulation, this implies the inclusion of an additional piece into the Lagrangian density, the so-called θ term. In this way, the complete Lagrangian would be the sum of two

pieces,

$$\mathcal{L}_{\theta\text{-QCD}} = \mathcal{L}_{\text{QCD}} + i\theta \frac{g^2}{64\pi^2} \epsilon_{\mu\nu\rho\sigma} F^a_{\mu\nu} F^a_{\rho\sigma}, \tag{2.8}$$

where $\mathcal{L}_{QCD}$ stands for the standard expression (1.4), which is both CP conserving and real. In contrast, the second piece in the right hand side of (2.8) breaks CP—as was stressed in the previous section—and, more importantly for the upcoming discussion, is a purely imaginary number.

The topological nature of the θ term has direct physical effects: the vacuum of the theory cannot be constructed as a quantum fluctuation around a classical definite state [97]. Therefore, in order to properly analyze in which way QCD depends on the θ parameter, a non-perturbative approach is required. Under this circumstances, it would seem adequate to deal with the inclusion of the extra term $\mathcal{L}_\theta$ within the lattice regularization formalism. In principle, it would suffice to find a proper discretization for the topological charge Q, and include its effects in the corresponding Monte Carlo algorithm. Inconveniently, this is far from being enough if non-vanishing values of the vacuum angle are to be explored, since the θ term amounts to a complex phase in the action that gives rise to a severe sign problem. Usual importance sampling methods are of no use in this situation, and workarounds need to be found. At present, much of the achieved progress in this topic involves computations of topological quantities at $\theta = 0$, where standard MC methods are still applicable. Although the definition of the topological charge on the lattice is a subtle question, it is possible to compute quantities such as the topological susceptibility χ, even with some difficulties [102]. However, little progress has been achieved in the last decades in what concerns the study of the $\theta > 0$ case.

It is worth noting that the inclusion of the θ term is not the only example of a sign problem being induced by a complex component into the action of QCD. Another major example is given by finite density QCD, which takes place when a non-zero chemical potential term is included into the fermionic matrix—a required addition when considering high baryonic densities. This, in fact, is a relevant scenario which affects several areas. It is needed in the studies of astrophysical objects such as neutron stars. Moreover, in early Universe investigations, dealing with extremely high values of both temperature and density is required. And, last but not least, particle collider facilities reproduce these conditions in heavy ion experiments. Although, thanks to asymptotic freedom, perturbative expansions can offer an insight for some limiting cases—namely high energy, which translates in high T or high μ—and the $\mu = 0$ case is accessible to the standard importance sampling techniques, almost the full $\mu - T$ phase diagram is beyond the reach of these approaches.

In both of the cases above, considering a complex action results in the appearance of a sign problem, which, as it was warned at the beginning of this thesis,

constitutes one of the Millenium problems—in particular one that is not expected to be solved with a positive outcome, which for our interests would be P=NP. Therefore, the community has directed their efforts towards the development of different alternatives that try to evade, or in some cases ameliorate, the sign problem in the systems of interest, i.e., in QCD or QCD-like models. In the next section, we mention some of the more popular strategies, including a brief review of the methods developed by Azcoiti et al [12, 13], which in fact are applied in Chapter 4, when reconstructing the θ dependence of the Schwinger model.

2.3 Trying to overcome the Sign Problem

In order to progress in the study of complex action systems, different methods have been developed over the years. In the cases where the sign problem is mild enough, such as in finite density QCD for small values of the chemical potential μ, several strategies can be followed with success. Perhaps the more straightforward approach is the technique known as *reweighting*. It introduces an auxiliary partition function with non-negative density, which is used to reformulate the expectation value of a given observable—computed in the original ensemble—in terms of other expected values that are to be determined within the auxiliary ensemble. Indeed, this change does not eliminate the problem, since the computational cost of this method escalates exponentially with the volume of the system; however, it is useful when applied to small systems, or in certain regions of the parameter space, such as QCD with a small chemical potential μ, where the effects of the sign problem are far from being severe. In this scenario, alternative approaches include Taylor expansions around $\mu = 0$ and analytic continuations from purely imaginary chemical potential, although its scope is heavily bounded by the presence of a SSP; for an extended discussion on this topic, we recommend the reader [103, 104].

Apart from the above methods, that provide some insight for mild sign problem regions—but fail to deliver otherwise—other procedures that have, in principle, greater scope, have been developed over the last decades. In chronological order, the first is *Complex Langevin*. The original works of Parisi and Klauder proposed to generalize the Langevin equation formalism to the case of a complex-valued distribution [9, 10]. Even when rigorous proofs were lacking—e.g., the existence of a stationary solution was a conjecture—the technique seemed to give correct results in some cases [105]. However, in other systems the algorithm failed to converge, or it did but to the wrong limit [106]. Interest in the method was rebounded when Berges and Stamatescu realized that the instabilities of the Langevin evolution can be dealt with if the stepsize is reduced enough [11]. In fact, using an adaptative stepsize eliminates this problem [107]. Notwithstanding its recent successes, the approach still has some caveats that need to be addressed, since in some scenarios

it continues to converge to a wrong result. Current efforts are devoted to identify under which conditions the proper solution can be reached, and what mechanisms can be used to monitor if the Langevin evolution is to be trusted; for a review on this topic, we refer to [108].

With a special focus on systems with a topological term in the action, a different strategy was proposed by Azcoiti et al in 2002 [12]. In summary, the topological charge dependence on θ is reconstructed from the probability distribution function at $\theta = 0$, which is to be computed from simulations at purely imaginary values of θ, possible since in this case the action becomes real. These results are to be adjusted to a suitable analytical expression that, once integrated, allows to obtain $q(\theta)$ with the help of multiprecision algorithms. This approach proved to work well in a number of systems, including the one dimensional Ising model and the $U(1)$ compact model in two dimensions, giving predictions for CP^3 and, in a later work, for CP^9—a model that, as QCD, exhibits confinement and asymptotic freedom [109]. Nevertheless, the scope of the approach gets hampered by the fact that it cannot reconstruct a non-monotone order parameter [21]. In other words, if a given model breaking CP gets this symmetry restored at $\theta = \pi$, then $q(\theta)$ needs to decrease at some point; in this situation, the method fails to reproduce this behavior and a flattening is observed—which, on the other hand, it is generally avoided in models with (spontaneously) broken symmetry at $\theta = \pi$.

Initially with the aim of crosschecking the above method, an alternative approach, using the same input—i.e., Monte Carlo simulations at imaginary values of the vacuum angle θ—was proposed in 2003 [13]. In this case, an additional assumption needs to be made, namely that in order to reconstruct the full θ dependence, no critical points are allowed, except at most at $\theta = \pi$. This poses a severe obstacle to its applicability in finite density QCD, where a rich phase diagram is expected, but is in principle well adapted to θ QCD, where only one phase transition—if any—is surmised, precisely at $\theta = \pi$ [102]. Besides the later assumption, a particular extrapolation is required, that needs certain observables to vary as slowly as possible. For this reason, the method is expected to work well, among others, in asymptotically free gauge theories. This approach, which has already obtained good results in a variety of models [109–111], has been applied in Chapter 4 to reconstruct the θ dependence of the massive Schwinger model; for a more extensive review, covering the specifics of the actual implementation, we refer the reader to Section 4.3.

Finally, other recent approaches to complex action systems can be mentioned, such as Lefschetz thimbles [14–16] or the density-of-states or LLR method [17–19]. Their details are beyond the scope of this thesis, since their application to QCD with a topological term seems, for now, remote.

Chapter 3

Ising model with a θ term

In this chapter we present our work on the two-dimensional antiferromagnetic Ising model with a purely imaginary magnetic field, which can be interpreted as a toy model for the usual θ physics, and that was published in [28]. Our motivation, as it was anticipated at the beginning of this thesis, is twofold. First, we pretend to provide a benchmark calculation in a system which suffers from a strong sign problem, so that our results can be used to test Monte Carlo methods developed to tackle such problems. In second place, we want to test the predictions of the method developed by Azcoiti et al. [13] regarding this system [21], since its performance with the expected non-trivial phase diagram could entail additional obstacles for its reliable application in other scenarios.

In the forecoming sections, we justify the choice of model and review their fundamentals. Then, we discuss the analytical techniques applied, including the exact computation of the first eight cumulants of the expansion of the effective Hamiltonian in powers of the inverse temperature, which allows to calculate physical observables for a large number of degrees of freedom with the help of standard multi-precision algorithms. Finally, we report accurate results for the free energy density, internal energy, standard and staggered magnetization, and the position and nature of the critical line, which confirm the mean-field qualitative picture of [21], and which should be quantitatively reliable, at least in the high-temperature regime, including the entire critical line.

3.1 Why Ising?

As has been argued along the first chapters of this work, numerical simulation of systems with a severe sign problem is one of the major challenges for high-energy theorists—a statement which is also valid for their solid-state colleagues. If we denote the microscopic states of a given physical system by s, and the thermody-

namics of such system is described by a partition function of the form

$$\mathcal{Z} = \sum_s P(s), \tag{3.1}$$

we say that the system in question presents a sign problem if the "weights" $P(s)$ are not real and positive: This implies that we cannot interpret $P(s)$ as a proper probability distribution, and the standard, efficient Monte Carlo algorithms cannot be applied. Not all sign problems are equally severe. Let us restrict ourselves for simplicity to the case where the $P(s)$ are real but not positive definite[1]. One can easily devise a reweighting algorithm that uses the absolute value $|P(s)|$ as the weight of each state, and shifts the sign of $P(s)$ into the observables. Now a standard Monte Carlo method is applicable, and in the limit of infinite statistics we should obtain the correct result. With finite statistics, however, a key quantity is the thermodynamic average of the sign of each contribution to the partition function, that is, $\langle \mathrm{sign}(P(s)) \rangle$. If this quantity goes to zero exponentially with the volume, $\langle \mathrm{sign} \rangle \propto e^{-\alpha V}$, then we would need an exponential amount (in the volume of the system V) of statistics to get correct results, which is of course impossible in practice. In this case we say that the sign problem is severe.

Beyond QCD at finite baryon density or QCD with a topological term in the action, there exist other physically relevant systems which suffer from a SSP. Some of the most popular examples include chains of quantum spins with antiferromagnetic interactions, the two-dimensional O(3) non linear sigma model with a topological term or the Hubbard model. The existence of a SSP is the main reason for the little progress made on the theoretical understanding of these physical systems outside of phenomenological models.

In order to check novel Monte Carlo methods designed to tackle such problems, it is highly desirable to have a set of benchmark calculations as extensive as possible. For very few systems an analytic solution is known, for example, the one-dimensional antiferromagnetic Ising model with an imaginary magnetic field, the two-dimensional compact U(1) model with topological term, or the two-dimensional Ising model with an imaginary magnetic field $h = i\pi/2$. In a few other cases the sign problem can be avoided by reformulating the physical system with new degrees of freedom, taking advantage of the fact that a good choice of these degrees of freedom provides an equivalent physical system free from the sign problem, which can therefore be simulated by standard methods; see e.g. [112] for a recent discussion on this dualization approach. Unfortunately this idea works only in a few cases which, until now, are not the most interesting physical systems—indeed none of the examples previously mentioned have been solved with this idea.

Within the above scenario, our intention in this work is to provide a benchmark calculation for a system for which we do not have an analytic solution available,

[1]The discussion for complex weights does not add any fundamental difficulty.

nor a reformulation that avoids the sign problem. We study the two-dimensional antiferromagnetic Ising model with a purely imaginary magnetic field, which can be thought of as a toy model for the usual θ physics. Indeed the Euclidean partition function for QCD with a nonvanishing θ term can be written in the form

$$\mathcal{Z}_V(\theta) = \sum_n p_V(n) e^{i\theta n} \tag{3.2}$$

where n, the topological charge, is an integer, and $p_V(n)$ is, up to a normalization, the probability of the topological sector n at $\theta = 0$. This has the same structure as the partition function of the antiferromagnetic Ising model in an external purely imaginary magnetic field, as we will see in detail later on, and we expect that the SSP in both systems should also be similar.

This system was studied in [20] by locating the zeros of the partition function in the complex temperature-magnetic field plane, and they found, for purely imaginary magnetic field, a rich phase structure with two phases characterized by a vanishing (nonvanishing) staggered magnetization, separated by a phase transition line. We study this system by an exact cumulant expansion to eighth order, followed by the analytic computation of the partition function and other physical quantities for a large number of degrees of freedom with the help of a standard multiprecision algorithm. This amounts essentially to the computation of the effective Hamiltonian up to order T^{-8}, and therefore is expected to work well in the high-temperature regime, and we provide strong evidence that this is indeed the case. Our results are consistent with [20], and extend the results of [21], obtained through the application of algorithms developed in [12, 13], and through a mean-field analysis. We are able to obtain a more precise quantitative determination of the transition line separating the paramagnetic and antiferromagnetic phases of the model.

For some systems with a SSP, we know *a priori* that the partition function will be positive, for example systems in thermal equilibrium with a (Hermitian) Hamiltonian description. Such is the case in a quantum field theory with a θ term. In the toy model we study here, although we do not have a rigorous proof in this case,[2] we have evidence that, at least in the region where the approximation we use is valid, the partition function is indeed positive (it is trivially always real).

Such evidence is twofold. First, we can prove rigorously that up to the fifth cumulant, the partition function is indeed positive. Unfortunately we have not been able to extend this proof to higher cumulants, but in our multiprecision calculations with up to eight cumulants, we have never seen an instance where

[2]This would imply a nontrivial restriction on the position of the Lee-Yang zeros for the antiferromagnetic Ising model. To the best of our knowledge, very little is rigorously known about such zeros.

the partition function is negative or vanishes. This is highly nontrivial: If instead of a constant imaginary magnetic field we try, for example, to put a staggered imaginary field in our lattice (this is of course equivalent to the ferromagnetic model with a constant imaginary field), we immediately get a fluctuating sign for the partition function.

Second, there have been studies locating the Lee-Yang zeros of the antiferromagnetic two-dimensional Ising model up to 14^2 lattices [113], and in 12×13 lattices [20]. Up to that size there is no sign of any zeros cutting the imaginary axis at any temperature.

Whereas this by no means amounts to a rigorous proof, we believe it provides a strong indication that, at least in the region of interest for our work, this model should have a positive partition function.

Hereafter, Section 3.2 is devoted to formulate the model and to recall the main ingredients and results of the mean-field approximation developed in [21]. In Sec. 3.3 we introduce the cumulant expansion, report the analytical results for the first eight cumulants in the two-dimensional model, and write the analytical expressions for the free energy and mean values of interesting physical quantities. The results for the staggered magnetization, susceptibility, and phase diagram of the model are reported in Sec. 3.4, where we also compare our results at $h = 0$ and $i\pi/2$ with the analytical solutions of [114–116]. In Sec. 3.5 we report our conclusions. The technical details of the analytical computation of the cumulant expansion can be found in Appendix A.

3.2 Two-dimensional Ising model

The Ising model [20, 114–119] has been studied for a long time now, and it has known analytical solutions in the one-dimensional case at any external magnetic field h [117], and in two dimensions only for the case without magnetic field h [114] and for $h = i\theta/2 = i\pi/2$ [115, 116]. The model with a pure imaginary magnetic field suffers from a SSP in any number of dimensions. In addition to that, the expected phase diagram for $d \geq 2$ is non trivial [21], making the reconstruction of the θ dependence of the observables even more challenging. All this makes the model a good theoretical laboratory to test new methods designed to deal with the SSP. It is therefore worthwhile to carry out a detailed study of this model at purely imaginary magnetic field, particularly because little progress has been achieved on reconstructing the θ dependence of the observables, apart from the analysis of [21] and the recent study in [120].

The partition function of the model, following the conventions of [21], is:

$$\mathcal{Z} = \sum_{\{s_i\}} \exp\left(F \sum_{<ij>} s_i s_j + i\theta \frac{1}{2} \sum_i s_i \right). \tag{3.3}$$

The half magnetization

$$\frac{M}{2} \equiv \frac{1}{2} \sum_i s_i, \tag{3.4}$$

is an integer taking any value between $-N/2$ and $N/2$, where N is an even number denoting the total number of spins in the lattice. It is in this sense that we identify $M/2$ with a topological charge and regard the imaginary magnetic field term in the action as a θ term. It is important to mention that, from now on, we will consider only the antiferromagnetic case $F < 0$, since the model with imaginary field does not define a unitary theory for arbitrary values of the ferromagnetic coupling [115, 121].

As we shall see in detail in the next section, by dividing the rectangular lattice into two sublattices, introducing the respective magnetizations M_1 and M_2, making a cumulant expansion and keeping only the first cumulant, we arrive at the following approximation to the partition function (where d denotes the dimensionality of the lattice):

$$\mathcal{Z}_{1c}(F,\theta) = \sum_{\{s_i\}} \exp\left(i\theta \frac{M_1 + M_2}{2} + 4\frac{Fd}{N} M_1 M_2 \right). \tag{3.5}$$

We recall now the mean-field analysis carried out in [21]. The resulting partition function,

$$\mathcal{Z}_{MF}(F,\theta) = \sum_{\{s_i\}} \exp\left(i\theta \frac{M_1 + M_2}{2} - \frac{Fd}{N} (M_1 - M_2)^2 \right), \tag{3.6}$$

is different from Eq. (3.5). However, it can be seen to give the same qualitative results for the observables and the phase diagram. In this regard, we will consider the first-cumulant expansion $\mathcal{Z}_{1c}$ as a mean-field approximation to $\mathcal{Z}$, and the general expansion itself as an improvement of it, at least for small F, where the expansion is expected to converge.

Applying standard saddle-point techniques to the mean-field partition function [21], one obtains the $F-\theta$ phase diagram shown in Fig. 3.1. A second order critical line,

$$dF_c = \frac{1}{2} \cos^2 \frac{\theta_c}{2}, \tag{3.7}$$

separates two different phases: a staggered one, with $\langle m_s \rangle \neq 0$, for $F > F_c(\theta)$, and a paramagnetic one, with $\langle m_s \rangle = 0$, for $F \leq F_c(\theta)$.

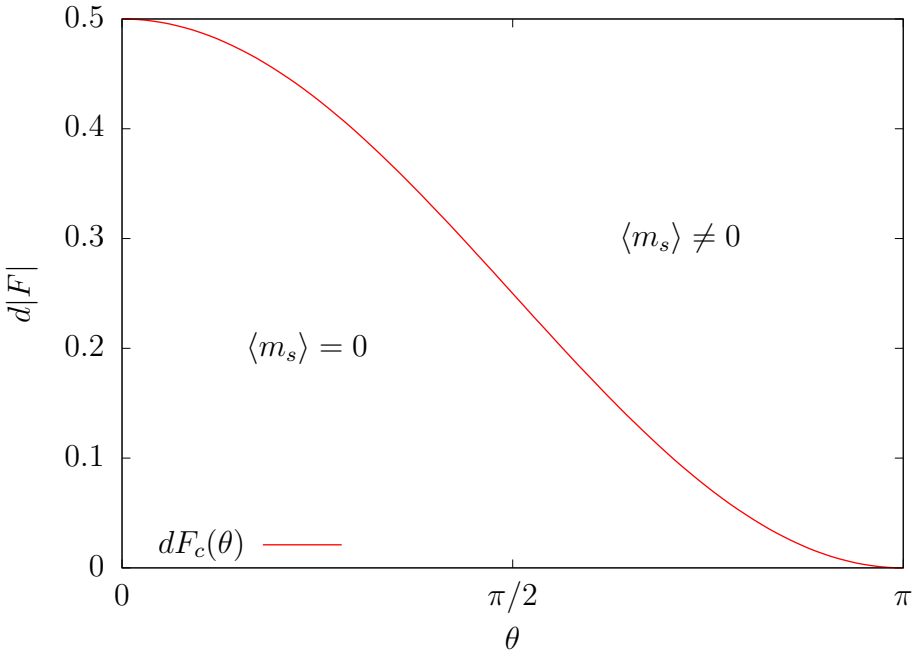

Figure 3.1: Phase diagram of the mean-field approach of [21] to the antiferromagnetic Ising model in the $F - \theta$ plane.

3.3 Cumulant expansion and observables

Our interest is focused on the antiferromagnetic model, where the staggered magnetization is a good order parameter. From now on we will work with a rectangular two-dimensional lattice, although the method is easily generalizable to any number of dimensions. We divide the lattice into two sublattices Ω_1 and Ω_2 in a chessboard fashion. In the two-dimensional lattice this means that if i and j index, respectively, the row and the column of a given spin, this spin will be in the first (second) sublattice if the sum $i + j$ is even (odd). For simplicity we will require both lengths of the lattice to be even. Denoting by N the total number of points in the lattice, we define the magnetization densities m_1 and m_2 as

$$m_j \equiv \frac{M_j}{N/2} \equiv \frac{\sum_{i \in \Omega_j} s_i}{N/2} \qquad j = 1, 2, \tag{3.8}$$

and the density of staggered magnetization is

$$m_s \equiv \frac{m_1 - m_2}{2}. \tag{3.9}$$

Let us denote by $g(m_1, m_2)$ the number of microstates with magnetization

densities m_1 and m_2 in sublattices Ω_1 and Ω_2, respectively, that is,

$$g(m_1, m_2) = \sum_{\{s_i\}} \delta\left(\sum_{i\in\Omega_1} s_i - M_1\right) \delta\left(\sum_{i\in\Omega_2} s_i - M_2\right). \tag{3.10}$$

A trivial computation gives:

$$g(m_1, m_2) = \binom{N/2}{N_{1+}}\binom{N/2}{N_{2+}}, \tag{3.11}$$

with $N_{j+} \equiv N(1+m_j)/4$ for $j = 1, 2$. Now, by restricting ourselves to the set of configurations with given magnetization densities m_1 and m_2, it is straightforward to define the expectation value of a general observable $\mathcal{O}(\{s_i\})$ within this subset—i.e., at fixed m_1, m_2—as:

$$\langle\mathcal{O}\rangle_{m_1,m_2} \equiv \frac{1}{g(m_1,m_2)} \sum_{\{s_i\}} \delta(\sum_{i\in\Omega_1} s_i - M_1)\delta(\sum_{i\in\Omega_2} s_i - M_2)\ \mathcal{O}(\{s_i\}). \tag{3.12}$$

Then, the sum over all possible spin configurations in the original partition function (3.3) can be partially summed up—at least formally—grouping together sectors with equal magnetization densities m_1, m_2. By doing so, and taking into account the above definitions, the reformulated partition function takes the following form:

$$\mathcal{Z} = \sum_{m_1,m_2} g(m_1, m_2) \left\langle \exp\left(i\frac{\theta}{2}\sum_i s_i + F\sum_{<ij>} s_i s_j\right)\right\rangle_{m_1,m_2}. \tag{3.13}$$

The θ term in Eq. (3.13) is just $i\theta\,(m_1+m_2)\,N/4$, and therefore constant at fixed m_1 and m_2; we can take it out of the expectation value, arriving at

$$\mathcal{Z} = \sum_{m_1,m_2} g(m_1, m_2) e^{\frac{1}{4}Ni\theta(m_1+m_2)} \left\langle \exp\left(F\sum_{<ij>} s_i s_j\right)\right\rangle_{m_1,m_2}. \tag{3.14}$$

We cannot evaluate exactly the expectation value in Eq. (3.14), as that would be equivalent to solving exactly the model for arbitrary values of the external field. Instead we perform a cumulant expansion and truncate at a given order. Let us recall the definition:

$$\left\langle e^{tX}\right\rangle \equiv \exp\left(\sum_{n=1}^{\infty} \kappa_n \frac{t^n}{n!}\right), \tag{3.15}$$

where the nth cumulant κ_n is an nth degree polynomial in the first n noncentral moments of X, given by the following recursion formula:

$$\kappa_n = \mu'_n - \sum_{m=1}^{n-1} \binom{n-1}{m-1} \kappa_m \mu'_{n-m}, \qquad \mu'_n \equiv \langle X^n\rangle. \tag{3.16}$$

By expanding in cumulants in our partition function, taking $t = F$ and $X = \sum s_i s_j$, we obtain

$$\mathcal{Z} = \sum_{m_1,m_2} g(m_1,m_2) \exp\left(\frac{1}{4}Ni\theta(m_1+m_2) + \sum_{n=1}^{\infty} \kappa_n(m_1,m_2)\frac{F^n}{n!}\right), \tag{3.17}$$

where now the moments are given by

$$\mu'_n = \left\langle \left(\sum_{<i,j>} s_i s_j\right)^n \right\rangle_{m_1,m_2} . \tag{3.18}$$

The computation of these quantities is somewhat involved, and we relegate the details to Appendix A. We calculate the cumulants using a numerical (but exact) method, up to $n = 8$. The results, at leading order in N[3], for $d = 2$, are

$$\begin{aligned}
\kappa_1 &= 2Nm_1m_2, \\
\kappa_2 &= 2N({m_1}^2-1)({m_2}^2-1), \\
\kappa_3 &= 8Nm_1m_2({m_1}^2-1)({m_2}^2-1), \\
\kappa_4 &= 4N(21{m_1}^2{m_2}^2 - 9({m_1}^2+{m_2}^2)+5) \\
&\quad \times({m_1}^2-1)({m_2}^2-1), \\
\kappa_5 &= 32N(51{m_1}^2{m_2}^2 - 39{m_1}^2 - 39{m_2}^2 + 31) \\
&\quad \times m_1m_2({m_1}^2-1)({m_2}^2-1), \\
\kappa_6 &= 64N(675{m_1}^4{m_2}^4 - 690[{m_1}^4{m_2}^2 + {m_1}^2{m_2}^4] \\
&\quad +705{m_1}^2{m_2}^2 + 75[{m_1}^4 + {m_2}^4 - {m_1}^2 - {m_2}^2] + 8) \\
&\quad \times({m_1}^2-1)({m_2}^2-1), \\
\kappa_7 &= 128N(10935m_1^4m_2^4 - 13950[m_1^4m_2^2 + m_1^2m_2^4] \\
&\quad +3375[m_1^4 + m_2^4] + 17760m_1^2m_2^2 - 4290[m_1^2 + m_2^2] \\
&\quad +1051)m_1m_2(m_1^2-1)(m_2^2-1).
\end{aligned}$$

[3]We can calculate the subleading terms also, but they become irrelevant as we approach the thermodynamic limit.

$$\begin{aligned}\kappa_8 &= 32N(1685565{m_1}^6{m_2}^6 - 2604735[{m_1}^6{m_2}^4 \\ &\quad +{m_1}^4{m_2}^6] + 994455[{m_1}^6{m_2}^2 + {m_1}^2{m_2}^6] \\ &\quad -55125[{m_1}^6 + {m_2}^6] + 4026645{m_1}^4{m_2}^4 \\ &\quad -1541085[{m_1}^4{m_2}^2 + {m_1}^2{m_2}^4] + 85575[{m_1}^4 + {m_2}^4] \\ &\quad +595077{m_1}^2{m_2}^2 - 33663[{m_1}^2 + {m_2}^2] + 2125) \\ &\quad \times(m_1^2 - 1)(m_2^2 - 1) \end{aligned} \tag{3.19}$$

Now we can compute an approximation to the expectation value of any observable that depends on the spin configuration only through the values of the magnetization densities m_1, m_2—i.e., of the form $\mathcal{O}(m_1, m_2)$—as follows:

$$\begin{aligned}\langle\mathcal{O}\rangle &= \frac{1}{\mathcal{Z}}\sum_{m_1,m_2}\mathcal{O}(m_1,m_2)g(m_1,m_2) \\ &\quad \times\exp\left\{i\theta\frac{M_1+M_2}{2} + \sum_{n=1}^{n_{max}}\frac{F^n}{n!}\kappa_n(m_1,m_2)\right\},\end{aligned} \tag{3.20}$$

where $\langle\mathcal{O}\rangle$ depends implicitly on the number of cumulants included in the approximation, n_{max}, and on the number of spins of the system N. Taking the limit of both n_{max} and N to infinity, we should recover the exact result in the thermodynamic limit. Using this technique, we have computed several observables, such as the density of free energy ϕ, the density of internal energy e, the specific heat c_v and both the usual and the staggered magnetization $\langle m\rangle$ and $\langle m_s\rangle$, respectively. The precise definitions of the computed observables are the following:

$$\phi \equiv -\frac{1}{NF}\log\mathcal{Z}, \tag{3.21}$$

$$e \equiv -\frac{1}{2N}\frac{\partial\log\mathcal{Z}}{\partial F}, \qquad c_v \equiv -F^2\frac{\partial}{\partial F}e, \tag{3.22}$$

$$\langle m\rangle \equiv \left\langle\frac{m_1+m_2}{2}\right\rangle, \qquad \langle m_s\rangle \equiv \left\langle\frac{m_1-m_2}{2}\right\rangle. \tag{3.23}$$

It must be noted that at $\theta = \pi$, where the model has an analytical solution, the free energy has a singularity at $F = 0$ [115, 116]. In the next section we will talk about its nonsingular part, which is simply the result of subtracting the singular term from the full expression:

$$\phi \equiv \phi_{ns} - \frac{1}{2F}\log(1 - e^{4F}). \tag{3.24}$$

As we have mentioned before, the complex-valued exponentials in Eq. (3.20) give rise to a severe sign problem. To deal with it we use a multiprecision algorithm, which allows us to keep as many digits as needed. In order to crosscheck our calculations we have used several multiprecision libraries (GMP, GNU MPFR, GNU MPC, gmpy2) to do the sum over m_1 and m_2. The computational cost when computing the observables grows on one hand with N^2 due to the number of summands in (3.20). In addition to that, the number of digits needed grows linearly with N, increasing the cost of each multiprecision operation.

3.4 Results

At $\theta = 0$ and π we know the analytical solution for the two-dimensional Ising model [114–116], and therefore we can compare the exact results with the approximations obtained from Eq. (3.20). We can see in Figs. 3.2 and 3.3 the density of free energy as a function of the coupling $|F|$, for different approximations. Concretely we show the approximations obtained by keeping only the first, up to the fourth, and up to the eighth cumulant. For clarity we show only the results corresponding to the largest size N that we have calculated, although we have carefully checked that the finite-size effects are tiny at that value of N. We can see that the agreement with the exact result, especially for the fourth and eighth approximations, is excellent at small $|F|$, where we can expect the cumulant expansion to be well behaved. At $|F| \gtrsim 0.57$ the approximations start to drift away from the analytic result, especially the eighth, possibly indicating the lack of convergence of the cumulant expansion at such larger couplings.

The above results are consistent with those of the density of internal energy, which we can see in Figs. 3.4-3.6. The same can be said about the specific heat for $\theta = \pi$, in Fig. 3.7. The results of the specific heat for $\theta = 0$, in Fig. 3.8, show also a good agreement with the analytical solution, as long as we are far from the critical point. In the neighborhood of the critical point we can see that keeping a finite number of cumulants has a strong impact. However, the results seem to converge to the exact solution quickly when we increase the number of cumulants, and indeed the peak when including all eight cumulants is not far from the analytic result.

The agreement with the exact results both at $\theta = 0$ and at π suggests that the cumulant expansion can be trusted at all values of θ, as long as $|F| \lesssim 0.57$.

We expect a nonvanishing value of $\langle m_s \rangle$ to signal the transition from the paramagnetic to the staggered phase. Because of translational symmetry, we cannot simply compute this observable, since for a finite N system it is always zero [permuting m_1 and m_2 leaves Eq. (3.20) invariant]. However, we can compute $\langle m_s^2 \rangle$, which also separates the weak and strong coupling phases.

In Fig. 3.9 we show results for $\langle m_s^2 \rangle$ at $\theta = 2$. One can see how, as we approach the thermodynamic limit, $\langle m_s^2 \rangle$ becomes a steeper function of $|F|$. To obtain the critical line for a given cumulant approximation, we numerically calculate the quantity $\frac{d}{d\theta}\langle m_s^2 \rangle$ (which should diverge in the thermodynamic limit at the critical line), and find the maximum along lines of constant θ. This gives us, for each size N and each value of θ, $F_c(\theta)$. We can see in Fig. 3.10 the behavior of such quantity as a function of F and N, for the specific value $\theta = 2$, in the eight cumulant approximation. The height of the peak does not scale as N, at least at the volumes we have been able to calculate, therefore suggesting a continuous phase transition; however, our data are not extensive enough to calculate the critical exponents.

The phase diagram obtained in this way is shown in Fig. 3.11, for several truncation orders of the cumulant expansion. The transition lines that we obtain lie entirely below $|F| = .45$, where we have good evidence that the cumulant expansion works well. The change from the line corresponding to $k = 1$ and 4 is very large, but the results seem to stabilize quickly with the order of the expansion, and the lines corresponding to $k = 4$ and 8 are quite close together. Therefore we expect the phase diagram for $k = 8$ to be a quite accurate approximation to the exact one. Further evidence of this is the agreement with the few maximal values for F_c estimated in [20] from the computation of the zeros of the partition function of the model in the complex temperature-magnetic field plane. As can be seen in the plot, they lie above but quite close to our $k = 8$ line.

As another crosscheck we show in Fig. 3.12 results for the specific heat at $\theta = 2$ in the eight cumulant approximation, computed for several system sizes. The behavior is similar to the one in Fig. 3.10: a peak of increasing height in the vicinity of the critical point, and smooth behavior and small finite N effects elsewhere.

3.5 Conclusions

We have analyzed the two-dimensional antiferromagnetic Ising model with an imaginary magnetic field by analytical techniques. We have calculated the first eight cumulants of what is essentially the expansion of the effective Hamiltonian in powers of the inverse temperature, and computed physical quantities for a large number of degrees of freedom with the help of multiprecision algorithms. The motivation for such a calculation was to have an example of a physical system with SSP and nontrivial phase structure, the dynamics of which is well known, at least in the high-temperature region.

Our results confirm the qualitative picture described in [21], and predict the existence of two phases in this model, which can be characterized by the staggered

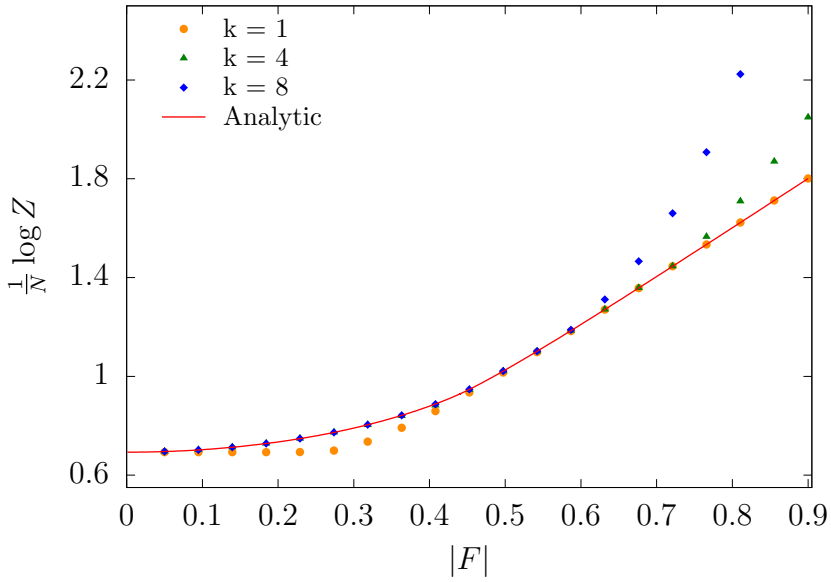

Figure 3.2: Free energy $(-F\phi)$ at $\theta = 0, N = 2000$ for the square-lattice AF Ising model in the kth cumulant approximation.

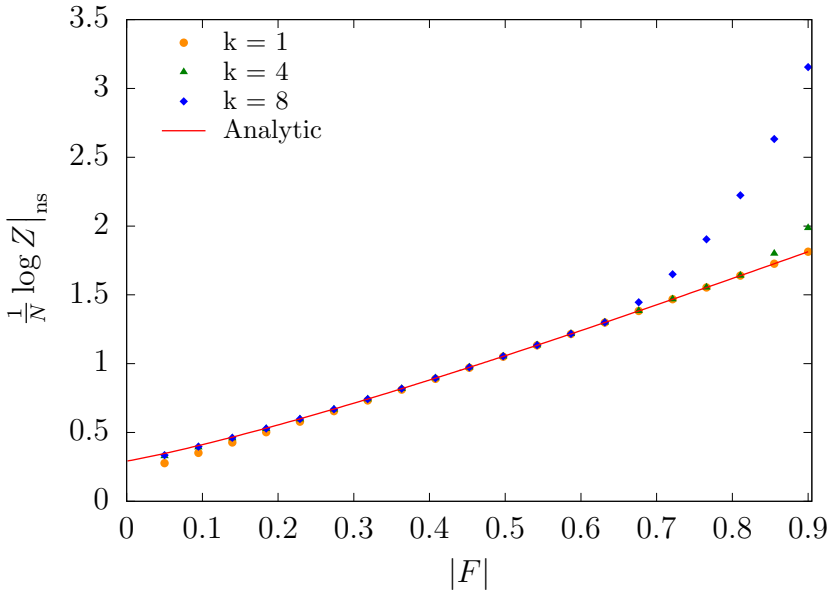

Figure 3.3: Nonsingular part of the free energy $(-F\phi)$ at $\theta = \pi, N = 2000$.

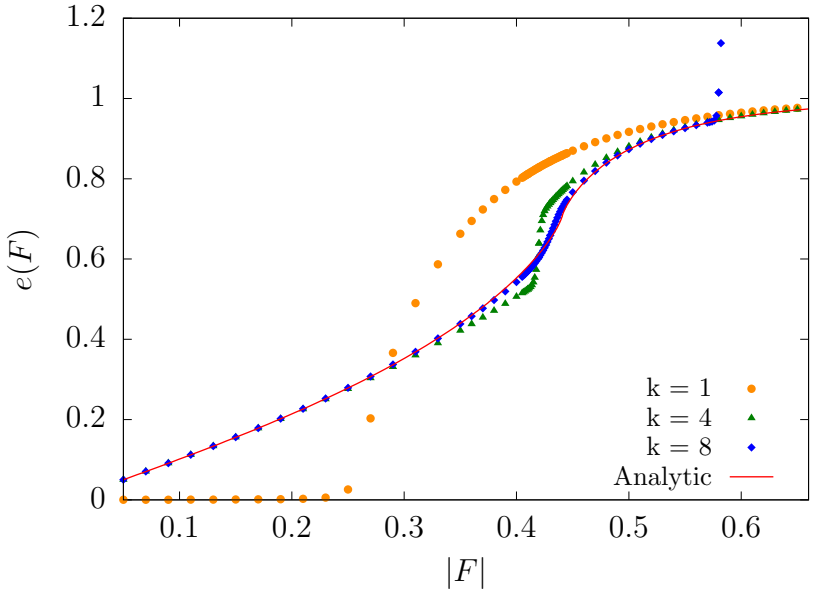

Figure 3.4: Internal energy $e(F)$ computed for one, four, and eight cumulants at $\theta = 0$ and $N = 2000$.

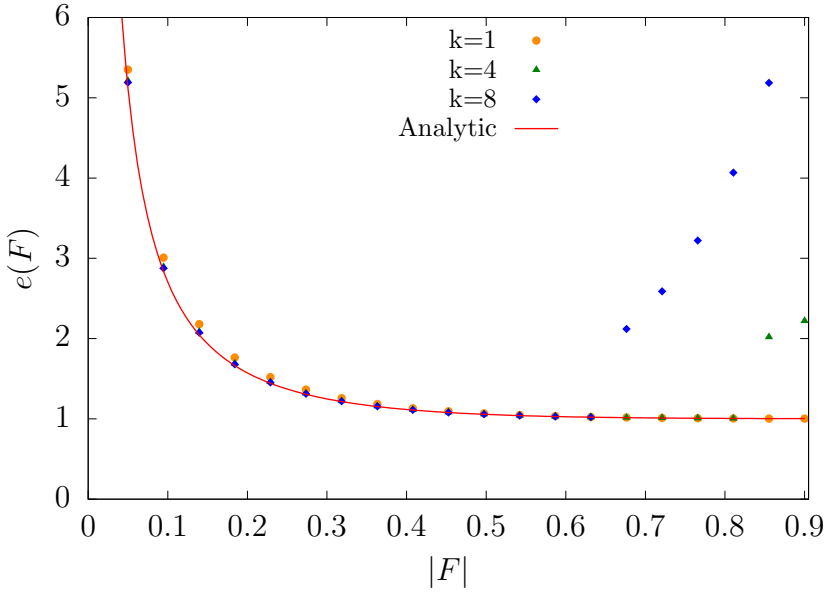

Figure 3.5: Internal energy density $e(F)$ at $\theta = \pi, N = 2000$ at several cumulant expansions.

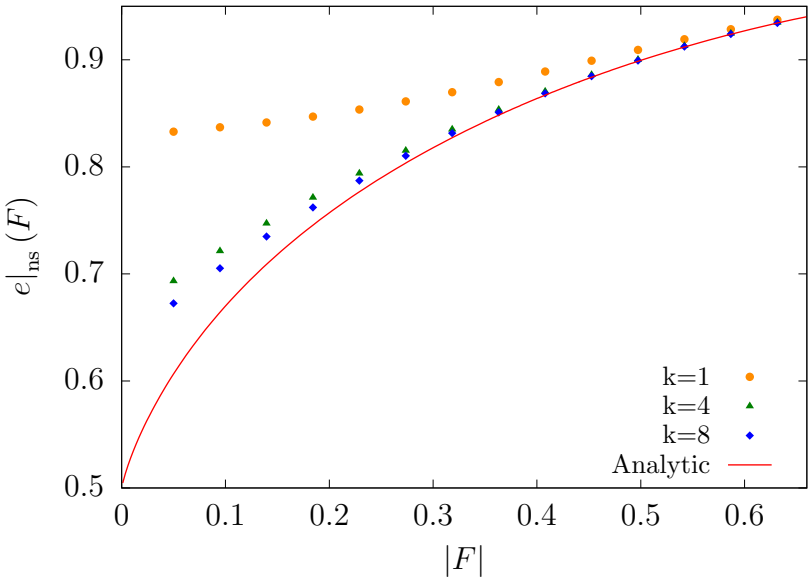

Figure 3.6: Nonsingular part of the internal energy at $\theta = \pi, N = 2000$.

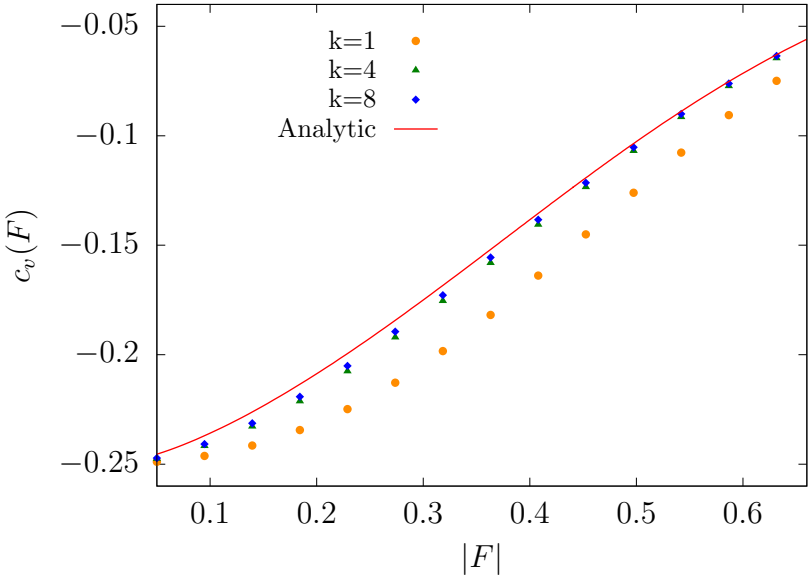

Figure 3.7: Specific heat at $\theta = \pi, N = 2000$, plotted against the analytical expression.

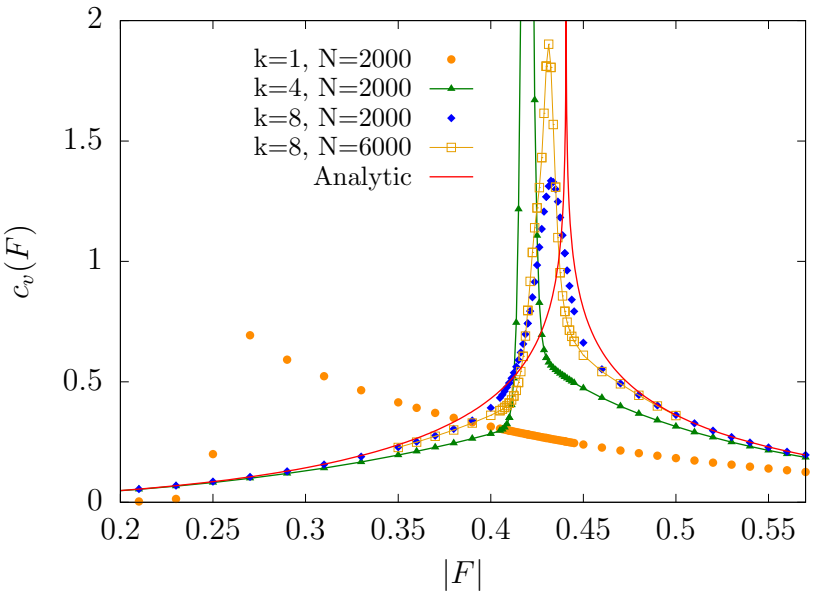

Figure 3.8: Specific heat at $\theta = 0$, plotted against the analytical solution. At $\theta = 0$, $F_c = \log(1+\sqrt{2})/2 \approx 0.4407$.

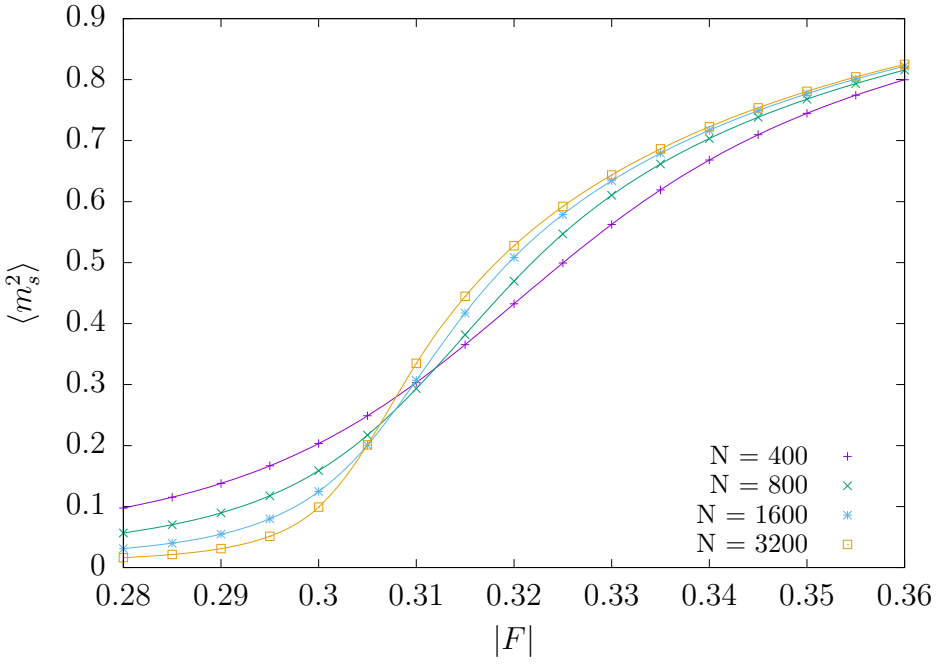

Figure 3.9: $\langle m_s^2 \rangle$ curves at $\theta = 2, k = 8$. Solid lines are just a guide to the eye.

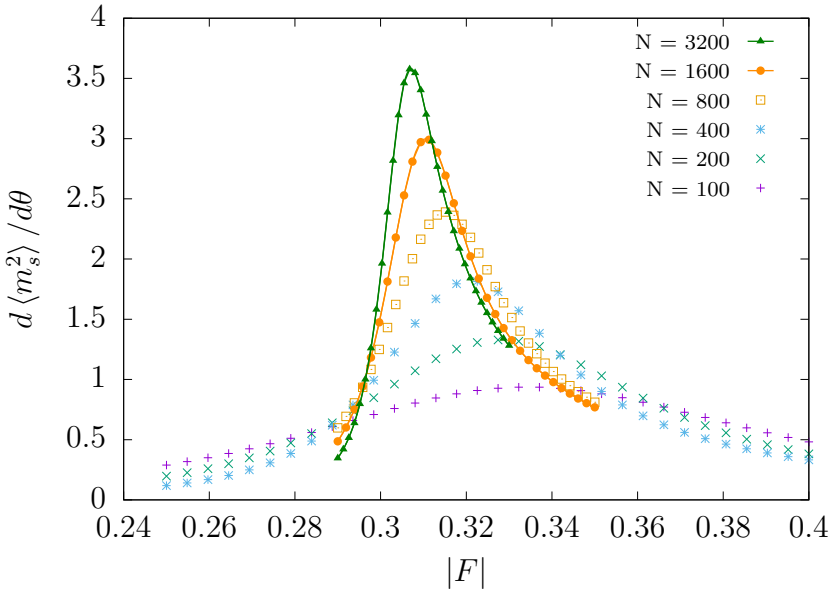

Figure 3.10: Scaling of $d\langle m_s^2\rangle/d\theta$ at $\theta = 2, k = 8$. Solid lines are a guide to the eye.

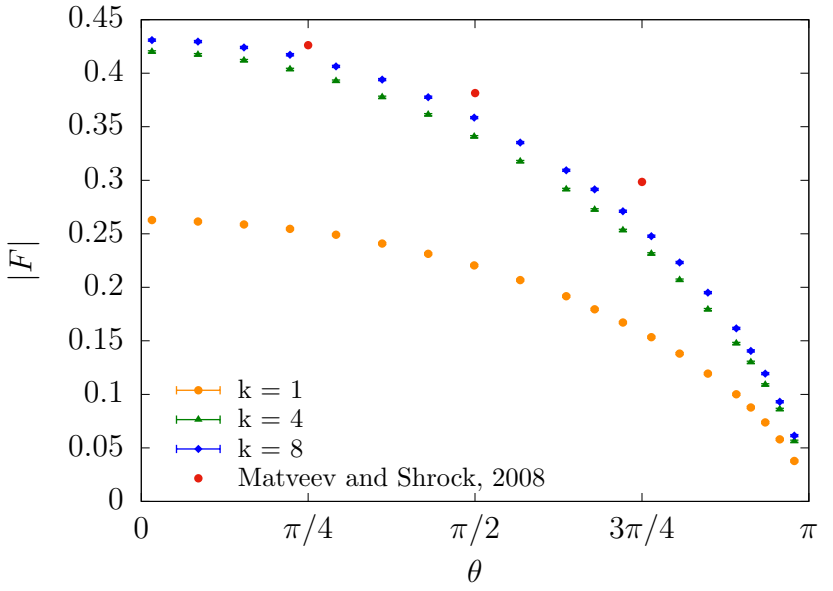

Figure 3.11: The critical line $F_c(\theta)$, computed as the maximum of $d\langle m_s^2\rangle/d\theta$ at $N = 2000$. The maximal F points obtained in [20] are also shown.

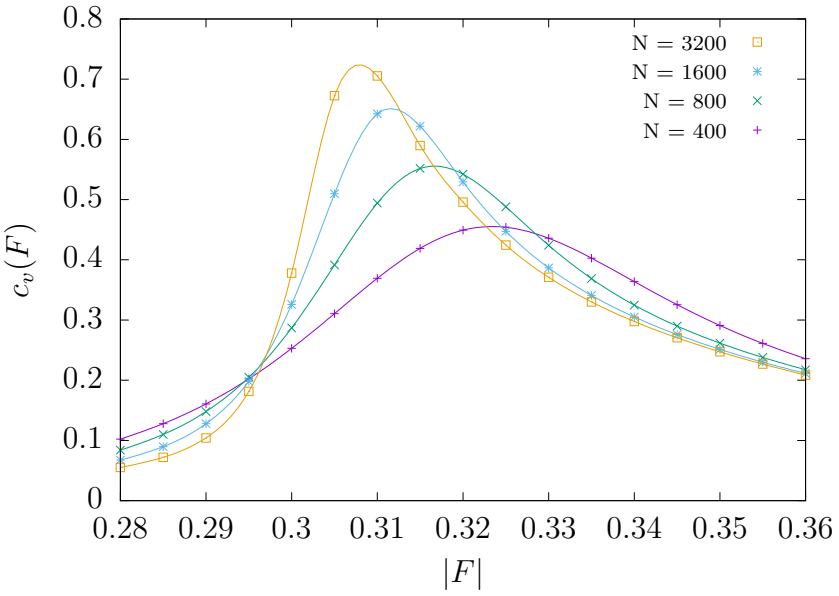

Figure 3.12: Specific heat c_v with $k = 8$ and $\theta = 2$. Solid lines are just a guide to the eye.

magnetization as an order parameter. The finite-size scaling suggests that the two phases are separated by a continuous phase transition line. The position of the critical point at $\theta = 0$ is in very good agreement with the exact result $F_c = \log(1 + \sqrt{2})/2 \approx 0.4407$, and the free and internal energy densities at $\theta = \pi$ agree also well with the analytical prediction, at least in the high-temperature regime, thus giving reliability to our results in this region. Therefore this model could be a good laboratory to check proposals to simulate physical systems afflicted by a SSP. Moreover, we have confirmed that the system under discussion has a more involved phase diagram than in the expected θ QCD case, which would have, at most, a single critical point in $\theta = \pi$. In this sense, the reconstruction method of [13], which when applied in [21] was capable of detecting the presence of a critical region, is strongly supported.

Chapter 4

Massive 1-flavor Schwinger model with a θ term

We analyze here the massive 1-flavor Schwinger model with a θ term and a quantized topological charge. Our work, published in [29], relies on the approach of Azcoiti et al in [13]. We are able to calculate the full dependence of the order parameter with θ in a system that includes dynamical fermions. Moreover, our results at $\theta = \pi$ are compatible with Coleman's conjecture [22] on the phase diagram of this model.

This chapter is organized as follows: after motivating the topic in the first section, we summarize some relevant features of the Schwinger model with a topological term in Sec. 4.2. Since the proposal [13] to analyze physical systems with a topological term in the action has been found to be particularly well suited to bypass the sign problem in asymptotically free gauge theories, we decided to apply it, and Sec. 4.3 contains a brief review of the method. In Sec. 4.4 we give some technical details concerning the lattice setup and the computer simulations performed. Sec. 4.5 shows our results for the topological charge density as a function of θ at several fermion masses and gauge couplings, and finally we end this chapter by reporting our conclusions.

4.1 Motivation

The nature and origin of dark matter constitute one of the most wide open questions in modern physics. To gain some insight in this puzzling problem, it is highly desirable to elucidate the existence of new low-mass, weakly interacting particles from a theoretical, phenomenological and experimental point of view. As was outlined in Chapter 2, the light particle that has gathered the most attention is the axion, predicted by Weinberg and Wilczek [99], and Wilczek [100] in the Peccei and

Quinn mechanism [98] to explain the absence of parity and temporal invariance violations induced by the QCD vacuum. The axion is one of the more interesting candidates to make the dark matter of the universe, and the axion potential, that determines the dynamics of the axion field, plays a fundamental role in this context.

The QCD axion model relates the topological susceptibility χ_T with the axion mass m_a and decay constant f_a through the relation $\chi_T = m_a^2 f_a^2$. The axion mass is, on the other hand, an essential ingredient in the calculation of the axion abundance in the Universe. Therefore, a precise computation of the topological properties of QCD and of their temperature dependence becomes of primordial interest in this context. Understanding the role of the θ parameter in QCD and its connection with the strong CP problem is one of the major challenges for high energy theorists [122].

The calculation of the topological susceptibility in QCD is already a challenge, but calculating the complete potential requires a strategy to deal with the presence of a highly oscillating term in the path integral; in other words, one needs to circumvent a severe sign problem. In fact euclidean lattice gauge theory, our main non-perturbative tool for studying QCD from first principles, has not been able to help us much because of the imaginary contribution to the action coming from the θ term, that prevents the applicability of the importance sampling method [102]. This is the main reason why the only progress in the analysis of the finite temperature θ dependence of the vacuum energy density in pure gauge QCD, outside of approximations, reduces to the computation of the first few coefficients in the expansion of the free energy density in powers of θ [123], and the situation in full QCD with dynamical fermions is, on the other hand, even worse [124–129].

Much experience has been developed in the last years concerning the strengths and weaknesses of the approaches [12,13], which aspire to eventually overcome the sign problem in θ QCD. As a matter of fact, it has been applied successfully to the computation of the vacuum energy density and the topological charge density in a handful of interesting physical systems [21,109–111,130]. Our purpose in the present chapter is to take advantage of this experience to perform a first step in the ambitious program of computing the θ dependence of the QCD vacuum energy density.

Thereby, we analyze the θ dependence of a toy model for QCD, the Schwinger model, on the lattice. Strictly speaking, the Schwinger model in the continuum is not asymptotically free, as QCD, since it is super-renormalizable and the Callan-Symanzik β-function vanishes. However, in the lattice version, since the continuum coupling is dimensionful, the continuum theory is reached at infinite inverse square gauge coupling $\beta = 1/e^2a^2$, much in the same way as four-dimensional asymptotically free gauge theories such as QCD. Furthermore the model is confining [131],

exactly solvable at zero fermion mass, has non-trivial topology and shows explicitly the $U_A(1)$ axial anomaly [132] through a non-vanishing value of the chiral condensate in the chiral limit, in the one-flavor case. These are basically the reasons why this model has been extensively used as a toy model for QCD.

It should be noted that, for two dimensional systems such as the Schwinger model with a θ term, there exist numerical methods such as Hamiltonian methods [133–135] and the Grassmann tensor renormalization group method [136] that have been applied successfully. However, such approaches are currently only applicable to two-dimensional systems, whereas our aim is to test a method that should, in principle, be applicable also to four-dimensional theories such as QCD.

4.2 The massive Schwinger model with a θ term

The Schwinger model is Quantum Electrodynamics in 1+1-dimensions [137]. The euclidean continuum action reads

$$S = \int d^2x \left\{ \bar{\psi}(x)\gamma_\mu \left(\partial_\mu + ieA_\mu(x)\right)\psi(x) + m\bar{\psi}(x)\psi(x) + \frac{1}{4}F_{\mu\nu}^2(x) \right\}, \qquad (4.1)$$

where m is the fermion mass and e is the electric charge or gauge coupling, which has the same dimension as m. After a simple rescaling of the fields the action can be written as

$$S = \int d^2x \left\{ \bar{\psi}(x)\gamma_\mu \left(\partial_\mu + iA_\mu(x)\right)\psi(x) + m\bar{\psi}(x)\psi(x) + \frac{1}{4e^2}F_{\mu\nu}^2(x) \right\}, \qquad (4.2)$$

where $F_{\mu\nu}(x) = \partial_\mu A_\nu(x) - \partial_\nu A_\mu(x)$ and γ_μ are 2×2 matrices satisfying the algebra

$$\{\gamma_\mu, \gamma_\nu\} = 2g_{\mu\nu}. \qquad (4.3)$$

where $g_{\mu\nu}$ stands for the Euclidean metric tensor.

At the classical level this action is invariant in the chiral limit under the $U_A(1)$ global transformations

$$\psi \rightarrow e^{i\alpha\gamma_5}\psi, \qquad (4.4)$$
$$\bar{\psi} \rightarrow \bar{\psi}e^{i\alpha\gamma_5}, \qquad (4.5)$$

leading to the conservation of the axial current

$$J_\mu^A(x) = \bar{\psi}(x)\gamma_\mu\gamma_5\psi(x). \qquad (4.6)$$

However the axial symmetry is broken at the quantum level because of the axial anomaly, as was discussed in detail in Section 1.3.3. The divergence of the axial current is

$$\partial_\mu J^A_\mu(x) = \frac{1}{2\pi}\epsilon_{\mu\nu}F_{\mu\nu}(x), \tag{4.7}$$

with $\epsilon_{\mu\nu}$ the antisymmetric tensor, and therefore does not vanish. The axial anomaly induces a topological θ term in the action of the form

$$S_{top} = \frac{i\theta}{4\pi}\int d^2x\epsilon_{\mu\nu}F_{\mu\nu}(x), \tag{4.8}$$

where the topological charge $Q = \frac{1}{4\pi}\int d^2x\epsilon_{\mu\nu}F_{\mu\nu}(x)$ is an integer.

Our purpose is then to analyze the θ dependence of the model described by the action (4.2)+(4.8)

$$S = \int d^2x \left\{ \bar{\psi}\gamma_\mu \left(\partial_\mu + iA_\mu\right)\psi + m\bar{\psi}\psi + \frac{1}{4e^2}F^2_{\mu\nu} + \frac{i\theta}{4\pi}\epsilon_{\mu\nu}F_{\mu\nu} \right\}. \tag{4.9}$$

A simple analysis of this model on the lattice suggests that it should undergo a phase transition at some intermediate fermion mass m and $\theta = \pi$, even at finite lattice spacing. Indeed the lattice model is analytically solvable in the infinite fermion mass limit (pure gauge two-dimensional electrodynamics with topological term) [138, 139], and it is well known that the density of topological charge approaches a non-vanishing vacuum expectation value at $\theta = \pi$ for any value of the inverse square gauge coupling β, exhibiting spontaneous symmetry breaking. On the other hand by expanding the vacuum energy density in powers of m, treating the fermion mass as a perturbation [140], one gets for the vacuum expectation value of the density of topological charge the following θ dependence:

$$\langle -iq\rangle = m\Sigma sin\theta + \frac{1}{2}m^2\sin\left(2\theta\right)\left(\chi_P - \chi_S\right) + \cdots, \tag{4.10}$$

with Σ the vacuum expectation value of the chiral condensate in the chiral limit and at $\theta = 0$ ($\Sigma = e^{\gamma_e}e/2\pi^{3/2}$ in the continuum limit), and χ_P and χ_S the pseudoscalar and scalar susceptibilities respectively. Equation (4.10) shows how the Z_2 symmetry at $\theta = \pi$ is realized order by order in the perturbative expansion of the topological charge in powers of the fermion mass m, and therefore a critical point separating the large and small fermion mass phases is expected.

Indeed the model was analyzed in the continuum by Coleman in [22], where he conjectured the existence of a phase transition at $\theta = \pi$, and some intermediate fermion mass m separating a "weak coupling" phase ($\frac{e}{m} << 1$), where the Z_2 symmetry of the model at $\theta = \pi$ is spontaneously broken, from a "strong coupling" phase ($\frac{e}{m} >> 1$) where the Z_2 symmetry is realized in the vacuum. This

conjecture was corroborated in [133, 134] using the lattice Hamiltonian approach with staggered fermions, and more recently in [136] using the Grassmann tensor renormalization group and Wilson fermions.

4.3 Computing the order parameter as a function of θ

To compute the θ dependence of the density of topological charge we use the approach proposed in reference [13]. The only assumption in this approach is the absence of phase transitions at real values of θ except at most at $\theta = \pi$. The method is based in extrapolating a suitably defined function to the origin. This function turns out to be very smooth in all the cases considered up to now [21, 109–111], and this makes us confident on the whole procedure. Here we summarize the main steps.

From numerical simulations of our physical system at imaginary values of $\theta = -ih$ (real values of h), which are free from the severe sign problem, we compute the density of topological charge $q(-ih)$ as a function of h, and introduce the following functions:

$$z = \cosh \frac{h}{2}, \tag{4.11}$$

$$y(z) = \frac{q(-ih)}{\tanh \frac{h}{2}}. \tag{4.12}$$

The procedure to find out the density of topological charge at real values of θ relies on scaling transformations [13]. We define the function $y_\lambda(z)$ as

$$y_\lambda(z) = y\left(e^{\frac{\lambda}{2}} z\right). \tag{4.13}$$

For negative values of λ, the function $y_\lambda(z)$ allows us to calculate the order parameter $\left(\tanh \frac{h}{2}\, y(z)\right)$ below the threshold $z = 1$. If $y(z)$ is non-vanishing for any positive z,[1] then we can plot y_λ/y against y. Furthermore, in the case that y_λ/y is a smooth function of y close to the origin, then we can rely on a simple extrapolation to $y = 0$. Of course, a smooth behavior of y_λ/y cannot be taken for granted; however no violations of this rule have been found in the exactly solvable models.

[1] Even though the possibility of a vanishing $y(z)$ for some value $z > 0$ cannot be completely excluded, it does not happen for any of the analytically solvable models we know.

The behavior of the model at $\theta = \pi$ can be ascertained from this extrapolation. At $\theta = \pi$ the model has the same Z_2 symmetry than at $\theta = 0$. We can define an effective exponent γ_λ by

$$\gamma_\lambda = \frac{2}{\lambda} \ln \left(\frac{y_\lambda}{y} \right). \tag{4.14}$$

As $z \to 0$, the order parameter $\tan \frac{\theta}{2}\, y \left(\cos \frac{\theta}{2} \right)$ behaves as $(\pi - \theta)^{\gamma_\lambda - 1}$. Therefore, a value of $\gamma_\lambda = 1$ implies spontaneous symmetry breaking at $\theta = \pi$. A value between $1 < \gamma_\lambda < 2$ signals a second order phase transition, and the corresponding susceptibility diverges. Finally, if $\gamma_\lambda = 2$, the symmetry is realized (at least for the selected order parameter), there is no phase transition and the free energy is analytic at $\theta = \pi$.[2]

We can take the information contained in the quotient $\frac{y_\lambda}{y}(y)$, and calculate the order parameter for any value of θ through an iterative procedure [13]. The outline of the procedure is the following:

- Beginning from a point $y(z_i) = y_i$, we find the value y_{i+1} such that $y_\lambda = y_i$. By definition, $y_{i+1} = y\left(e^{\frac{-\lambda}{2}} z_i \right)$.
- Replace y_i by y_{i+1}, and start again.

The procedure is repeated until enough values of y are know for $z < 1$ (see Fig. 4.1). This method can be used for any model, as long as our assumptions of smoothness and absence of singular behavior are verified during the numerical computations. The reliability of our approach in practical applications is better when the following conditions are met:

1. $y(z)$ takes small values for values of z of order 1.
2. The dependence on y of the functions y_λ / y and γ_λ is soft enough to allow a reliable extrapolation.

In the one-dimensional Ising model within an imaginary magnetic field these two properties are realized in the low temperature regime [13], and the two and three-dimensional models also show a very good behavior in this regime [21]. Indeed the relevant feature, at least in what concerns point 1, is that, at low temperatures, the magnetic susceptibility at small values of the real external magnetic field takes small values. In the more interesting case of asymptotically free models, the analogue of the magnetic susceptibility is the topological susceptibility, and it is well known that topological structures are strongly suppressed near the continuum

[2] Other possibilities are allowed, for instance, any $\gamma_\lambda > 1, \quad \gamma_\lambda \in \mathbb{N}$ leads to symmetry realization for the order parameter at $\theta = \pi$ and to an analytic free energy. If γ_λ lies between two natural numbers, $p < \gamma_\lambda < q, \quad p, q \in \mathbb{N}$, then a transition of order q takes place.

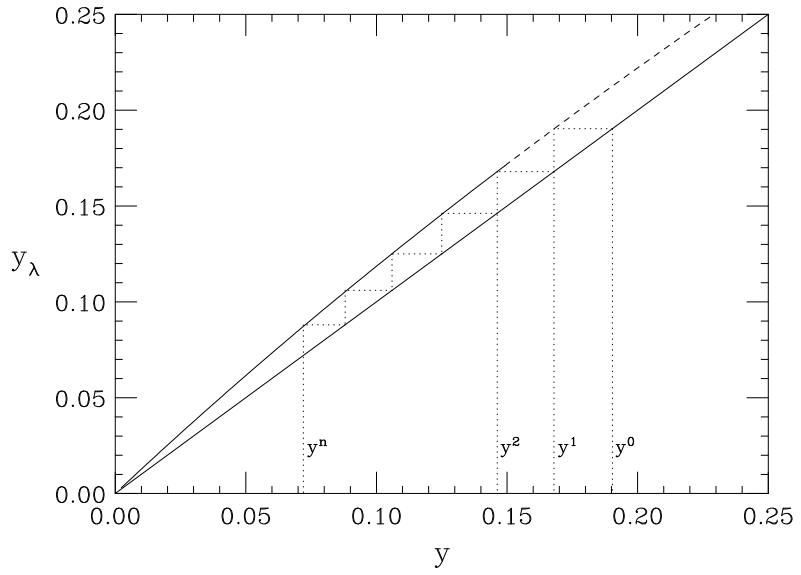

Figure 4.1: Iterative method used to compute the different values of $y(z)$. y_λ is plotted as a function of y using a dashed line in the region where direct measurements are available, and a continuous line in the extrapolated region. The straight continuous line represents $y_\lambda = y$. Reproduced from [13].

limit. Therefore, and on qualitative grounds, we expect a good implementation of our method in the Schwinger model or in QCD, at least close enough to the continuum limit.

The high reliability of this method has been tested in several models. In reference [13], where the approach was proposed, the θ-dependence of the density of topological charge in CP^3 was computed at $\beta = 0.4$ on 100×100 lattices, and the numerical results were compared with the corresponding results obtained from a completely independent method, the one proposed in [12], based on the computation of the probability distribution function of the density of the topological charge, finding a perfect agreement between the two independent approaches. In [109] the two independent methods [12, 13] were also applied to the analysis of the θ dependence of the CP^9 model. The results of the two methods were again in agreement within statistical errors at the % level. Furthermore a very good agreement of the scaling of the density of topological charge with the prediction of the

renormalization group equation was also found in [109], this being the strongest indication that the continuum θ dependence of CP^9 was fully reconstructed and that CP symmetry is spontaneously broken at $\theta = \pi$, as predicted by the large N expansion. In [110] the method described in this section was applied to the analysis of the critical behavior of CP^1 at $\theta = \pi$, finding a region outside the strong coupling regime where Haldane's conjecture [141] is verified. Lastly, in [111], the critical behavior at $\theta = \pi$ of the two-dimensional $O(3)$ nonlinear sigma model with topological term on the lattice was investigated, also using the method described in this section; the results were compatible with a second-order phase transition, with the critical exponent of the $SU(2)_1$ Wess-Zumino-Novikov-Witten model, for sufficiently small values of the coupling.

All these results show the high reliability of [13], especially when applied to asymptotically free theories, or in the weak coupling regime. However since this chapter deals with the Schwinger model, we want to add a new test of our method intimately related to this model. It is well known that pure gauge compact electrodynamics in two dimensions with a topological term can be analytically solved on a lattice of infinite extent [138, 139]. In Fig. 4.2 we plot our results for the topological charge density of this model against the θ-parameter, obtained using our method, in a 20×20 lattice, and $\beta = 4$. The continuous line shows the analytical result in the thermodynamic limit. As can be seen the agreement is very good.

4.4 Details of the simulation

We use the lattice version of the continuum action (4.9) with staggered fermions and standard Wilson form for the pure gauge part. It reads as follows,

$$\begin{aligned} S &= \frac{1}{2}\sum_{n,\mu}\eta_\mu(n)\bar{\chi}(n)\{U_\mu(n)\chi(n+\hat{\mu}) \\ &\quad -U_\mu^\dagger(n-\hat{\mu})\chi(n-\hat{\mu})\} + m\sum_n \bar{\chi}(n)\chi(n) \\ &\quad -\beta\sum_n Re\left(U_1(n)U_2(n+\hat{1})U_1^\dagger(n+\hat{2})U_2^\dagger(n)\right) \\ &\quad -i\theta\sum_n q(n), \end{aligned} \tag{4.15}$$

where the notation is standard. The compact gauge variable $U_\mu(n)$ is related to the non-compact gauge field $A_\mu(n)$ in the usual way

$$U_\mu(n) = e^{iaA_\mu(n)} = e^{i\phi_\mu(n)}, \tag{4.16}$$

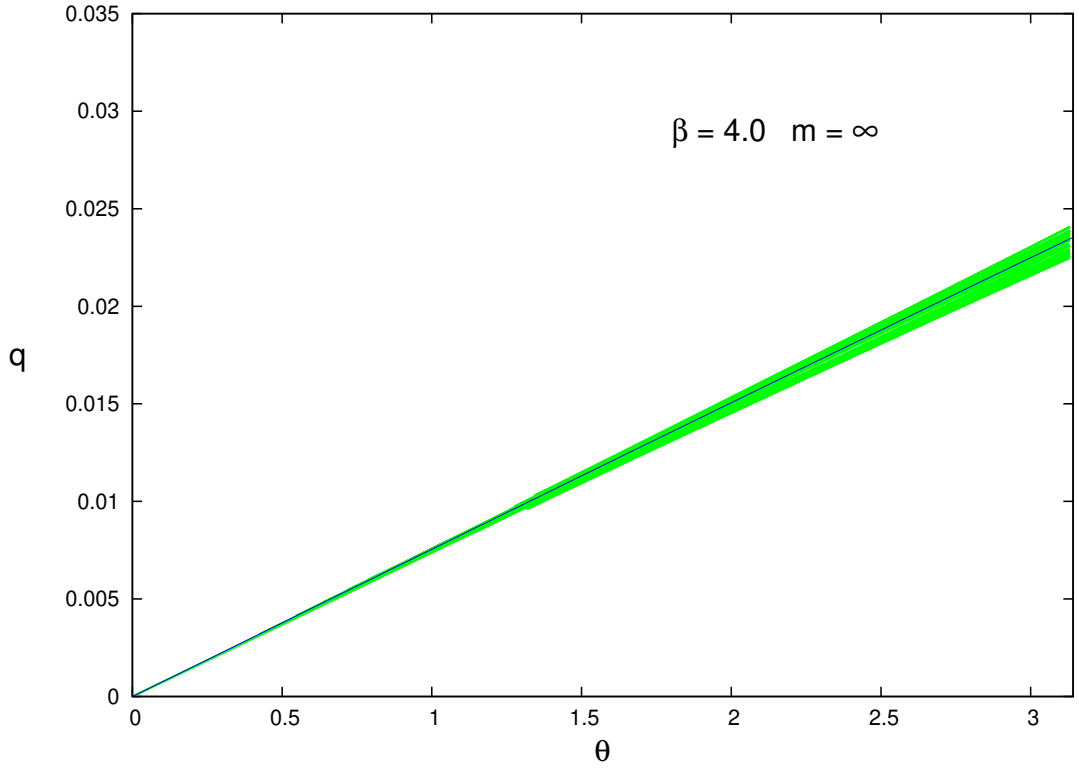

Figure 4.2: Order parameter as a function of θ for $\beta = 4.0$ in the pure gauge theory, $m \to \infty$. The continuous blue line is the exact result.

with a the lattice spacing, and the local topological charge $q(n)$ is given by

$$\begin{aligned} q(n) &= \frac{1}{2\pi}\left(\phi_1(n) + \phi_2(n+\hat{1})\right. \\ &\quad \left. - \phi_1(n+\hat{2}) - \phi_2(n) \ \ mod\ 2\pi\right). \end{aligned} \tag{4.17}$$

An important point is that this charge is quantized, and therefore the partition function of the model has exact 2π periodicity in θ, as is the case in the continuum theory.[3]

We will analyze in what follows the model given by action (4.15), taking the square root of the fermion determinant in order to describe only one flavor. There is ample evidence that this procedure leads to the correct physics in the continuum limit, including the effects of the anomaly. For example, the Microcanonical Fermion Average (MFA) approach [143] was applied years ago to simulate the one-flavor Schwinger model on the lattice at $\theta = 0$, using the standard Wilson

[3]This is an important difference with the approach in [142], which makes a comparison with our results at finite lattice spacing difficult.

action for the gauge field and staggered fermions. The results [144] reproduce the exact value of the chiral condensate in the chiral continuum limit up to 3 decimal places.[4]

As explained in Sec. 4.3, in order to find the dependence on θ of the density of topological charge q, we need to compute the expected value of q for imaginary values of θ. In this case standard Monte Carlo algorithms work well, and we can sample the distribution e^{-S} generated by (4.15) with any of these methods. We have used a standard Metropolis approach, trying to update each link sequentially in every sweep.

We want to use an exact Monte Carlo method, and the fermionic part of the action forces us to recompute the whole fermion determinant at each attempt to update one link, that is, N times each sweep. Indeed, this is the most expensive part of the algorithm. All our lattices are of size 16×16, and we computed the eigenvalues of the fermion matrix with the GNU Scientific Library, taking advantage of the standard even-odd decomposition of the staggered fermions Dirac operator. The simulations have been run at the U-LITE computer facility at the INFN National Laboratories of Gran Sasso.

We present in the following section results for several masses m, gauge couplings β, and fields h (imaginary θ). At each point of the parameter space, we run the algorithm and take up to 100k measurements, each one made every ten sweeps. For the $\beta = 3, m = 0.05$ case, where more precision was needed, nine independent runs were performed. Between 5-10% of the initial configurations are discarded for thermalization. The errors of the expected values are estimated by a standard jackknife binning.

4.5 Results

Our results for the exponent γ are summarized in Figures 4.3 and 4.4. As is apparent in Fig. 4.3, the behavior at fixed β is very different as we vary the fermion mass. The data corresponding to $m = 0.5$ lie essentially on top of the analytic $m = \infty$ curve (that is, pure gauge theory [139]), and therefore this mass corresponds to the phase with broken symmetry at $\theta = \pi$. On the other hand, the data for both the $m = 0.05$ and the $m = 0$ case extrapolate to a value clearly above 1, indicating symmetry restoration at $\theta = \pi$, although our data are not precise enough to make a definite statement on the value of γ. In Fig. 4.4 we present the results at fixed $m = 0$ for the various coupling constants we have studied. We see as before a clear extrapolation to a value of γ above 1,[5] in stark contrast with the pure gauge theory case.

[4] See also [145, 146].

[5] This is also the case for $\beta = 3$, $m = 0.05$, which is not shown in these figures.

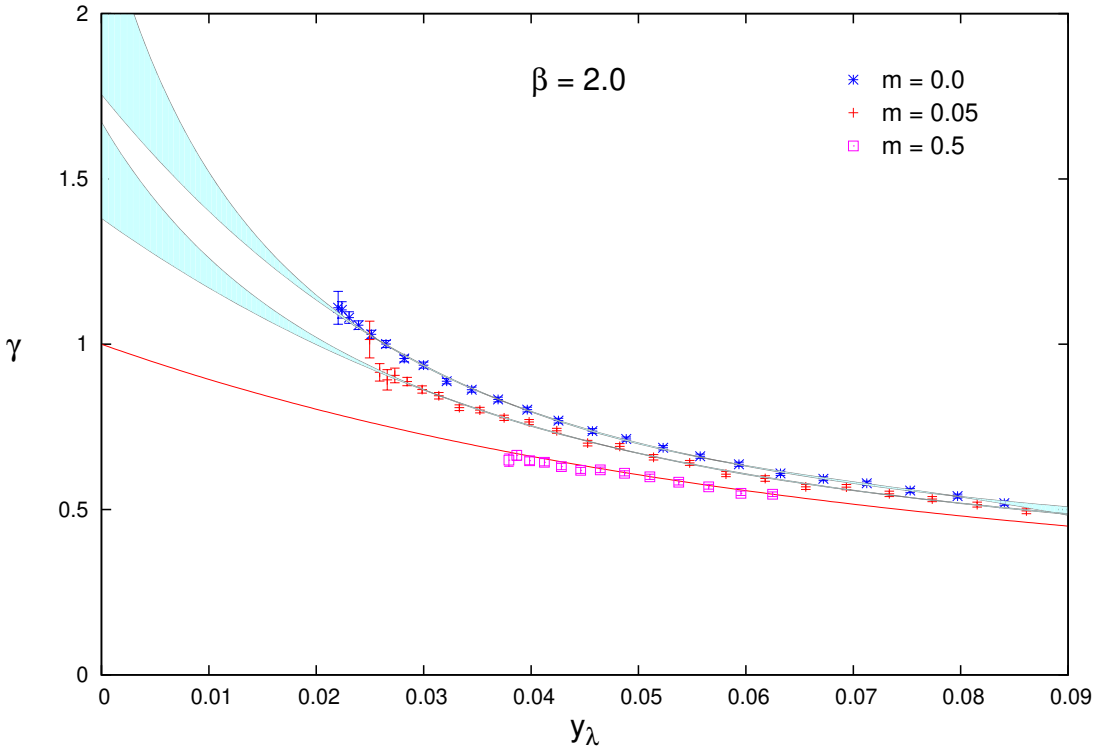

Figure 4.3: Exponent γ for $\beta = 2.0$ and various fermion masses. The shaded areas give an estimation of the ambiguity in the extrapolation to $y_\lambda = 0$. The continuous red line is the analytic result in the pure gauge theory.

We have also been able to extract the full dependence of the order parameter as a function of the angle, $q(\theta)$. In Fig. 4.5 we show details of the fit y versus y_λ for a particular value of the parameters, in order to give an idea of the precision of our data. This will be followed by the iterative procedure depicted in Sec. 4.3 in order to produce the curve $q(\theta)$. Regarding the error estimation, it is impossible to follow the error propagation from the values of q at imaginary θ to the final result of $q(\theta)$. To overcome this impasse we proceed in the following way: first we generate 20 sets of synthetic data for $q(h)$ having the same mean value and distribution of the actual Monte Carlo data; then we compute, following the same scheme (fit of y vs. y_λ and iterative procedure), 20 realization of $q(\theta)$; from the distribution of these values around the curve computed from the real data, we can infer the error associated to each value of $q(\theta)$, which will be shown in the following figures as a shaded band. Moreover, for the $\beta = 3, m = 0.05$ case, where we have data from several independent runs, we have also done the analysis in a different way: we divide the data into four independent sets, and we analyze each set independently.

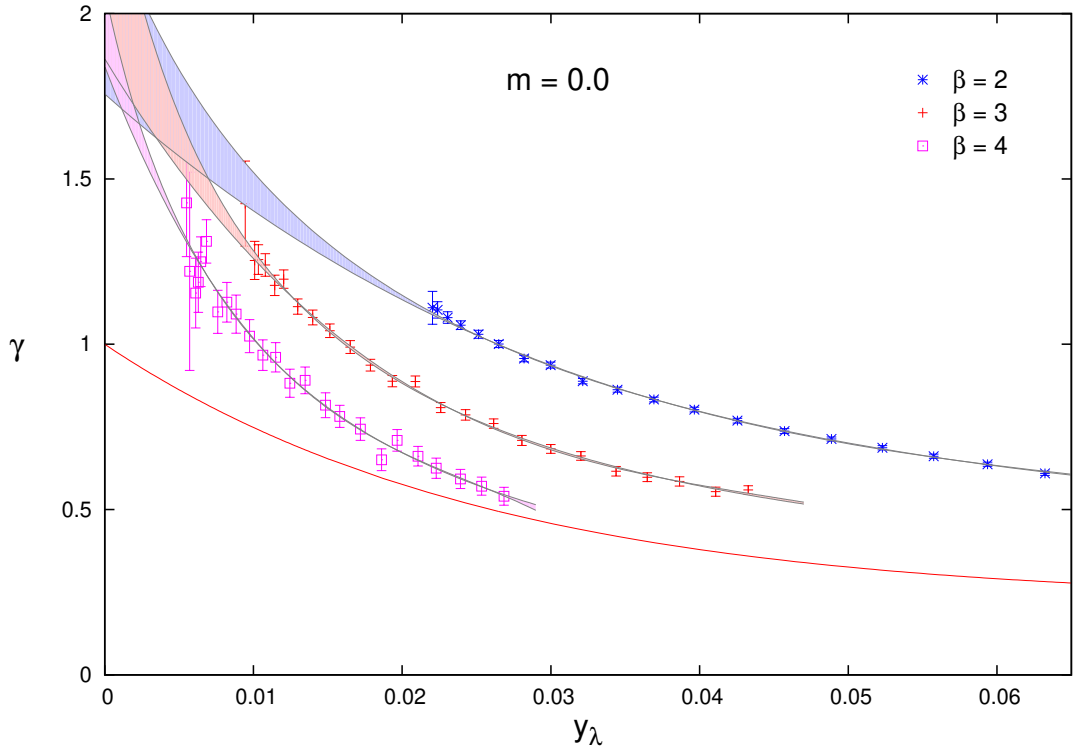

Figure 4.4: Exponent γ for $m = 0.0$ and various coupling constants. The shaded areas give an estimation of the ambiguity in the extrapolation to $y_\lambda = 0$. The continuous red line is the analytic result in the pure gauge theory, corresponding to infinite fermion mass.

We plot in Fig. 4.6 the results of each of the independent analysis for an interval of θ. As can be seen, the errors we would obtain by averaging the independent points are fully consistent with the synthetic-data estimation.

In Fig. 4.6 we present $q(\theta)$ at $\beta = 3$ for two masses in the symmetry restored phase, as well as at $\beta = 2$ and $m = 0.5$, in the symmetry broken phase (and also the corresponding analytic results for the pure gauge case at both values of β for comparison).

In Fig. 4.7 we show the results for $m = 0$ and the three different values of the coupling constant we have simulated. We can clearly see the restoration of the symmetry as we approach $\theta = \pi$. In Fig. 4.8 we show, for $\beta = 3.0$ and $m = 0$, the order parameter $q(\theta)$ in the vicinity of $\theta = \pi$. Fitting $q(\theta)$ near $\theta = \pi$ in the symmetry restored phase allows us to extract the exponent $(\pi - \theta)^\epsilon$, which is related to γ by $\epsilon = \gamma - 1$.[6] We present in Table 4.1 our results for ϵ.

[6]The numerical procedure used to extract the two exponents is different, and therefore the

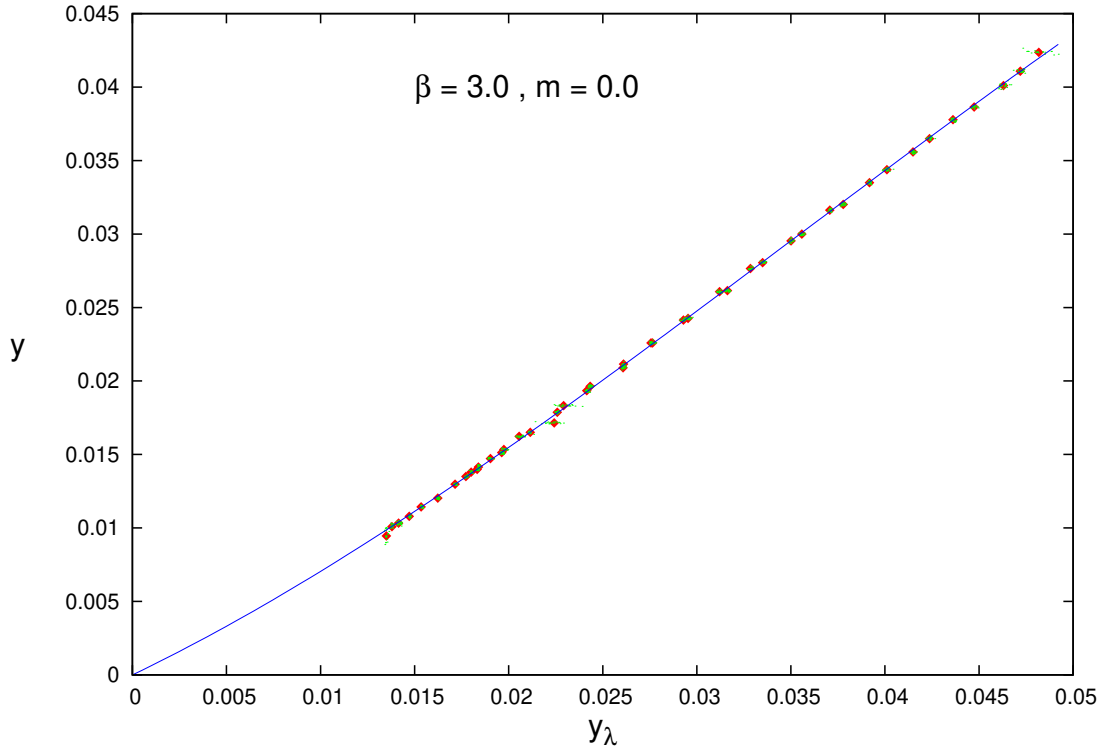

Figure 4.5: Fit of y versus y_λ.

Table 4.1:

β	m	ϵ
2.0	0.0	0.67(4)
2.0	0.05	0.43(5)
3.0	0.0	0.92(7)
3.0	0.05	0.70(21)
4.0	0.0	0.94(19)

To finish this Sec. we want to discuss a little bit more on the results for the massless Schwinger model reported in Fig. 4.7. It is well known that the continuum formulation of the massless Schwinger model shows no θ dependence, because the θ term in the action can be canceled by an anomalous chiral transformation which

results, although compatible within errors, will also be different.

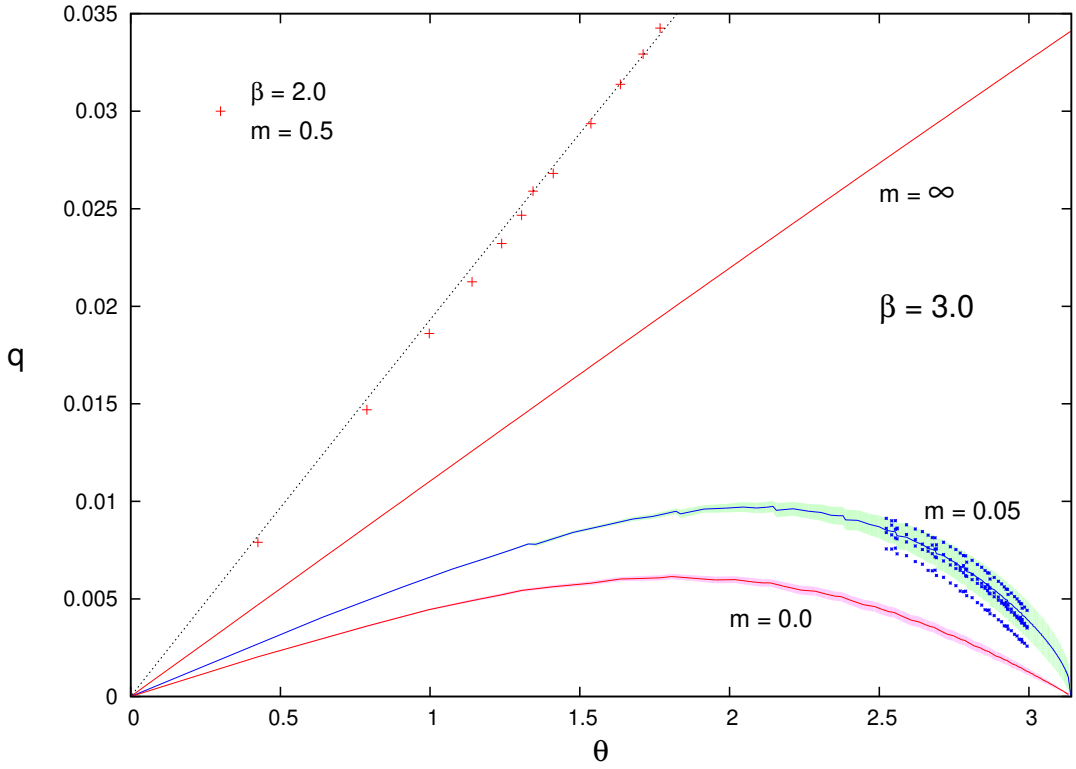

Figure 4.6: Order parameter as a function of θ. The data at $m = 0.0$ and $m = 0.05$ correspond to $\beta = 3.0$, whereas the points at $m = 0.5$ correspond to $\beta = 2$. Blue points, corresponding to the results of four independent runs, are also shown, to provide a different estimate of the error. The continuous line labeled $m = \infty$ is the pure gauge analytic result for $\beta = 3.0$, whereas the dotted line is the corresponding analytic result for $\beta = 2.0$.

does not change the fermion-gauge action if the fermion mass vanishes. Hence the non-trivial θ dependence of the density of topological charge shown in Fig. 4.7 may seem surprising. However, the massless staggered Dirac operator does not have exact zero-modes, and therefore, for a given gauge configuration, a nonzero value of the quantized topological charge Q does not imply the existence of a corresponding number of zero-modes in the staggered Dirac operator, as would be the case, for example, with the overlap Dirac operator. What we should expect instead is that, as we approach the continuum limit, the topological charge density vanishes. This is indeed what seems to happen, as is suggested by Fig. 4.9.

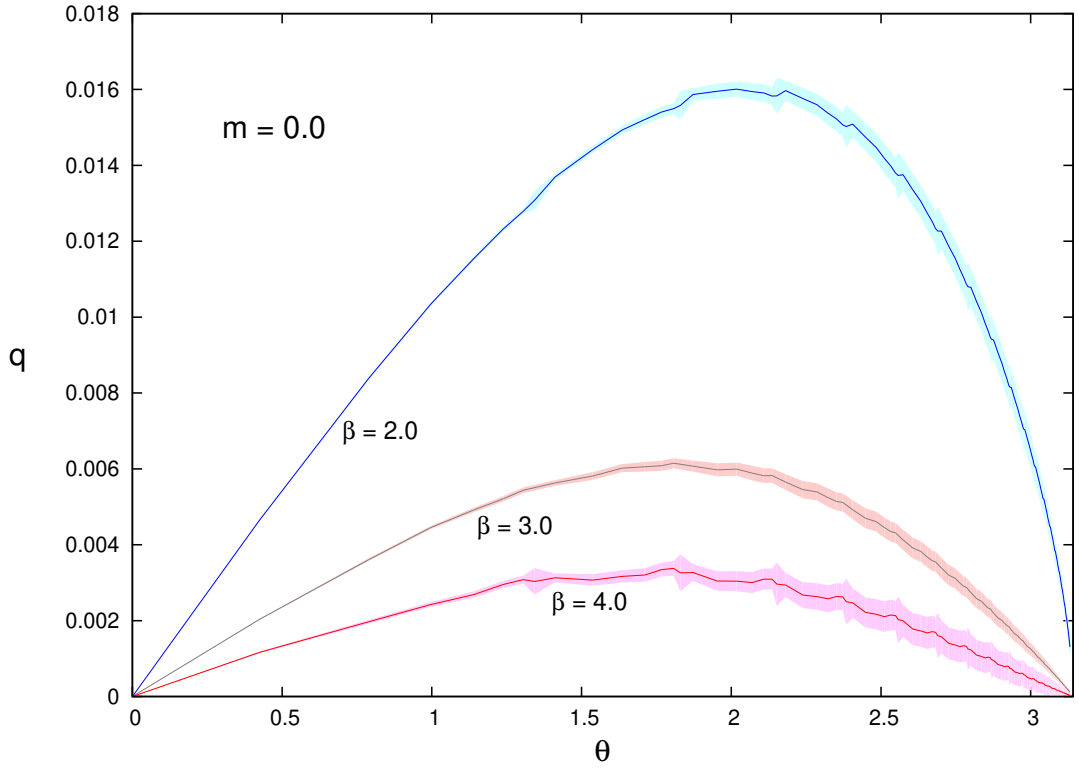

Figure 4.7: Order parameter as a function of θ, at $m = 0.0$ and different coupling constants.

4.6 Conclusions and outlook

All our results are compatible with the standard lore on this model, and in particular with Coleman's conjecture on the existence of two distinct phases at $\theta = \pi$, a symmetry breaking phase at large mass, and a symmetry restored phase at small mass.

Our simulations are a proof of concept, and are not extensive enough to determine precisely the position of the critical mass at $\theta = \pi$ or its properties in detail. But the important point is that we have succeeded in calculating the full dependence of the order parameter in θ in a gauge theory with fermions and a quantized topological charge, using a method that should, in principle, work also in higher dimensional theories.

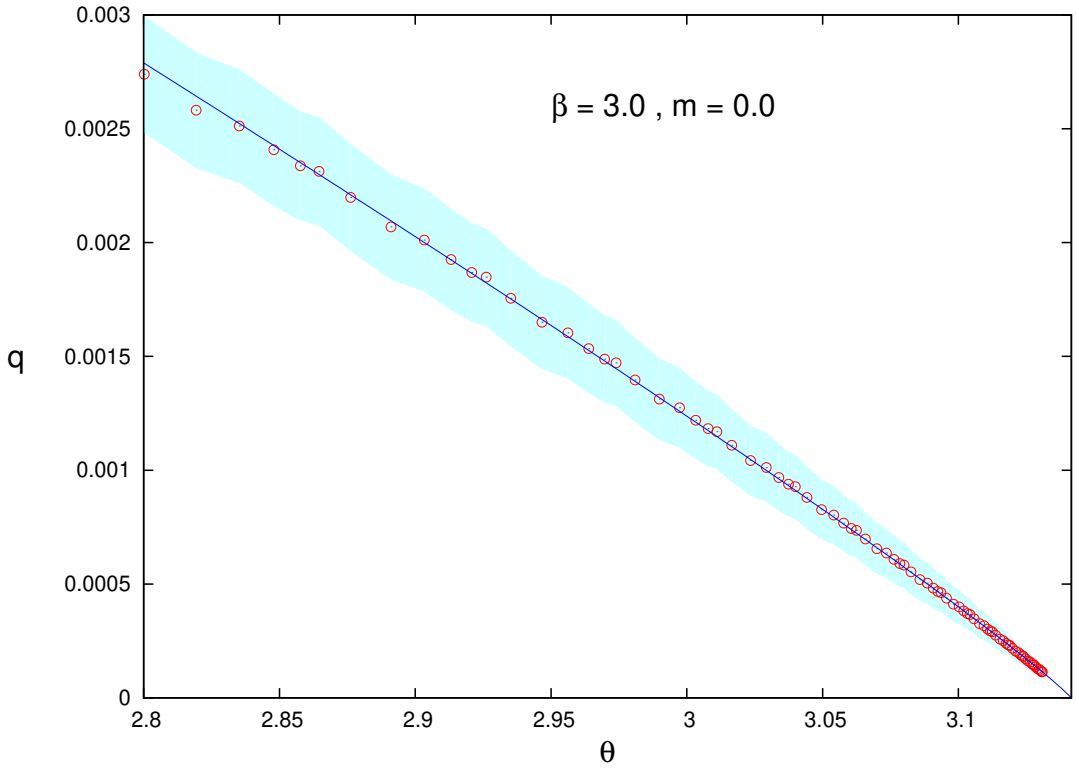

Figure 4.8: Order parameter as a function of θ near $\theta = \pi$.

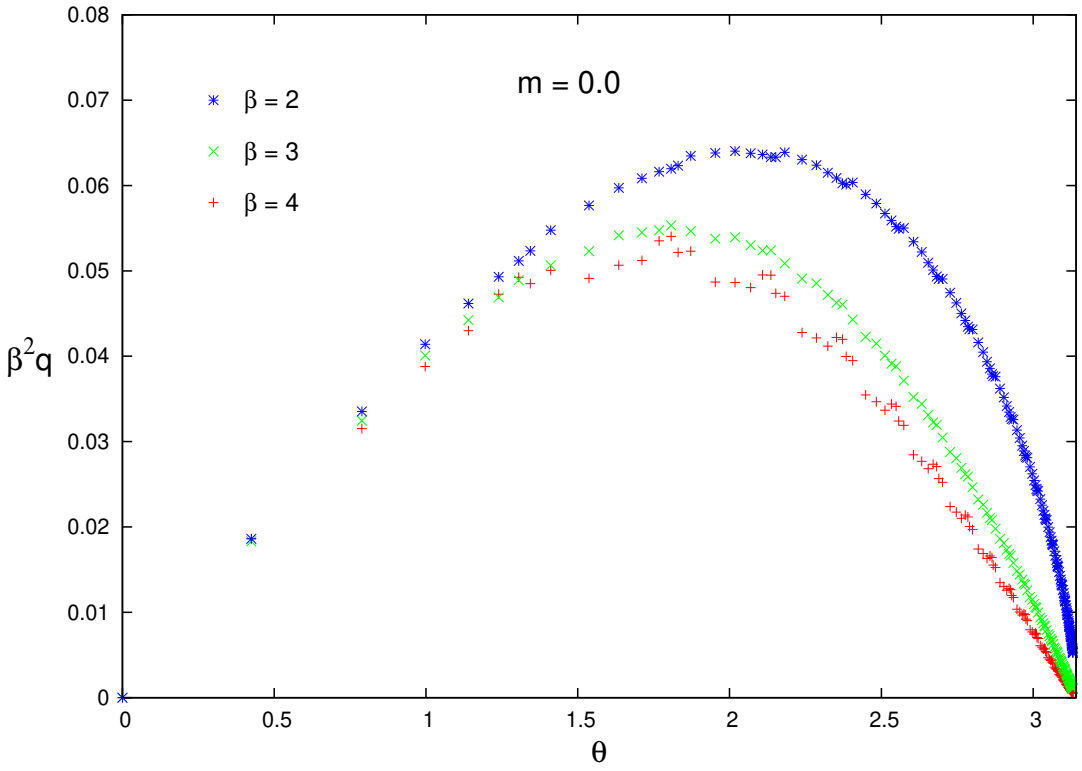

Figure 4.9: Rescaled topological charge density at $m = 0.0$ and different coupling constants.

Chapter 5

Preliminary results on two-flavor Schwinger—a pseudofermionic approach

Hereafter we present our work with the massive Schwinger model with a θ term and two distinct fermionic species. Although the starting point of the study consists in the application of the same Monte Carlo algorithm that was developed for Chapter 4—a standard implementation of Kogut-Susskind fermions with a Metropolis update—a search for more efficient algorithms proves to be necessary in order to fully test the capabilities of the $q(\theta)$ reconstruction approach of [13].

5.1 Motivation

The study of the Schwinger model with a single flavor of massive fermions and the inclusion of a θ term was carried out in the previous chapter with considerable success, since the dependence of the topological charge on θ was determined on the lattice for the whole domain of the vacuum angle, up to $\theta = \pi$. This was achieved thanks to standard Monte Carlo simulations performed at purely imaginary values of θ, which are the basic input for the reconstruction method of [13]. In these real-action computations, staggered (Kogut-Susskind) fermions were used, and the determinant of the fermionic matrix was calculated at every Metropolis step by extracting numerically all its eigenvalues—a technique as reliable as inefficient. In order to adjust the computation to the one-flavor case, the square root of this determinant needs to be taken; since the actual weight employed by the algorithm depends on the logarithm of the determinant, this *rooting* procedure amounts to multiplying by a factor of $1/2$. If instead we consider a factor of $N_f/2$, the discussion is valid for the Schwinger model with N_f fermion species—in fact, this

is the only change required in the algorithm.

Having developed an algorithm that can be trivially extended to the multi-flavored case, it seems natural to apply it, at least, to the cases that are closely related to one of our main interests during this thesis: the study of topological objects on lattice gauge theories, and its implications in QCD. In fact, this is the case for the two-flavored version of the model: its action holds a $U(2)$ symmetry in the chiral limit, of which its axial $U(1)$ subgroup is broken by the anomaly, much in the same way as QCD. The remaining $SU(2)$ group constitutes a true symmetry of the theory that, contrary to what occurs in low temperature QCD, is exactly preserved—as granted by a Theorem due to Coleman,[1] a continuous symmetry cannot be spontaneously broken in a two-dimensional system, as long as interactions are kept sufficiently local. This exactly preserved symmetry results to be an interesting property, as long as it is shared by the high temperature phase of QCD. In other words, QCD at high temperatures has in the chiral limit an exactly preserved chiral symmetry (contrary to the less exotic low temperature phase, as was discussed in Section 1.3.3). This fact favors the study the two-flavor Schwinger model as a mechanism to gain insight about the topological properties of finite temperature QCD.

Beyond its interest as a toy model of QCD, the $N_f = 2$ Schwinger model presents a more involved θ behaviour than its single flavored counterpart. The later presents, at $\theta = \pi$, two distinct phases depending on the coupling e/m. While P symmetry is spontaneously broken at weak coupling, in the strong coupling (or light mass) limit the vacuum energy density can be expanded in terms of the fermion mass m, its leading contribution being

$$E(\theta) \sim me\cos\theta. \tag{5.1}$$

As a consequence, the symmetry is exactly preserved and the topological susceptibility remains finite. By the contrary, the two-flavor version of the model, which has a similar behavior in the weak coupling region, has a more involved θ dependence on the vacuum angle. As it was shown by Coleman [22], a strong coupling approximation allows to write the energy density θ dependence as

$$E(\theta) \sim m^{\frac{4}{3}} e^{\frac{2}{3}} \cos^{\frac{4}{3}} \frac{\theta}{2}, \tag{5.2}$$

which eventually leads to P exact conservation at $\theta = \pi$, but with a divergent topological susceptibility—the characteristic of a continuous phase transition. This approximation, valid in principle when $e/m >> 1$, implies a value of $\delta = 1/3$ for the

[1] Although this result is proven by Coleman in the context of quantum field theories [147], it is commonly known as Mermin-Wagner theorm, since they arrived to the same conclusions in statistical physics [148].

associated critical exponent, which describes how the topological charge density vanishes as θ approaches π. Additionally, the lightest bosons of the spectrum are predicted to be an isotriplet and an isosinglet, the quotient of its masses being $\sqrt{3}$. It is worth noting that precisely this mass ratio has been recently the subject of some controversy, since a recent work by Azcoiti [149] found a subtantial discrepancy with respect to the original computation of Coleman [22]. Furthermore, Georgi [150] has drown even more attention to this model, by proposing a solution to the three questions posed by Coleman in [22] that could entail the existence of a novel mechanism, capable of generating the appearance of fine-tuning in low-energy effective theories and, consequently, with promising potential concerning any of the hierarchy problems that afflict the Standard Model. In any case, since a critical point is expected in this model at $\theta = \pi$, this system poses a relevant challenge for the reconstruction method that was applied during Chapter 4; to this effect, it serves as an additional motivation to this work—a particularly pragmatic one, arguably.

5.2 The model

The action of the one-flavor massive Schwinger model with a θ term can be easily generalized to its multi-flavor version by adding an index f, running from 1 to N_f, to the original expression (4.9). In this manner, the action for N_f flavors of equal charge e and mass m yields

$$S_{N_f} = \int d^2x \left\{ \sum_{1}^{N_f} \bar{\psi}_f \left[\gamma_\mu \left(\partial_\mu + iA_\mu \right) + m \right] \psi_f + \frac{1}{4e^2} F_{\mu\nu}^2 + \frac{i\theta}{4\pi} \epsilon_{\mu\nu} F_{\mu\nu} \right\}. \tag{5.3}$$

Following the reasoning of the previous chapter, it is possible to discretize the above continuum action by using Kogut-Susskind fermions and the standard Wilson action for the gauge part, as in (4.15). At this point we recall that a procedure commonly known as rooting was needed to get the one-flavor theory from the corresponding lattice action, since staggered fermions are not completely free of the doubling problem—they describe two degenerate species of fermions, in two dimensions. But, as long as we are interested in the two-flavor version, it suffices to consider the exact same action (4.15) and dismiss the rooting step.

The next step would imply performing a Monte Carlo simulation, much in the same way as in Chapter 4. However, while in our one-flavor study it was enough to perform a proof-of-concept calculation, our aim with the $N_f = 2$ case is to determine more involved quantities, such as the critical exponent of the expected $\theta = \pi$ phase transition. Even if the *brute force* approach of the previous chapter was able to deliver results in, roughly speaking, a few months of computer

time—which are to be multiplied by a factor of 160: the cores available to be run independently in a cluster facility—the time required for the present analysis, with similar computing resources, would need to be counted in years, thereby exceeding the lifespan of this thesis. In this situation, the main purpose of the chapter is to find an alternative to our previous algorithm, that is capable to give sufficiently precise results for the θ reconstruction technique to work.

5.3 Pseudofermions come into play

In order to achieve a greater computational efficiency, even at the cost of introducing some systematic errors, we have chosen to implement an algorithm based on the pseudofermion approach of Fucito et al [23]. As was discussed in Chapter 1, and particularly detailed in Section 1.3.1, the fermionic degrees of freedom present in the lattice partition function can be analytically integred out. Nontheless, this procedure has a cost: the introduction of the fermionic determinant, an involved object which depends in a highly non-linear way on the gauge fields—and so, implies a prohibitive computational price for any Monte Carlo simulation.

The key ingredient of [23] is to substitute the exact determination of the fermionic determinant M by a suitable estimation. To this end, auxiliary bosonic degrees of freedom are introduced, ruled by their own dynamics. If we label them by $\bar{\Phi}, \Phi$, the inverse of the determinant can be formulated as an integral,

$$\frac{1}{\det M} = \int \prod_i d\bar{\Phi}_i d\Phi_i \exp\left(- \sum_{j,k} \bar{\Phi}_j M_{jk} \Phi_k \right). \tag{5.4}$$

In fact, since what is needed for our Monte Carlo process is the ratio of two determinants (and in the case of a Metropolis-like algorithm, with relatively close associated matrices) an immediate corollary of the above is given by

$$\frac{\det M}{\det (M + \delta M)} = \left\langle \exp\left(- \sum_{j,k} \bar{\Phi}_j \delta M_{jk} \Phi_k \right) \right\rangle_{\text{PSF}}, \tag{5.5}$$

where $\langle \cdot \rangle_{\text{PSF}}$ is to be understood as the expectation value within the pseudofermions $\bar{\Phi}, \Phi$ ensemble, distributed precisely as indicated in (5.4).

Equation (5.5) makes the ratio between determinants suitable to be computed by means of an *additional* Monte Carlo algorithm. That is, at each step of the original algorithm (which consist in proposing a change in the gauge fields $U_\mu(n)$ that can be accepted or rejected) a new ensemble of pseudofermions $\bar{\Phi}, \Phi$ needs to be generated, in order to evaluate the observable $\bar{\Phi}_j \delta M_{jk} \Phi_k$, which eventually delivers an estimation for the ratio of determinants. In practice, the ensemble

of pseudofermions—its size grows linearly with the system—is updated a small number of times, n, and the observable is computed at each of these steps and averaged. The procedure is then exact in the limit of large n, and introduces systematic errors, as well as statistical ones, when keeping the number of steps finite.

A number of legitimate questions can be asked about the feasibility of this approach within the context of the Schwinger model with a topological term in the action. A non-exahustive list would include how large shoud be n in order to give a sufficiently precise result, what is the magnitude of the systematic errors when computing $q(\theta = ih)$, for suitable values of h, or what is the magnitude of the computing efficiency increase—and if it is enough to achieve the objectives stated at the beginning of the chapter. In the forthcoming section we try to answer and illustrate these questions.

5.4 Results and conclusions

The pseudofermion method of Fucito et al [23] has been applied in many scenarios, and their strengths and limitations have been already studied. Our purpose here is to analyze the potential of this method when applied to the Schwinger model—a system with both dynamical fermions and a topological term in the action. To this aim, we have performed a number of tests that help to delimit which section of the parameter space of the model is amenable to the use of this technique.

To begin with, we recall that the algorithm makes use of two distinct dynamics in its Monte Carlo evolution. Whereas the gauge fields evolve according to the action described in Section 5.2, the pseudofermion fields are regulated by (5.5), performing n Metropolis *inner* sweeps each time a tentative change for the gauge fields is proposed. In this manner, a pseudofermion sweep consists in sequentially trying to update each one of the complex bosonic variables Φ. Real and imaginary parts of the proposed complex shifts are randomly distributed, and also bounded by the technical parameter δ_{max}. In Figure 5.1 we show the result of choosing a relatively high value for this parameter in the one-flavor model, since for n as high as 80 the result obtained shows a systematic deviation from that obtained with the standard approach.

The first conclusion is the following: the dependence on the δ_{max} parameter needs to be taken into account to avoid too large systematic errors. In Figure 5.2 it can be seen how a larger value of this parameter implies a greater number n of the steps needed by the algorithm to reach the correct solution. For this reasons, and after considering similar tests, the value of δ_{max} is fixed in what follows to $\delta = 0.25$.

Another point that could compromise the viability of the method is the strength

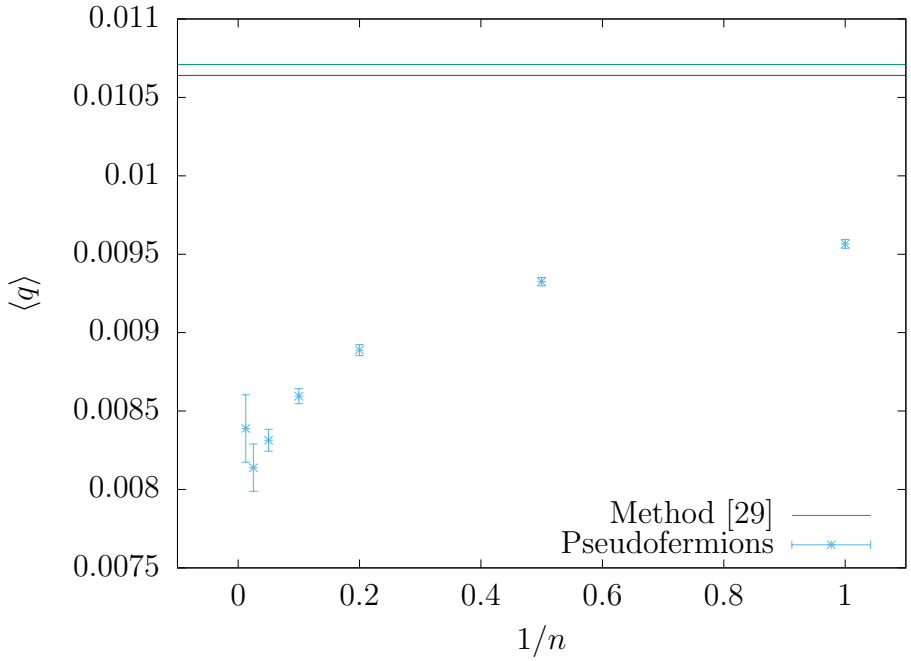

Figure 5.1: Results for a 16×16 lattice, with $\beta = 3, h \approx 1.51, m_f = 0.05, N_f = 1$ and $\delta_{max} = 1$. The expectation value of the topological charge density, $< q >$, is computed for several values of the number of pseudofermion Metropolis sweeps, namely for $n = 1, 2, 5, 10, 20, 40, 80$. Solid lines are to be identified with the upper and lower confidence intervals provided by the approach of [29], described in Chapter 4.

of the topological term, measured by h in our simulations at pure imaginary values of the parameter $\theta = ih$. In fact, this dependence on h can be seen in Figs. 5.3 and 5.4, which show results for the two-flavor Schwinger model. While for $h = 0.3$ the pseudofermion approach seems to reach the *correct* value as soon as for $n = 2$, a stronger topological term, of $h = 1.7$, results in a spoiled convergence, with systematic deviations still appearing for $n = 40$.

At this point we want to stress that, for a 16×16 lattice, as in Figs. 5.3 and 5.4, the computational efficiency of the standard method of Chapter 4 is roughly on par with the pseudofermion approach when $n = 80$. Since the cost of the latter depends linearly on n, this means that, e.g., using $n = 2$ would give a factor of 40 speed-up with respect to the former algorithm.

Taking into account the above conclusions, we have performed resource intensive simulations (allocated in the LNGS cluster), comparing both methods, in the two-flavored model for $\beta = 3$ and $m = 0.12$, using $\delta_{max} = 0.25$ and $n = 10$. The

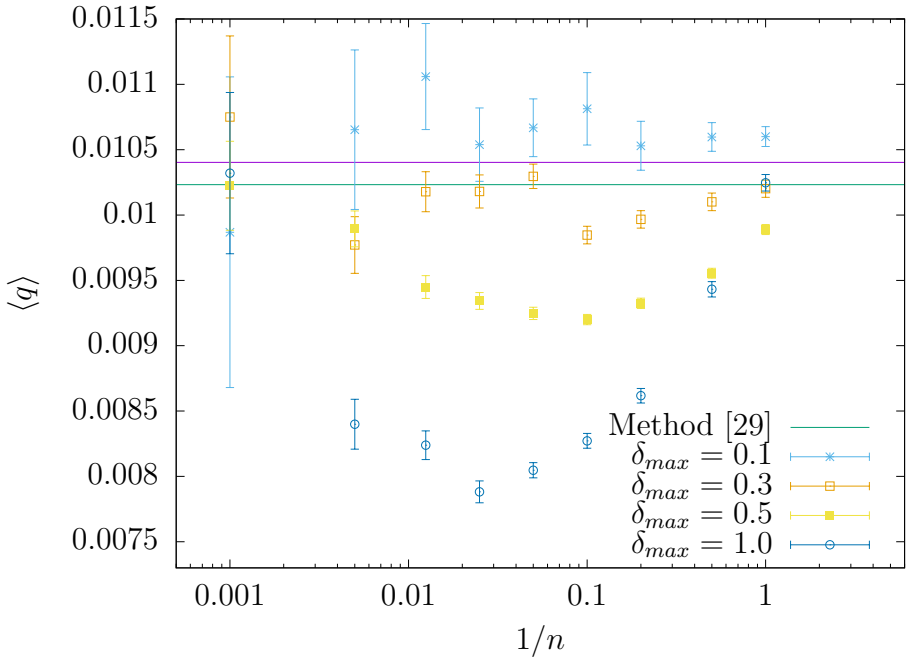

Figure 5.2: The dependence of the pseudofermion approach on δ_{max} is studied in a 8×8 lattice, with $\beta = 3, h \approx 1.51, m_f = 0.05$ and $N_f = 1$. Several δ_{max} curves are presented, showing a varying convergence rate. The number of sweeps n required to match the correct result grows rapidly with δ_{max}.

corresponding results are displayed in Fig. 5.5, where a very good agreement is observed up to $h = 0.5$; beyond that point, systematic deviations appear—bigger than statistical errors—slowly increasing with h.

In the light of the above results, it results convenient to clarify at least two issues. First, that we have compared the efficiency of two approaches in a particular area of the parameter space, suited to the determination of the critical exponent mentioned in the beginning of this chapter [22, 149]. In a 16^2 lattice, the cost is balanced at $n = 80$ pseudofermion Metropolis sweeps. We recall that the need of such comparison arise from the practical inability of the method of Chapter 4 to be extended to larger lattice sizes, which are required to elucidate the $N_f = 2$ case. While both approaches have a computational cost that escalates with N—i.e., the number of gauge fields that have to tentatively change—an extra factor due to the computation of the associated weight is needed. This is the main difference between the compared algorithms; while the determination of all the eigenvalues of the fermionic matrix is very costly, of order N^3 (even being sparse, it is never better than N^2), the pseudofermion evolution grows linearly with the number of

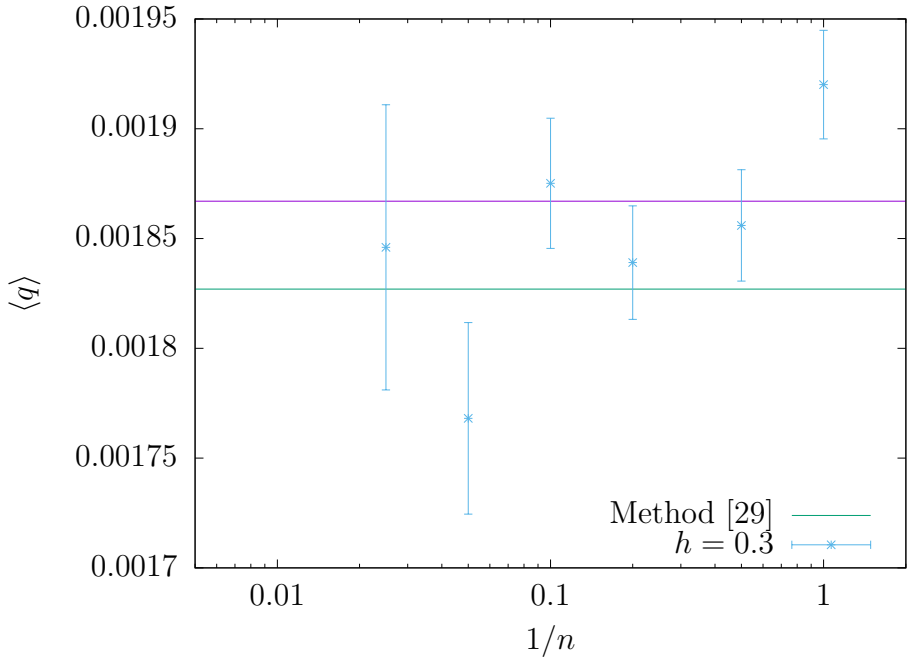

Figure 5.3: Results for the two-flavor Schwinger model in a 16×16 lattice, with $\beta = 3, h = 0.3$ and $m_f = 0.12$. δ_{max} is kept at 0.25 and the number of pseudofermion sweeps varies between 1 and 40. At this value of h, a very rapid convergence is observed.

degrees of freedom. This leads to a linear dependence on the size of the lattice N, which yields a total factor of N^2. For this reason, the algorithm presented in this chapter, being faster than its standard counterpart in a 16^2 lattice, is expected to perform way better at larger lattice sizes.

A second question that should be answered is how important are the systematic effects introduced by the pseudofermion approximation. As we noted above, this depends on the strength of the topological term. For small values of h, the differences are unnoticeable, appearing around $h > 0.5$ and growing consistently with this parameter. However, the aim of performing simulations at purely imaginary values of θ is to apply the reconstruction method of [13], as in Chapter 4. In order to perform the required extrapolation, the most important values of h to be analyzed are those close to the origin. Thereby, the pseudofermion approach gives with reliable accuracy precisely the region of interest for the θ dependence study. Moreover, at small values of h the number of n steps needed to reduce systematic errors decreases, giving an additional potential source of optimization.

All in all, a better dependence on the lattice size together with a good perfor-

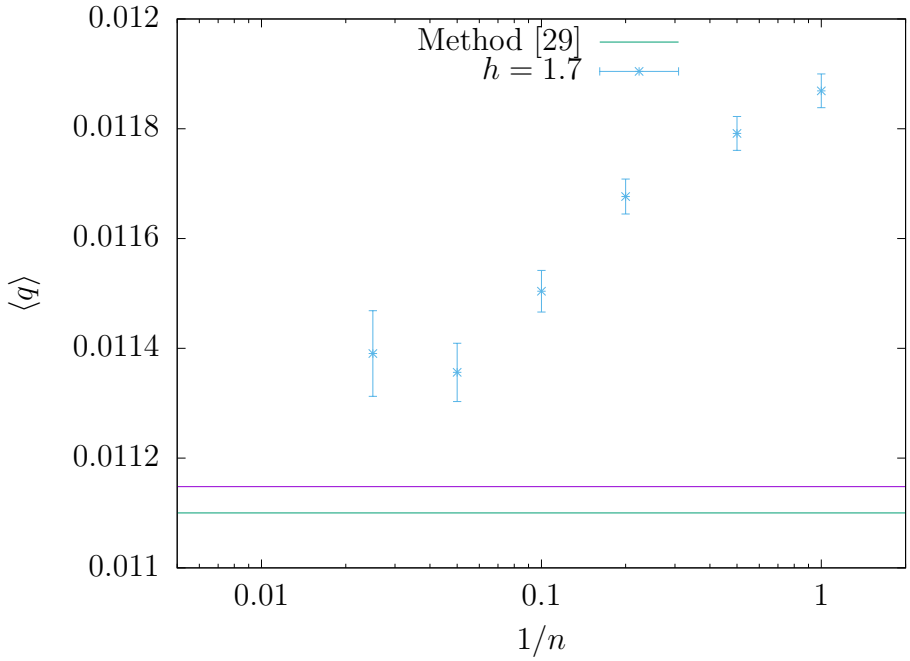

Figure 5.4: Results for the two-flavor Schwinger model in a 16×16 lattice, with $\beta = 3, h = 0.3$ and $m_f = 0.12$. δ_{max} is kept at 0.25 and the number of pseudofermion sweeps varies between 1 and 40. At this value of h, much higher than in the previous figure, convergence can only be guessed to occur beyond $n = 40$.

mance at low imaginary θ (real h), makes the pseudofermion approach an interesting candidate to explore the phase diagram of the multi-flavored Schwinger model with a θ term. The next step, that transcends the scope of this chapter, would imply a large-scale simulation, including larger lattice sizes, which could provide some insight into several aspects of the system under study and, consequently, of finite temperature QCD.

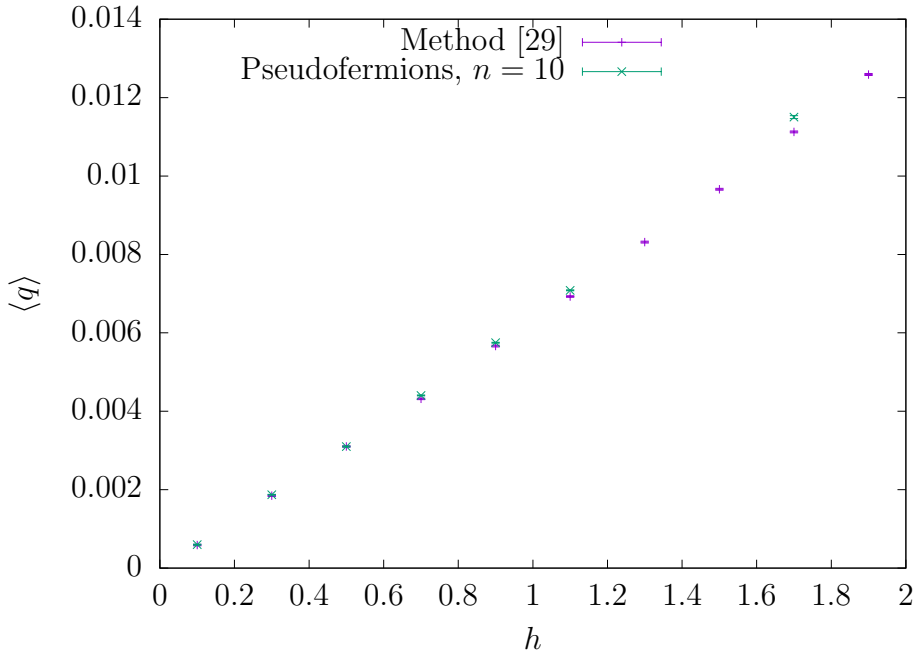

Figure 5.5: Results for the two-flavor Schwinger model in a 16×16 lattice, with $\beta = 3$ and $m_f = 0.12$. $\delta_{max} = 0.25$ and $n = 10$. The pseudofermion approach is confronted with the method of Chapter 4, with great agreement for small values of h, although systematic deviations are otherwise observed.

Chapter 6

Exploratory ghost-gluon study on α_S with HISQ fermions

In this last chapter we put aside the study of topological effects to face a non-perturbative quantity of the utmost relevance in QCD—its running coupling constant α_s. Our intention is to explore the dependence of the coupling on the momentum transfer q, by means of a purely gluonic method, following Sternbeck et al [26]. In this way, it is possible to compute gluon and ghost propagators, $G(q^2)$ and $D(q^2)$, in the lattice, eventually leading to the determination of $\alpha_s(q^2)$.

In the following sections we motivate the topic and review briefly the most relevant mathematical relations, describing with some detail the technical issues involved in the propagators determination. After that, our results—obtained from large sets of configurations generated by the MILC collaboration—are presented. The chapter is finished with some considerations concerning how the present study could be extended.

6.1 Motivation

The determination of the α_s coupling constant constitutes a very active field of research. In fact, the Particle Data Group periodically provide a *global average* of this quantity, including both theoretical calculations of lattice simulations and experimental determinations, such as from hadronic τ decays or e^+e^- annihilation processes, that allow to give an estimate—at a given scale, usually that of the Z boson—of the strong coupling α_s [2]. Remarkably enough, the last decade has been marked by a setback of the precision achieved when calculating the *global average* of this quantity, in part due to the existence of previously underestimated sources of systematic error that were present in lattice computations.

In this situation, there cohabit several independent approaches within the lat-

tice formalism, developed by a number of international collaborations such as HPQCD [4, 151, 152], PACS-CS [153], ETM [154], and other research groups [155, 156]. These approaches differ in a number of technicalities, including how fermions are implemented on the lattice. Moreover, different observables can be studied in order to extract α_s, an example being heavy quark correlators in [152], or the determination of the static potential in [156], which in fact gives a value for $\alpha_s(M_Z)$ that exhibits some tension with the rest of lattice predictions.

Our intention in the current chapter is to explore the potential of combining the ghost-gluon vertex technique of Sternbeck et al [26], which was already applied to twisted mass fermions in [154], with the highly improved staggered action (HISQ), used by the HPQCD collaboration [78]. To this aim, we will analyze ghost and gluon fields in a collection of ensembles generated by the MILC collaboration with the HISQ action [157].

6.2 α_s and the ghost-gluon vertex

Before going any further, it should be noted that the running coupling α_s is not a physically observable quantity. Instead, it acquires a precise meaning only in the context of perturbation theory. Then, in order to compare two given results for the coupling it is necessary to take into account the renormalization scheme. Typical choices in the literature are momentum subtraction schemes, the more common including MS, $\overline{\text{MS}}$ and MOM. While the standard computed value of $\alpha_s(M_Z)$ is tipically given in the literature in the $\overline{\text{MS}}$ scheme [2], the present approach is defined in a MOM scheme, in which renormalization constants are defined by requiring two- and three-point functions to equal their tree level expressions at a given energy scale μ [158].

There exist a number of ways that allow to calculate the value of the running coupling α_s on the lattice. As it has been just mentioned, the present work follows the approach of Sternbeck et al [26], although with the focus set in a different region (since we are not particularly interested in the infrared limit of α_s). Hereafter, we review the essentials of the method.

The computation of α_s in the lattice starts by realizing how ghost and gluon propagators can be exploited. Its dressing functions can be used to determine the running coupling as a renormalization group invariant, in a momentum subtraction scheme [25], as

$$\alpha_s(q^2) = \frac{g_0^2}{4\pi} Z_D(q^2) Z_G^2(q^2), \tag{6.1}$$

where Z_D and Z_G are respectively the bare dressing functions of gluon and ghost propagators; we discuss how to compute these functions in the next sections.

Although in usual lattice computations, as we reviewed in Chapter 1, fixing the gauge is not necessary, the mathematical expressions for ghost and gluon propagators adopt a simpler form in the Landau gauge—which in fact makes the whole computation feasible. Consequently, in what follows all expressions will be understood to be valid within the Landau gauge.

6.3 The gluon propagator

To begin with, the starting point is the standard 4-dimensional lattice of V sites, and $4V$ link variables $U_{x,\mu} \in SU(N_c = 3)$. The lattice gluon fields, which *live* in the mid-point of each link, $A_{x,\mu} \equiv A_\mu(x + \hat{\mu}/2)$, are defined as

$$A_{x,\mu} := \frac{1}{2i}(U_{x,\mu} - U^\dagger_{x,\mu}) - \frac{\mathbb{1}}{6i}\,\mathrm{Tr}(U_{x,\mu} - U^\dagger_{x,\mu}). \tag{6.2}$$

Additionally, we recall that the color components $A^a_{x,\mu}$ of the gluon field can be computed as

$$A^a_{x,\mu} := 2\,\mathrm{Tr}(T^a A_{x,\mu}) = 2 \cdot \mathfrak{Im}\,\mathrm{Tr}(T^a U_{x,\mu}), \tag{6.3}$$

where the definition (6.2) has been used. With these expressions, we can compute the bare gluon propagator on the lattice as

$$D^{ab}_{\mu\nu}(k) = \left\langle \tilde{A}^a_\mu(k)\tilde{A}^b_\nu(-k)\right\rangle_U, \tag{6.4}$$

where $\tilde{A}_\mu = \tilde{A}^a_\mu T^a$ are the Fourier transformed gluon fields. In other words,

$$D^{ab}_{\mu\nu}(q(k)) = \frac{1}{V}\left\langle \sum_{x,y} A^a_{x,\mu} A^b_{y,\nu} e^{ik\cdot(x+\hat{\mu}/2)} e^{-ik\cdot(y+\hat{\nu}/2)} \right\rangle_U, \tag{6.5}$$

where the momentum $q(k)$ is given by

$$q_\mu(k_\mu) = \frac{2}{a}\sin\left(\frac{\pi k_\mu}{L_\mu}\right). \tag{6.6}$$

If we assume now that $D^{ab}_{\mu\nu}(q(k))$ has the same tensor structure than its continuum counterpart,

$$D^{ab}_{\mu\nu}(q) = \delta^{ab}\left(\delta^{\mu\nu} - \frac{q_\mu q_\nu}{q^2}\right) D(q^2), \tag{6.7}$$

it suffices a bit of algebra to obtain an expression for the scalar part of the propagator $D(q^2)$,

$$D(q^2) = \frac{1}{(D-1)(N_c^2-1)} \sum_{a\mu} D^{aa}_{\mu\mu}(q), \tag{6.8}$$

which is related with the dressed propagator simply by

$$Z_D(q^2) \equiv q^2 D(q^2). \tag{6.9}$$

In practical terms, the key step in this computation—in terms of computational complexity—is the Fourier transformation of the gauge fields. Fortunately, Fast Fourier Transform algorithms allow to compute very efficiently expression (6.5), especially taking into account that a single application of the algorithm delivers the propagator for every lattice value of the momenta q_μ at once.

6.4 The ghost propagator

Following [27], the ghost propagator in the lattice is defined in the Landau gauge as

$$G^{ab}(k) = a^2 \left\langle \sum_{xy} \left(M^{-1}\right)^{ab}_{xy} e^{ik\cdot(x-y)} \right\rangle = \delta^{ab} G(q), \tag{6.10}$$

where the real symmetric matrix M is the Fadeev-Popov operator, defined by

$$M^{ab}_{xy} = \sum_{\mu} \left(A^{ab}_{x,\mu}\delta_{x,y} - B^{ab}_{x,\mu}\delta_{x+\hat{\mu},y} - C^{ab}_{x,\mu}\delta_{x-\hat{\mu},y} \right) \tag{6.11}$$

with

$$A^{ab}_{x,\mu} = \mathfrak{Re}\,\mathrm{Tr}\left[\{T^a, T^b\}(U_{x,\mu} + U_{x-\hat{\mu},\mu})\right], \tag{6.12}$$

$$B^{ab}_{x,\mu} = 2\cdot\mathfrak{Re}\,\mathrm{Tr}\left[T^b T^a U_{x,\mu}\right], \tag{6.13}$$

$$C^{ab}_{x,\mu} = 2\cdot\mathfrak{Re}\,\mathrm{Tr}\left[T^a T^b U_{x-\hat{\mu},\mu}\right]. \tag{6.14}$$

In order to compute (6.10), the following system of equations needs to be solved

$$\begin{cases} M_{ax,by}\boldsymbol{c}^{by}_c = \delta^{ac}\cos(k\cdot x), \\ M_{ax,by}\boldsymbol{s}^{by}_c = \delta^{ac}\sin(k\cdot x). \end{cases} \tag{6.15}$$

The $8V$-component vectors $\boldsymbol{c}_c, \boldsymbol{s}_c$ are computed with the conjugate gradient method and can be used to determine the inverse of M. Together with (6.10), and assuming the tensor structure of the continuum, $G^{ab}(q_\mu) = \delta^{ab}G(q^2)$, we have

$$G(q^2) = \frac{1}{(N_c^2-1)}\sum_{ax}\left[\cos(k\cdot x)\,\boldsymbol{c}^{ax}_a + \sin(k\cdot x)\,\boldsymbol{s}^{ax}_a\right], \tag{6.16}$$

with the corresponding dressed propagator being given by

$$Z_G(q^2) \equiv q^2 G(q^2). \tag{6.17}$$

β	m'_l/m'_s	m'_s	m'_c	$N_s^3 \times N_t$	a (fm)	# of cnfgs
6.00	1/5	0.0509	0.0635	$24^3 \times 64$	0.1218(7)	1053
6.30	1/5	0.0370	0.0440	$32^3 \times 96$	0.0879(5)	1008
6.72	1/5	0.0240	0.0286	$48^3 \times 144$	0.0573(4)	1017

Table 6.1: Details of the three ensembles studied.

In contrast with the gluon determination of the previous section, the steps here described are much more expensive in computational terms. In particular, numerically solving the system of equations (6.15) is a very demanding task which, at large lattice sizes—as the ones studied in this chapter are—requires large resources, both in terms of memory and processing time. Furthermore, lattice artifacts are expected to be more intense both at large and at off-diagonal momenta, due to the lack of rotational symmetry on the lattice in the latter case [159]. For this reasons, the ghost propagator, and as a consequence also α_s, have been computed only for a handful of selected diagonal momenta.

6.5 Results

We have analyzed three sets of configurations, made available by the MILC collaboration [157]. The details of their parameters are summarized in Table 6.1. Prior to the propagators determination, we fixed every configuration to Landau gauge. To this end, it is necessary to make use of an iterative optimization algorithm. As is well known, this type of algorithms could suffer from a severe critical slowing down problem. In the case of large lattices, as some of the ones analyzed here, this obstacle can turn insurmountable. However, we have evaded this difficulty by applying a Fourier-accelerated algorithm, originally proposed by Davies et al [160], which allows to alleviate the computational overhead, making the gauge fixing procedure feasible. In this process, the fixing procedure was stopped only when every local gauge field verified the transversality condition—the lattice version of $\partial_\mu A_\mu = 0$—up to $\Theta < 10^{-14}$, with the same definition of [160]. Such level of precision was proved to be necessary, since the propagators are quite sensitive to the gauge condition.

Once the whole sets were fixed to Landau gauge, we have computed both propagators, $G(q^2)$ and $D(q^2)$, for a total of seven diagonal momenta,

$$\mathbf{k} = (n, n, n, n) \qquad \text{for} \quad n = 1, \ldots, 7. \tag{6.18}$$

As we mentioned earlier, the ghost computation, and in a lesser way the gauge

# of configurations	1	1053
Landau gauge-fixing time (core-h)	7.1	7.1k
Propagators for 7 momenta (core-h)	19.7	20.8k
Total time (7 momenta) (core-h)	26.9	28.3k
Each additional momentum (core-h)		+3.0k

Table 6.2: Distribution of computing times involved in the $24^3 \times 64$ ensemble.

fixing procedure, are very demanding in terms of computing resources. This being the case, actual calculations have required to be performed in large cluster facilities, which provide both the computing power and the memory needed to store the largest configurations. To this end, the University of Cambridge computing services have been used, including the cluster Darwin, and its 2017 update CSD3. For the first set, of volume $24^3 \times 64$, 28k core-hours were used in Darwin; to exemplify how these are distributed, see Table 6.2. For the $32^3 \times 96$ set, a total of 135k core-hours, also in Darwin, were used. Finally, the ensemble corresponding to the bigger lattice size, $48^3 \times 144$, was analyzed with a total cost of 452k core-hours of the newer cluster CSD3.

Our results for both bare unrenormalized propagators are shown in Figure 6.1, as a function of the squared lattice momenta in physical units. By means of Eq. 6.1, the previous results can be applied to determine α_s. Taking into account that, according with the particular implementation of the HISQ action in the analysed MILC configurations,

$$g_0^2 \equiv \frac{5}{3}\frac{2N_c}{\beta} = \frac{10}{\beta}, \tag{6.19}$$

our final results for the unrenormalized version of the running coupling are shown in Fig. 6.2. As a preliminary conclusion, these results can be checked to be qualitatively in agreement with those of the literature, see e.g. [25, 26, 154]. In any case, in order to provide an estimate for the $\alpha_s(M_Z)$ in the $\overline{\text{MS}}$ renormalization scheme, the corresponding β function should be carefully studied and integrated, together with a thorough study of present volume effects and lattice artifacts, since the knowledge of its dependence would allow to estimate the systematic errors of the method. Finally, the relatively low value of the estimated statistical errors in the studied ensembles drive us to conclude that completing the present analysis would be worthwhile, potentially leading to a valuable contribution to the world average of the strong running coupling.

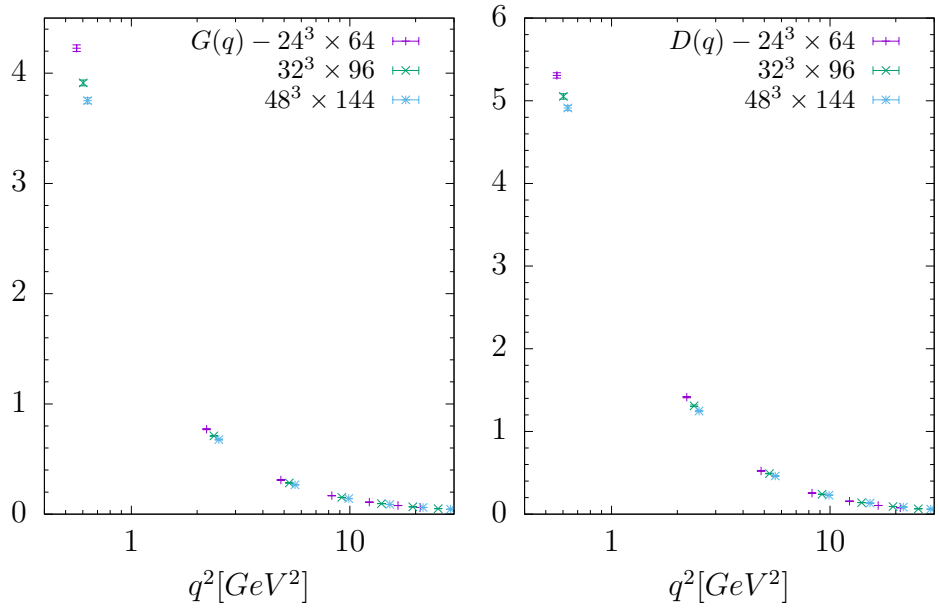

Figure 6.1: Ghost and gluon bare propagators, in physical units.

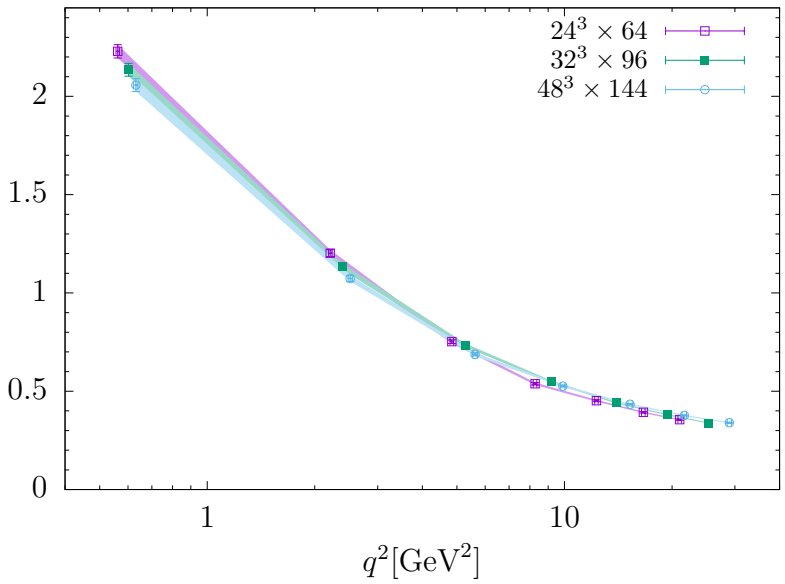

Figure 6.2: The running coupling $\alpha_s(q^2)$ as defined in Eq. 6.1. Shaded areas connect 1σ intervals.

Conclusions and outlook

In the beginning of this thesis we emphasized the key role of lattice QCD as the main tool capable of dealing with non-perturbative phenomena, in QCD and beyond. Their successes are many, as it has been documented in Chapter 1. Up to the present day, there exist several international collaborations that work intensively to provide theoretical estimates that match the ever-increasing precision of the experimental measures. But, notwithstanding the achievements in phenomenology grounds, there exist open questions that seem to evade any attempt of resolution. Indeed, this is the case of QCD when the topological θ term is included into its action, as it has been reviewed in Chapter 2.

Deeply connected with the strong CP problem, and of great importance in axion physics, the study of the θ dependence of QCD has been the long-sighted goal of this thesis. Certainly, this is an ambitious objective, since there exist many difficulties when considering θ QCD on the lattice, one of the most fundamental being the presence of a severe sign problem that makes the system unattainable to standard Monte Carlo simulations. In this scenario, our efforts have been first directed towards the testing of a promising method that would in principle allow to reconstruct the full θ dependence of observables as the topological charge [13]. Thereby, in Chapter 3, following [28], we have crosschecked a previous work that, making use of the reconstruction method of Azcoiti et al, found signs of a rich phase structure in the antiferromagnetic Ising model within an imaginary magnetic field—which can be thought of as a θ term [21]. By making use of a combination of analytical and numerical—but exact—techniques, our results have supported the previous qualitative picture, thus confirming the potential of the reconstruction method in a theory that, when compared to θ QCD, holds a more intricate phase diagram. In the same spirit, Chapter 4 has been devoted to the study of the massive one-flavor Schwinger model with a θ term in the action, which frequently serves as a toy model of QCD, as presented in [29]. To apply the reconstruction method [13] in this system implies a stringent exam concerning its possibilities of being successfully applied to full QCD, as it shares many of its potential obstacles—but not all, since it holds a very elementary definition of the topological charge, in contrast with the difficulties that appear in the $SU(3)$ 4d theory. Actually, we have

been able to obtain the full $q(\theta)$ dependence of the model for some selected points of the parameter space. These results are coherent with the existent literature, confirming a previous conjecture due to Coleman, and thus reinforcing the viability of the reconstruction approach.

Initially devised as an extension of the previous study, in Chapter 5 we have presented our work with the 2-flavor version of the Schwinger model with a θ term in the action. Our motivation was two-fold: first, the model is expected to have a second order phase transition at $\theta = \pi$ and, in this sense, it poses a challenge to the reconstruction method. Moreover, the mass ratio of the lightest bosons of the spectrum has been the subject of a recent controversy [149], and an independent computation could clarify the issue. Secondly, the 2-flavor system serves as a toy model for the high temperature phase of QCD, since both theories share an exactly preserved $SU(2)$ chiral symmetry. Since the direct approach applied in Chapter 4 didn't have the required computational efficiency, we have developed an algorithm based on the use of pseudofermions, following the original prescription of [23]. Our results support a more intensive calculation involving larger lattice sizes, since the region where the pseudofermion approach delivers better coincides with the one required by the reconstruction approach.

Last, in Chapter 6 we have set aside the study of systems with a sign problem, focusing our interest in the determination of the strong running coupling $\alpha_s(M_Z)$. As the Particle Data Group reports periodically [2], many efforts are devoted to obtain a precise value for this perturbative-defined quantity, both from the experimental and the theoretical perspectives. In the later case, there exist several lattice approaches that try to provide the most accurate result. With this aim, we have explored the potential of applying the ghost-gluon vertex approach of [25], to three large HISQ ensembles, provided by the MILC collaboration. Our results show promising statistical errors, and we conclude that a complete analysis of lattice artifacts and other systematic errors would be worthwile, possibly leading to a valuable contribution to the lattice world-average of the running coupling.

To give a closure to this thesis, and in particular to our study of θ physics, we want to stress out some final ideas. First, there are clear signs, according to the results presented in Chapters 3 and 4, that point to the viability of applying the reconstruction approach [13] to full QCD. To implement this program would require simulations at pure imaginary values of θ in the $SU(3)$ theory, including some variety of fermions. However, if compared with the Schwinger model analysis, QCD comes with an additional obstacle—the computation of the topological charge. In essence, the determination of the θ dependence would require, at the very least, a sufficiently well-behaved lattice definition of the topological charge, which additionally should be computationally tractable, in order to be included into the corresponding Monte Carlo dynamics. To found a balanced solution to

this problem is left out of the scope of this document—this endeavor should be confronted in future works.

Conclusiones

Al comenzar esta tesis enfatizábamos el papel clave de *lattice* QCD como la herramienta principal capaz de enfrentarse a fenómenos no perturbativos, en QCD y más allá. Sus éxitos son muchos, como ha quedado documentado en el Capítulo 1. Hasta el día de hoy, existen varias colaboraciones internacionales que trabajan intensivamente para ofrecer estimaciones teóricas que igualen la creciente precisión de las medidas experimentales. Pero, sin desmerecer los logros en el área de la fenomenología, existen preguntas abiertas que parecen evadir cualquier intento de resolución. Por supuesto, este es el caso de QCD cuando el término topológico θ se incluye en su acción, como se repasó en el Capítulo 2.

Profundamente conectado con el problema CP fuerte, y de gran importancia en física de axiones, el estudio de la dependencia en θ de QCD ha sido el objetivo a largo plazo de esta tesis. Ciertamente, se trata de un objetivo ambicioso, toda vez que existen varias dificultades importantes cuando se considera θ QCD en el retículo, siendo una de las más fundamentales la presencia de un problema de signo severo que hace el sistema inalcanzable a las simulaciones de Montecarlo usuales. En este escenario, nuestros esfuerzos se han dirigido en primer lugar hacia la corroboración de un método prometedor que podría permitir, en principio, reconstruir completamente la dependencia en θ de observables como la carga topológica [13]. Así, en el Capítulo 3, siguiendo [28], hemos comprobado un trabajo previo que, haciendo uso del método de reconstrucción de Azcoiti et al, encontró signos de una estructura de fases rica en el modelo de Ising antiferromagnético con campo magnético puramente imaginario—que puede verse como un término θ [21]. Haciendo uso de una combinación de técnicas analíticas y numéricas (pero exactas), nuestros resultados apoyan la imagen cualitativa anterior, confirmando así el potencial del método de reconstrucción en una teoría que, si se compara con θ QCD, posee un diagrama de fases más enrevesado. Con el mismo espíritu, el Capítulo 4 se ha dedicado al estudio del modelo de Schwinger masivo con un único *flavor* y término θ en la acción, que sirve frecuentemente como *toy model* de QCD, tal y como se presenta en [29]. Aplicar el método de reconstrucción [13] en este sistema implica un exigente examen a sus posibilidades de ser aplicado en QCD, ya que comparte muchos de sus obstáculos potenciales—aunque no todos, ya que

mantiene una definición muy elemental de la carga topológica, en contraste con las dificultades que aparecen en la teoría $SU(3)$ en 4 dimensiones. De hecho, hemos conseguido obtener la dependencia completa $q(\theta)$ para el modelo en algunos puntos seleccionados del espacio de parámetros. Estos resultados son coherentes con la literatura existente, confirmando una conjetura previa de Coleman, y reforzando así la viabilidad del método de reconstrucción.

Inicialmente concebido como una extensión del estudio anterior, en el Capítulo 5 hemos presentado nuestro trabajo con la versión de dos *flavors* del modelo de Schwinger con un término θ en la acción. Nuestra motivación era doble: primero, en este modelo se espera una transición de fase de segundo orden en $\theta = \pi$ y, en este sentido, plantea un desafío al método de reconstrucción. Además, la ratio entre las masas de los bosones más ligeros del espectro ha sido el sujeto de una controversia reciente [149], y un cálculo independiente podría clarificar la situación. En segundo lugar, el sistema de dos *flavors* sirve como *toy model* para la fase de alta temperatura de QCD, dado que ambas teorías comparten una simetría quiral $SU(2)$ que es preservada de forma exacta. Como el enfoque directo aplicado en el Capítulo 4 no tenía la eficiencia computacional requerida, hemos desarrollado un algoritmo basado en el uso de pseudofermiones, siguiendo la prescripción original de [23]. Nuestros resultados apoyan un cálculo más extenso que incluya retículos de mayor tamaño, dado que la región en la que el método basado en pseudofermiones se comporta mejor coincide con la requerida por el método de reconstrucción.

Por último, en el Capítulo 6 hemos dejado a un lado el estudio de sistemas con un problema de signo, centrando nuestro interés en la determinación del *running coupling* de la interacción fuerte, $\alpha_s(M_Z)$. Tal y como el *Particle Data Group* refiere periódicamente [2], son dedicados muchos esfuerzos a la obtención de un valor preciso para esta cantidad definida perturbativamente, tanto desde perspectivas experimentales como teóricas. En este último caso, existen varios enfoques que, desde el retículo, tratan de ofrecer el resultado más preciso. Con este objetivo, hemos explorado el potencial de aplicar el método del vértice ghost-gluon de [25] a tres grandes conjuntos de configuraciones HISQ, facilitadas por la colaboración MILC. Nuestos resultados muestran unos errores estadísticos prometedores, y concluimos que un análisis completo de los artefactos del retículo y otras fuentes de errores sistemáticos sería provechoso, pudiendo llevar a una contribución valiosa para la media mundial del *running-coupling*.

Para dar un cierre a esta tesis, y en particular a nuestro estudio de la dependencia en θ, queremos recalcar algunas ideas finales. En primer lugar, existen signos claros, de acuerdo con los resultados presentados en los Capítulos 3 y 4, que apuntan a la viabilidad de la aplicación del método de reconstrucción [13] a QCD. Implementar este programa requeriría de simulaciones a valores puramente imaginarios de θ en la teoría $SU(3)$, incluyendo alguna de las variedades de

fermiones. Sin embargo, si se compara con el análisis del modelo de Schwinger, QCD conlleva un obstáculo adicional—la computación de la carga topológica. En esencia, la determinación de la dependencia en θ requeriría, como mínimo, de una definición que se comportase lo suficientemente bien en el retículo y que, a su vez, fuese computacionalmente tratable, para así poder ser incluida en la dinámica de Montecarlo correspondiente. Encontrar una solución equilibrada a este problema se deja fuera del alcance de este documento—este cometido deberá ser afrontado en trabajos futuros.

Appendix A

Computation of the cumulants κ_η

In order to use expressions (3.17) and (3.20), we need to compute the cumulants κ_n. The nth cumulant can be calculated in terms of the first n noncentral moments μ'_n,

$$\mu'_n \equiv \left\langle \left(\sum_{<ij>} s_i s_j \right)^n \right\rangle_{m_1,m_2}, \tag{A.1}$$

by means of the recursion relation (3.16). The summation over $< ij >$ runs over each couple of neighboring spins, or in other words, over each link. Two neighboring spins always belong to different sublattices.

Before going further, let us comment on two intermediate results. First, we consider a lattice of N spins, the magnetization of which is the sum $m = \sum_i s_i$, and ask about the expected value of the product of n of these spins at fixed m (or fixed N_+, the number of positive spins), that is, $\langle s_1 s_2 \cdots s_n \rangle_m$. One can perform this calculation by means of the microcanonical formalism, arriving at

$$\langle s_1 s_2 \cdots s_n \rangle_m = \frac{1}{\binom{N}{N_+}} \sum_{k=0}^{n} (-1)^k \binom{n}{k} \binom{N-n}{N_+ - n + k}. \tag{A.2}$$

In the above expression, k can be read as the number of negative spins in the product $s_1 s_2 \cdots s_n$. In this way, the first summand, $k = 0$, counts the number of states with zero negative spins in the product $s_1 s_2 \cdots s_n$ and multiplies it by the expectation value of the product in this case, $(-1)^0 = 1$. The second one, $k = 1$, does the same for one negative spin in $s_1 \cdots s_n$, and so on. Dividing the sum by the total number of configurations with magnetization $m = 2N_+/N - 1$, one obtains the previous expectation value at fixed m. Secondly, consider an observable $\mathcal{O}(m_1, m_2)$ in our two sublattice system, with a dependence on m_1 and m_2 such as we can write it as $\mathcal{O}_1(m_1)\mathcal{O}_2(m_2)$. In this case, from the definition

(3.12) of the expectation value at fixed m_1 and m_2, we have

$$\langle \mathcal{O}_1(m_1)\mathcal{O}_2(m_2)\rangle_{m_1,m_2} = \langle \mathcal{O}_1(m_1)\rangle_{m_1} \langle \mathcal{O}_2(m_2)\rangle_{m_2} . \tag{A.3}$$

This immediately applies to the spin product $s_1 s_2 \cdots s_n$. We can always divide it into two products $s_a \cdots s_b$ and $s_\alpha \cdots s_\beta$, each one containing the spins of one of the sublattices, and then

$$\langle s_1 s_2 \cdots s_n\rangle_{m_1,m_2} = \langle s_a \cdots s_b\rangle_{m_1} \langle s_\alpha \cdots s_\beta\rangle_{m_2} . \tag{A.4}$$

With the previous couple of results, we come back to Eq. (A.1), and apply the linearity of the expectation value, arriving at

$$\mu'_n = \sum_{<ij>,<kl>,\cdots,<pq>} \langle s_i s_j s_k s_l \cdots s_p s_q\rangle_{m_1,m_2} , \tag{A.5}$$

which is the sum of the expectation values of the product of n links, running over all permutations with repetitions of these links. Then, in every summand we have the product of $2n$ spins, in some cases with some of them identical. Taking into account that $s_i^2 = 1\ \forall i$, each summand can be reduced to the expectation value of the product of $n_1 + n_2$ different spins, n_1 and n_2 being the number of spins in each sublattice. Since by means of Eq. (A.2) we already have an expression that computes $\langle s_1 \cdots s_n\rangle_m$, the problem is reduced to count how many summands in Eq. (A.5) have (n_1, n_2) spins. We call these numbers *geometrical factors*, and denote them by $\mathcal{G}(n_1, n_2)$. Following this convention, we can write the nth central moment as

$$\mu'_n = \sum_{\{n_1,n_2\}} \mathcal{G}(n_1,n_2) \langle \underbrace{s_a \cdots s_b}_{n_1 \text{ spins}}\rangle_{m_1} \langle \underbrace{s_\alpha \cdots s_\beta}_{n_2 \text{ spins}}\rangle_{m_2}, \tag{A.6}$$

where the sum runs over the couples of integers (n_1, n_2) the sum of which is even and less than or equal to n.

The computation of the geometrical factors $\mathcal{G}(n_1, n_2)$ can be done by hand for the first few cumulants. As an example, for the second noncentral moment μ'_2 we have to compute four cases: the two links being the same (sharing both spins), sharing only one spin belonging to the first or the second sublattice, and finally not sharing any spin at all. That is, in terms of the previous notation,

$$\{(n_1, n_2)\} = \{(0,0), (2,0), (0,2), (2,2)\}. \tag{A.7}$$

The factors $\mathcal{G}(n_1, n_2)$ can be computed easily in this case, even for an hypercubic lattice of arbitrary dimension d, arriving at the following expression for the second moment

$$\begin{aligned} \mu'_2 &= Nd\langle 1\rangle + Nd(d-1)(\langle s_1 s_2\rangle_{m_1} + \langle s_1 s_2\rangle_{m_2}) \\ &\quad + Nd(Nd - 2(d-1) - 1)\langle s_1 s_2\rangle_{m_1}\langle s_1 s_2\rangle_{m_2}. \end{aligned} \tag{A.8}$$

We can use this expression to calculate the second cumulant κ_2,

$$\kappa_2 = \mu'_2 - \mu'^2_1 \xrightarrow{N\to\infty} Nd(m_1^2 - 1)(m_2^2 - 1), \tag{A.9}$$

where we have taken the thermodynamic limit, keeping only the terms of order $\mathcal{O}(N)$, which is the leading order for all cumulants. Subleading orders can be preserved if needed, but they are not relevant for our paper. The difficulty of the previous computation escalates quickly with the order n of the cumulant, and it is quite cumbersome for just $n \geq 4$. In order to get beyond this limitation, we have developed a program which computes the geometrical factors $\mathcal{G}(n_1, n_2)$ numerically for a finite $L \times L$ bidimensional lattice. Since these factors $\mathcal{G}(n_1, n_2)$ are polynomials in N of order $\leq n$ (and with integer coefficients), we can run the program for lattices of $n + 1$ different sizes, obtaining a set of (N,$\mathcal{G}(N)$) points, which we can use to recover the exact integer coefficients of each geometrical factor, by means of the Lagrange interpolation formula.

The basic idea of the program is very simple. We just construct a periodic rectangular $L \times M$ lattice, with $L, M > n$, n being the order of the cumulant we want to compute. With this restriction we avoid products of links crossing the entire lattice, that would not appear in the thermodynamic limit for any finite cumulant. Once we have this, we start a loop running over all the permutations with repetitions of n links, and perform the following steps,

- We have a product of n links, or equivalently $2n$ spins, $s_1 \cdots s_{2n}$.
- Recursively, we remove couples of equal spins from this product.
- We classify the remaining product by the number of spins in each sublattice, (n_1, n_2).
- We add one to the geometric factor $\mathcal{G}(n_1, n_2)$ and proceed to the next iteration.

When the algorithm finishes, we obtain all the $\mathcal{G}(n_1, n_2)$ values for a given $N = LM$. The computational cost is associated to the number of iterations of the main loop, which grows as $(LM)^n$, that is, exponentially with the order of the cumulant. In practice, we have only reached the computation of the fourth cumulant with this program. However, a number of optimizations can be implemented in order to reach higher order cumulants, which we summarize in what follows.

A.1 Translational symmetry

Our lattice is symmetric under translations, implying that all geometrical factors are proportional to Nd, the number of links. Fixing, e.g., the first link of the

product, one obtains the same $\mathcal{G}(n_1, n_2)$, but divided by a common factor Nd. The same factor is gained in the overall speed of the program. In addition to that, the degree of the polynomials $\mathcal{G}(n_1, n_2)$ is also reduced by one, and it suffices with n (instead of $n+1$) different sizes in order to recover the N dependence. One can go even further by realizing that the geometrical factor corresponding to non-neighboring links, $\mathcal{G}(n, n)$, is the only one with maximum degree N^{n-1}. This allows us to express it in terms of the remaining factors,

$$\begin{aligned} \frac{1}{Nd}\mathcal{G}(n,n) &= (Nd)^{n-1} \\ &\quad -\frac{1}{Nd}\sum_{\{(n_1,n_2)\}\setminus(n,n)} \mathcal{G}(n_1,n_2), \end{aligned} \tag{A.10}$$

which are only of order $n-2$ or less. This means that it is enough to run the program for $n-1$ lattice sizes, compute all the geometrical factors but $\mathcal{G}(n, n)$ via the Lagrange interpolator, and then with the previous expression find the N dependence of this last factor.

A.2 From permutations to combinations

The product of links commutes, so its contribution to the geometrical factors is the same regardless of the order. Then, we can change the main loop over permutations with repetition to a loop over combinations with repetition, by taking into account the multiplicity of each combination. Schematically, we perform

$$\begin{aligned} \textstyle\sum_{i,j,\ldots,k} & \ \mathrm{contrib}(l_i l_j \cdots l_k) \\ & \to \sum_{i\le j\le\cdots\le k} \mathrm{mult} \times \mathrm{contrib}(l_i l_j \cdots l_k), \end{aligned} \tag{A.11}$$

where *contrib* represents a function in our program that takes a product of links and returns the contribution to the geometrical factors. If there are r different links, each one appearing $k_1, \ldots, k_r$ times, the multiplicity of the combination is given by

$$\mathrm{mult} = \frac{n!}{k_1! \cdots k_r!}. \tag{A.12}$$

A.3 Blocks - Grouping links together

Many of the link products have few, if any, repeated spins, and their contributions to the geometrical factors can be counted without having to analyze one by one each of them. This is possible by grouping them in sets of links that we will call in

what follows *blocks*, and replacing the loop over link products by a loop over block products. When the blocks in a product are not neighbors (i.e., they do not have any common spin), we do not need to perform the computation link by link and the contribution can be summed up trivially. Let b_1 and b_3 be two non-neighboring blocks, each one composed by N_b links, and let us denote the contributions to the geometrical factors by $\lambda(n_1, n_2)$, where λ is an integer counting how many products of links have n_1 (n_2) spins in the first (second) sublattice. Then we have

$$contrib(b_1 b_3) = N_b^2(2, 2), \tag{A.13}$$

or in general, for the product of k non-neighboring blocks, $N_b^k(k, k)$. Following this strategy, we divide our lattice into *unidimensional* blocks of $2M$ links, in a way that the jth block, b_j, contains all links the first spin of which belongs to the jth column. As a consequence, b_j is a neighbor of blocks $j-1$ and $j+1$, and, taking into account the boundary conditions, b_0 and b_{L-1} are neighbors too.

When we have a product of neighboring blocks, we proceed as before, analyzing the link products one by one, and there is no computational saving. But when the n blocks are not neighbors, we move from $(Nd)^n$ iterations to a single one.

A.4 Clusters of blocks

The block method, as defined above, fails to save any computation time if two or more blocks are neighbors in a given block product. However, we can extend the method by dividing each block product into several subproducts, which we will denote as *clusters*. In each cluster, one can always connect one block to another by the equivalence relation of being neighbors (sharing spins). And in the same way, in each product different clusters never share any spin. This allows us to compute the contributions of each cluster separately, and then compose them with the following law,

$$\lambda_1(a, b) \oplus \lambda_2(c, d) = \lambda_1 \lambda_2(a + c, b + d). \tag{A.14}$$

If the contributions of the clusters involve more than one geometrical factor, linearity applies,

$$\sum_{ab} \lambda_{ab}(a, b) \quad \oplus \quad \sum_{cd} \lambda_{cd}(c, d) = \sum_{ab,cd} \lambda_{ab} \lambda_{cd}(a + c, b + d). \tag{A.15}$$

Processing one cluster with k blocks takes a computing time proportional to $(Nd)^k$. So dividing the whole block product in smaller clusters implies for almost every

block product a significant amount of time saved. Only when all the blocks are part of the same cluster there is no speed up.

Another major optimization can be performed by realizing that translational invariance can also be applied here, since a given cluster, say $b_0 b_1 b_1$, and any of its translations, $b_{0+t} b_{1+t} b_{1+t}$, have the same contribution to the geometrical factors. Then, when a cluster is going to be computed, we can express it in terms of its equivalence class, compute its contribution, and store it in memory. Every time one of its translations appears, we just take the value from the memory, saving a lot of computing time. In addition to that, once we have computed the factors $\mathcal{G}(n_1, n_2)$ for the first size $L \times M$, we know in advance *all* the cluster contributions for any $L' \times M$ lattice (the blocks keep its size constant). Since almost all the computing time is spent in figuring out the cluster contributions, we reduce in this way the full problem of computing the geometrical factors in lattices of $n-1$ different sizes to *only* one size, the smallest one, $M \times M$. In practice, the time spent by the rest of the sizes needed is barely the $1-2\%$ of that of the first size.

A.5 Computation of a cluster

The last optimization concerns the computation of the clusters themselves. Until now it is done simply by performing a loop over each possible permutation of links belonging to each of the blocks in the cluster. However, one can go one step further and divide the blocks composing the cluster into smaller sets, that we will call *sites*. A site is simply the set of two links the first spin of which lies in the site i, j, that is,

$$\text{site}(i,j) \equiv \{s_{ij} s_{i+1,j}, s_{ij} s_{i,j+1}\}. \tag{A.16}$$

With this new subdivision, we can apply in the same way the techniques described above. In order to compute the cluster $b_1 \dots b_k$, we start a loop over every permutation of sites $s_1 \dots s_k$, with $s_i \in b_i$. Each site product is divided into clusters, the contributions of which can be summed with Eq. (A.15) and are calculated by performing another loop over each link product (2^k iterations for a site product of k elements). Finally, by summing up each site product contribution, we obtain the whole cluster contribution.

All the described optimizations do not remove the exponential dependence on n of the algorithm. However, they allow us to reach the eighth cumulant, which takes about three days of computing time in a modern laptop.

Bibliography

[1] J. C. Collins, D. E. Soper, and G. F. Sterman, "Factorization of Hard Processes in QCD," *Adv. Ser. Direct. High Energy Phys.* **5** (1989) 1–91, arXiv:hep-ph/0409313 [hep-ph].

[2] **Particle Data Group**, M. Tanabashi *et al.*, "Review of Particle Physics," *Phys. Rev. D* **98** (Aug, 2018) 030001.

[3] K. G. Wilson, "Confinement of quarks," *Phys. Rev. D* **10** (Oct, 1974) 2445–2459.

[4] **HPQCD and UKQCD Collaborations and MILC Collaboration and HPQCD and Fermilab Lattice Collaborations**, C. T. H. Davies, E. Follana, A. Gray, G. P. Lepage, Q. Mason, M. Nobes, J. Shigemitsu, H. D. Trottier, M. Wingate, C. Aubin, C. Bernard, T. Burch, C. DeTar, S. Gottlieb, E. B. Gregory, U. M. Heller, J. E. Hetrick, J. Osborn, R. Sugar, D. Toussaint, M. D. Pierro, A. El-Khadra, A. S. Kronfeld, P. B. Mackenzie, D. Menscher, and J. Simone, "High-precision lattice qcd confronts experiment," *Phys. Rev. Lett.* **92** (Jan, 2004) 022001.

[5] S. Dürr, Z. Fodor, J. Frison, C. Hoelbling, R. Hoffmann, S. D. Katz, S. Krieg, T. Kurth, L. Lellouch, T. Lippert, K. K. Szabo, and G. Vulvert, "Ab initio determination of light hadron masses," *Science* **322** no. 5905, (2008) 1224–1227, http://science.sciencemag.org/content/322/5905/1224.full.pdf.

[6] S. Borsanyi, S. Durr, Z. Fodor, C. Hoelbling, S. D. Katz, S. Krieg, L. Lellouch, T. Lippert, A. Portelli, K. K. Szabo, and B. C. Toth, "Ab initio calculation of the neutron-proton mass difference," *Science* **347** no. 6229, (2015) 1452–1455, http://science.sciencemag.org/content/347/6229/1452.full.pdf.

[7] K. G. Wilson, "Ab initio quantum chemistry: A source of ideas for lattice gauge theorists," *Nuclear Physics B - Proceedings Supplements* **17** (1990) 82 – 92.

[8] L. Fortnow, "The status of the p versus np problem," *Commun. ACM* **52** no. 9, (Sept., 2009) 78–86.

[9] G. Parisi, "On complex probabilities," *Physics Letters B* **131** no. 4, (1983) 393 – 395.

[10] J. R. Klauder, "STOCHASTIC QUANTIZATION," *Acta Phys. Austriaca Suppl.* **25** (1983) 251–281.

[11] J. Berges and I.-O. Stamatescu, "Simulating nonequilibrium quantum fields with stochastic quantization techniques," *Phys. Rev. Lett.* **95** (Nov, 2005) 202003.

[12] V. Azcoiti, G. Di Carlo, A. Galante, and V. Laliena, "New proposal for numerical simulations of thetavacuum - like systems," *Phys. Rev. Lett.* **89** (2002) 141601, `arXiv:hep-lat/0203017 [hep-lat]`.

[13] V. Azcoiti, G. Di Carlo, A. Galante, and V. Laliena, "theta vacuum systems via real action simulations," *Phys. Lett.* **B563** (2003) 117, `arXiv:hep-lat/0305005 [hep-lat]`.

[14] E. Witten, "Analytic Continuation Of Chern-Simons Theory," *AMS/IP Stud. Adv. Math.* **50** (2011) 347–446, `arXiv:1001.2933 [hep-th]`. (Aug, 2010).

[15] E. Witten, "A New Look At The Path Integral Of Quantum Mechanics," `arXiv:1009.6032 [hep-th]`. (Sep, 2010).

[16] **AuroraScience Collaboration**, M. Cristoforetti, F. Di Renzo, and L. Scorzato, "New approach to the sign problem in quantum field theories: High density qcd on a lefschetz thimble," *Phys. Rev. D* **86** (Oct, 2012) 074506.

[17] K. Langfeld, B. Lucini, and A. Rago, "Density of states in gauge theories," *Phys. Rev. Lett.* **109** (Sep, 2012) 111601.

[18] K. Langfeld, B. Lucini, R. Pellegrini, and A. Rago, "An efficient algorithm for numerical computations of continuous densities of states," *Eur. Phys. J. C* **76** no. 6, (2016) 306, `arXiv:1509.08391 [hep-lat]`.

[19] K. Langfeld, "Density-of-states," *PoS* **LATTICE2016** (2017) 010, `arXiv:1610.09856 [hep-lat]`.

[20] V. Matveev and R. Shrock, "On properties of the ising model for complex energy/temperature and magnetic field," *Journal of Physics A: Mathematical and Theoretical* **41** no. 13, (Mar, 2008) 135002.

[21] V. Azcoiti, E. Follana, and A. Vaquero, "Progress in numerical simulations of systems with a $\theta-$vacuum like term: The two and three-dimensional Ising model within an imaginary magnetic field," *Nucl. Phys.* **B851** (2011) 420, `arXiv:1105.1020 [hep-lat]`.

[22] S. R. Coleman, "More About the Massive Schwinger Model," *Annals Phys.* **101** (1976) 239.

[23] F. Fucito, E. Marinari, G. Parisi, and C. Rebbi, "A proposal for monte carlo simulations of fermionic systems," *Nuclear Physics B* **180** no. 3, (1981) 369 – 377.

[24] A. Deur, S. J. Brodsky, and G. F. de Téramond, "The qcd running coupling," *Progress in Particle and Nuclear Physics* **90** (2016) 1 – 74.

[25] A. Sternbeck, E.-M. Ilgenfritz, M. Müller-Preussker, and A. Schiller, "Towards the infrared limit in $su(3)$ landau gauge lattice gluodynamics," *Phys. Rev. D* **72** (Jul, 2005) 014507.

[26] A. Sternbeck, K. Maltman, L. von Smekal, A. G. Williams, E. M. Ilgenfritz, and M. Muller-Preussker, "Running alpha(s) from Landau-gauge gluon and ghost correlations," *PoS* **LATTICE2007** (2007) 256, `arXiv:0710.2965 [hep-lat]`.

[27] R. Aouane, V. G. Bornyakov, E.-M. Ilgenfritz, V. K. Mitrjushkin, M. Müller-Preussker, and A. Sternbeck, "Landau gauge gluon and ghost propagators at finite temperature from quenched lattice qcd," *Phys. Rev. D* **85** (Feb, 2012) 034501.

[28] V. Azcoiti, G. Di Carlo, E. Follana, and E. Royo-Amondarain, "Antiferromagnetic ising model in an imaginary magnetic field," *Phys. Rev. E* **96** (Sep, 2017) 032114.

[29] V. Azcoiti, E. Follana, E. Royo-Amondarain, G. Di Carlo, and A. Vaquero Avilés-Casco, "Massive schwinger model at finite θ," *Phys. Rev. D* **97** (Jan, 2018) 014507.

[30] C. M. G. Lattes, H. Muirhead, G. P. S. Occhialini, and C. F. Powell, "PROCESSES INVOLVING CHARGED MESONS," *Nature* **159** (1947) 694–697. [,42(1947)].

[31] M. Gell-Mann, "The Eightfold Way: A Theory of strong interaction symmetry," Tech. Rep. CTSL-20, TID-12608, California Inst. of Tech., Pasadena. Synchrotron Lab., 1961.

[32] V. E. Barnes, P. L. Connolly, D. J. Crennell, B. B. Culwick, W. C. Delaney, W. B. Fowler, P. E. Hagerty, E. L. Hart, N. Horwitz, P. V. C. Hough, J. E. Jensen, J. K. Kopp, K. W. Lai, J. Leitner, J. L. Lloyd, G. W. London, T. W. Morris, Y. Oren, R. B. Palmer, A. G. Prodell, D. Radojičić, D. C. Rahm, C. R. Richardson, N. P. Samios, J. R. Sanford, R. P. Shutt, J. R. Smith, D. L. Stonehill, R. C. Strand, A. M. Thorndike, M. S. Webster, W. J. Willis, and S. S. Yamamoto, "Observation of a hyperon with strangeness minus three," *Phys. Rev. Lett.* **12** (Feb, 1964) 204–206.

[33] G. Zweig, "An SU_3 model for strong interaction symmetry and its breaking; Version 2," Tech. Rep. CERN-TH-412, CERN, Feb, 1964. `http://cds.cern.ch/record/570209`. Version 1 is CERN preprint 8182/TH.401, Jan. 17, 1964.

[34] H. Fritzsch and M. Gell-Mann, "Light cone current algebra," in *Proceedings, International conference on duality and symmetry in hadron physics: Tel Aviv, Israel, April 5-7,1971*, pp. 317–374. 1971. `arXiv:hep-ph/0301127 [hep-ph]`. `http://tuvalu.santafe.edu/~mgm/Site/Publications_files/MGM%2077.pdf`.

[35] W. A. Bardeen, H. Fritzsch, and M. Gell-Mann, "Light cone current algebra, π^0 decay, and e^+e^- annihilation," in *Topical Meeting on the Outlook for Broken Conformal Symmetry in Elementary Particle Physics Frascati, Italy, May 4-5, 1972.* 1972. `arXiv:hep-ph/0211388 [hep-ph]`. `http://tuvalu.santafe.edu/~mgm/Site/Publications_files/MGM%2079.pdf`.

[36] H. Fritzsch and M. Gell-Mann, "Current algebra: Quarks and what else?," *eConf* **C720906V2** (1972) 135–165, `arXiv:hep-ph/0208010 [hep-ph]`.

[37] H. Fritzsch, M. Gell-Mann, and H. Leutwyler, "Advantages of the color octet gluon picture," *Physics Letters B* **47** no. 4, (1973) 365 – 368.

[38] D. J. Gross and F. Wilczek, "Ultraviolet behavior of non-abelian gauge theories," *Phys. Rev. Lett.* **30** (Jun, 1973) 1343–1346.

[39] H. D. Politzer, "Reliable perturbative results for strong interactions?" *Phys. Rev. Lett.* **30** (Jun, 1973) 1346–1349.

[40] K. G. Wilson, "QUARK CONFINEMENT AND LATTICE CALCULATION," *AIP Conf. Proc.* **48** (2008) 9–16.

[41] M. Creutz, L. Jacobs, and C. Rebbi, "Experiments with a gauge-invariant ising system," *Phys. Rev. Lett.* **42** (May, 1979) 1390–1393.

[42] A. A. Migdal, "Recursion Equations in Gauge Theories," *Sov. Phys. JETP* **42** (1975) 413. [,114(1975)].

[43] K. G. Wilson, "MONTE CARLO CALCULATIONS FOR THE LATTICE GAUGE THEORY," *NATO Sci. Ser. B* **59** (1980) 363–402.

[44] M. Creutz, "Monte carlo study of quantized su(2) gauge theory," *Phys. Rev. D* **21** (Apr, 1980) 2308–2315.

[45] D. Weingarten, "Monte carlo evaluation of hadron masses in lattice gauge theories with fermions," *Physics Letters B* **109** no. 1, (1982) 57 – 62.

[46] H. Hamber and G. Parisi, "Numerical estimates of hadronic masses in a pure su (3) gauge theory," *Phys. Rev. Lett.* **47** (Dec, 1981) 1792–1795.

[47] V. Azcoiti and A. Nakamura, "Monte carlo simulation of su(2) lattice gauge theory with internal quark loops," *Phys. Rev. D* **27** (May, 1983) 2559–2562.

[48] H. W. Hamber, "On fermion polarization effects in lattice gauge theories," *Nuclear Physics B* **251** (1985) 182 – 198.

[49] Z. Fodor and C. Hoelbling, "Light hadron masses from lattice qcd," *Rev. Mod. Phys.* **84** (Apr, 2012) 449–495.

[50] C. Davies, "Lattice QCD," in *Heavy flavor physics: Theory and experimental results in heavy quark physics and CP violation. Proceedings, 55th Scottish Universities Summer School in Physics, SUSSP 2001, St. Andrews, UK, August 7-23, 2001*, pp. 105–146. 2002. `arXiv:hep-ph/0205181 [hep-ph]`.

[51] C. Gattringer and C. B. Lang, "Quantum chromodynamics on the lattice," *Lect. Notes Phys.* **788** (2010) 1–343.

[52] R. P. Feynman, "A relativistic cut-off for classical electrodynamics," *Phys. Rev.* **74** (Oct, 1948) 939–946.

[53] R. P. Feynman, "Space-time approach to non-relativistic quantum mechanics," *Rev. Mod. Phys.* **20** (Apr, 1948) 367–387.

[54] K. Osterwalder and R. Schrader, "Axioms for euclidean green's functions," *Comm. Math. Phys.* **31** no. 2, (1973) 83–112. https://projecteuclid.org:443/euclid.cmp/1103858969.

[55] K. Osterwalder and R. Schrader, "Axioms for euclidean green's functions. II," *Comm. Math. Phys.* **42** no. 3, (1975) 281–305. https://projecteuclid.org:443/euclid.cmp/1103899050.

[56] W. Pauli and F. Villars, "On the invariant regularization in relativistic quantum theory," *Rev. Mod. Phys.* **21** (Jul, 1949) 434–444.

[57] K. Symanzik, "Continuum limit and improved action in lattice theories: (i). principles and ϕ^4 theory," *Nuclear Physics B* **226** no. 1, (1983) 187 – 204.

[58] K. Symanzik, "Continuum limit and improved action in lattice theories: (ii). o(n) non-linear sigma model in perturbation theory," *Nuclear Physics B* **226** no. 1, (1983) 205 – 227.

[59] **CP-PACS**, S. Aoki *et al.*, "Quenched light hadron spectrum," *Phys. Rev. Lett.* **84** (2000) 238–241, arXiv:hep-lat/9904012 [hep-lat].

[60] **CP-PACS**, S. Aoki *et al.*, "Light hadron spectrum and quark masses from quenched lattice QCD," *Phys. Rev.* **D67** (2003) 034503, arXiv:hep-lat/0206009 [hep-lat].

[61] **ALPHA, UKQCD**, J. Garden, J. Heitger, R. Sommer, and H. Wittig, "Precision computation of the strange quark's mass in quenched QCD," *Nucl. Phys.* **B571** (2000) 237–256, arXiv:hep-lat/9906013 [hep-lat].

[62] **UKQCD**, K. C. Bowler *et al.*, "Quenched QCD with O(a) improvement. 1. The Spectrum of light hadrons," *Phys. Rev.* **D62** (2000) 054506, arXiv:hep-lat/9910022 [hep-lat].

[63] E. Witten, "Current Algebra Theorems for the U(1) Goldstone Boson," *Nucl. Phys.* **B156** (1979) 269–283.

[64] G. Veneziano, "U(1) Without Instantons," *Nucl. Phys.* **B159** (1979) 213–224.

[65] L. Del Debbio, L. Giusti, and C. Pica, "Topological susceptibility in the SU(3) gauge theory," *Phys. Rev. Lett.* **94** (2005) 032003, arXiv:hep-th/0407052 [hep-th].

[66] N. H. Christ, C. Dawson, T. Izubuchi, C. Jung, Q. Liu, R. D. Mawhinney, C. T. Sachrajda, A. Soni, and R. Zhou, "The η and η' mesons from Lattice QCD," *Phys. Rev. Lett.* **105** (2010) 241601, arXiv:1002.2999 [hep-lat].

[67] L. H. Karsten and J. Smit, "Lattice Fermions: Species Doubling, Chiral Invariance, and the Triangle Anomaly," *Nucl. Phys.* **B183** (1981) 103. [,495(1980)].

[68] H. B. Nielsen and M. Ninomiya, "Absence of Neutrinos on a Lattice. 1. Proof by Homotopy Theory," *Nucl. Phys.* **B185** (1981) 20.

[69] H. B. Nielsen and M. Ninomiya, "Absence of Neutrinos on a Lattice. 2. Intuitive Topological Proof," *Nucl. Phys.* **B193** (1981) 173–194.

[70] H. B. Nielsen and M. Ninomiya, "No Go Theorem for Regularizing Chiral Fermions," *Phys. Lett.* **105B** (1981) 219–223.

[71] P. H. Ginsparg and K. G. Wilson, "A Remnant of Chiral Symmetry on the Lattice," *Phys. Rev.* **D25** (1982) 2649.

[72] M. Luscher, "Exact chiral symmetry on the lattice and the Ginsparg-Wilson relation," *Phys. Lett.* **B428** (1998) 342–345, arXiv:hep-lat/9802011 [hep-lat].

[73] P. Hasenfratz, V. Laliena, and F. Niedermayer, "The Index theorem in QCD with a finite cutoff," *Phys. Lett.* **B427** (1998) 125–131, arXiv:hep-lat/9801021 [hep-lat].

[74] B. Sheikholeslami and R. Wohlert, "Improved Continuum Limit Lattice Action for QCD with Wilson Fermions," *Nucl. Phys.* **B259** (1985) 572.

[75] **Alpha**, R. Frezzotti, P. A. Grassi, S. Sint, and P. Weisz, "Lattice QCD with a chirally twisted mass term," *JHEP* **08** (2001) 058, arXiv:hep-lat/0101001 [hep-lat].

[76] L. Susskind, "Lattice Fermions," *Phys. Rev.* **D16** (1977) 3031–3039.

[77] E. Marinari, G. Parisi, and C. Rebbi, "Monte Carlo Simulation of the Massive Schwinger Model," *Nucl. Phys.* **B190** (1981) 734. [,595(1981)].

[78] **HPQCD, UKQCD**, E. Follana, C. T. H. Davies, G. P. Lepage, and J. Shigemitsu, "High Precision determination of the pi, K, D and D(s) decay constants from lattice QCD," *Phys. Rev. Lett.* **100** (2008) 062002, arXiv:0706.1726 [hep-lat].

[79] C. Bernard, M. Golterman, and Y. Shamir, "Observations on staggered fermions at non-zero lattice spacing," *Phys. Rev.* **D73** (2006) 114511, arXiv:hep-lat/0604017 [hep-lat].

[80] G. Lepage, "Flavor symmetry restoration and Symanzik improvement for staggered quarks," *Phys. Rev. D* **59** (1999) 074502, arXiv:hep-lat/9809157.

[81] **HPQCD, UKQCD**, E. Follana, Q. Mason, C. Davies, K. Hornbostel, G. Lepage, J. Shigemitsu, H. Trottier, and K. Wong, "Highly improved staggered quarks on the lattice, with applications to charm physics," *Phys. Rev. D* **75** (2007) 054502, arXiv:hep-lat/0610092.

[82] R. Narayanan and H. Neuberger, "A Construction of lattice chiral gauge theories," *Nucl. Phys.* **B443** (1995) 305–385, arXiv:hep-th/9411108 [hep-th].

[83] H. Neuberger, "Exactly massless quarks on the lattice," *Phys. Lett. B* **417** (1998) 141–144, arXiv:hep-lat/9707022.

[84] H. Neuberger, "More about exactly massless quarks on the lattice," *Phys. Lett. B* **427** (1998) 353–355, arXiv:hep-lat/9801031.

[85] D. B. Kaplan, "A Method for simulating chiral fermions on the lattice," *Phys. Lett. B* **288** (1992) 342–347, arXiv:hep-lat/9206013.

[86] Y. Shamir, "Chiral fermions from lattice boundaries," *Nucl. Phys. B* **406** (1993) 90–106, arXiv:hep-lat/9303005.

[87] S. L. Adler, "An Overrelaxation Method for the Monte Carlo Evaluation of the Partition Function for Multiquadratic Actions," *Phys. Rev. D* **23** (1981) 2901.

[88] C. Whitmer, "OVERRELAXATION METHODS FOR MONTE CARLO SIMULATIONS OF QUADRATIC AND MULTIQUADRATIC ACTIONS," *Phys. Rev. D* **29** (1984) 306–311.

[89] M. Creutz, "Overrelaxation and Monte Carlo Simulation," *Phys. Rev. D* **36** (1987) 515.

[90] D. J. Callaway and A. Rahman, "The Microcanonical Ensemble: A New Formulation of Lattice Gauge Theory," *Phys. Rev. Lett.* **49** (1982) 613.

[91] D. J. Callaway and A. Rahman, "Lattice Gauge Theory in Microcanonical Ensemble," *Phys. Rev. D* **28** (1983) 1506.

[92] S. L. Adler, "Axial vector vertex in spinor electrodynamics," *Phys. Rev.* **177** (1969) 2426–2438.

[93] J. Bell and R. Jackiw, "A PCAC puzzle: $\pi^0 \to \gamma\gamma$ in the σ model," *Nuovo Cim. A* **60** (1969) 47–61.

[94] S. Weinberg, "The U(1) Problem," *Phys. Rev. D* **11** (1975) 3583–3593.

[95] A. Belavin, A. M. Polyakov, A. Schwartz, and Y. Tyupkin, "Pseudoparticle Solutions of the Yang-Mills Equations," *Phys. Lett. B* **59** (1975) 85–87.

[96] G. 't Hooft, "Symmetry breaking through bell-jackiw anomalies," *Phys. Rev. Lett.* **37** (Jul, 1976) 8–11.

[97] R. Jackiw and C. Rebbi, "Vacuum Periodicity in a Yang-Mills Quantum Theory," *Phys. Rev. Lett.* **37** (1976) 172–175.

[98] R. Peccei and H. R. Quinn, "CP Conservation in the Presence of Instantons," *Phys. Rev. Lett.* **38** (1977) 1440–1443.

[99] S. Weinberg, "A new light boson?" *Phys. Rev. Lett.* **40** (Jan, 1978) 223.

[100] F. Wilczek, "Problem of strong P and T invariance in the presence of instantons," *Phys. Rev. Lett.* **40** (Jan, 1978) 279.

[101] I. G. Irastorza and J. Redondo, "New experimental approaches in the search for axion-like particles," *Prog. Part. Nucl. Phys.* **102** (2018) 89–159, `arXiv:1801.08127 [hep-ph]`.

[102] E. Vicari and H. Panagopoulos, "Theta dependence of SU(N) gauge theories in the presence of a topological term," *Phys. Rept.* **470** (2009) 93, `arXiv:0803.1593 [hep-th]`.

[103] P. de Forcrand, "Simulating QCD at finite density," *PoS* **LAT2009** (2009) 010, `arXiv:1005.0539 [hep-lat]`.

[104] G. Aarts, "Complex Langevin dynamics and other approaches at finite chemical potential," *PoS* **LATTICE2012** (2012) 017, `arXiv:1302.3028 [hep-lat]`.

[105] F. Karsch and H. Wyld, "Complex Langevin Simulation of the SU(3) Spin Model With Nonzero Chemical Potential," *Phys. Rev. Lett.* **55** (1985) 2242.

[106] J. Ambjorn and S. Yang, "Numerical Problems in Applying the Langevin Equation to Complex Effective Actions," *Phys. Lett. B* **165** (1985) 140.

[107] G. Aarts, F. A. James, E. Seiler, and I.-O. Stamatescu, "Adaptive stepsize and instabilities in complex Langevin dynamics," *Phys. Lett. B* **687** (2010) 154–159, arXiv:0912.0617 [hep-lat].

[108] E. Seiler, "Status of Complex Langevin," *EPJ Web Conf.* **175** (2018) 01019, arXiv:1708.08254 [hep-lat].

[109] V. Azcoiti, G. Di Carlo, A. Galante, and V. Laliena, "θ dependence of the CP^9 model," *Phys. Rev.* **D69** (2004) 056006, arXiv:hep-lat/0305022 [hep-lat].

[110] V. Azcoiti, G. Di Carlo, and A. Galante, "Critical Behaviour of CP^1 at $\theta = \pi$, Haldane's Conjecture, and the Relevant Universality Class," *Phys. Rev. Lett.* **98** (2007) 257203, arXiv:0710.1507 [hep-lat].

[111] V. Azcoiti, G. Di Carlo, E. Follana, and M. Giordano, "Critical behaviour of the $O(3)$ nonlinear sigma model with topological term at $\theta = \pi$ from numerical simulations," *Phys. Rev.* **D86** (2012) 096009, arXiv:1207.4905 [hep-lat].

[112] C. Gattringer and K. Langfeld, "Approaches to the sign problem in lattice field theory," *Int. J. Mod. Phys.* **A31** no. 22, (2016) 1643007, arXiv:1603.09517 [hep-lat].

[113] S.-Y. Kim, "Yang-lee zeros of the antiferromagnetic ising model," *Phys. Rev. Lett.* **93** (Sep, 2004) 130604.

[114] L. Onsager, "Crystal statistics. i. a two-dimensional model with an order-disorder transition," *Phys. Rev.* **65** (Feb, 1944) 117–149.

[115] T. D. Lee and C. N. Yang, "Statistical theory of equations of state and phase transitions. ii. lattice gas and ising model," *Phys. Rev.* **87** (Aug, 1952) 410–419.

[116] B. M. McCoy and T. T. Wu, "Theory of Toeplitz Determinants and the Spin Correlations of the Two-Dimensional Ising Model. II," *Phys. Rev.* **155** (1967) 438.

[117] E. Ising, "Beitrag zur theorie des ferromagnetismus," *Zeitschrift für Physik* **31** no. 1, (Feb, 1925) 253–258.

[118] V. Matveev and R. Shrock, "Complex temperature properties of the 2-D Ising model with Beta H = (+- i pi/2)," *J. Phys.* **A28** (1995) 4859–4882, arXiv:hep-lat/9412105 [hep-lat].

[119] B. M. McCoy and T. T. Wu, *The Two-Dimensional Ising Model*. Harvard University Press, Cambridge, MA, 1973.

[120] P. de Forcrand and T. Rindlisbacher, "The density of states method applied to the ising model with an imaginary magnetic field," 8, 2016. `https://conference.ippp.dur.ac.uk/event/530/session/3/contribution/58`.

[121] V. Azcoiti and A. Galante, "Parity and ct realization in qcd," *Phys. Rev. Lett.* **83** (Aug, 1999) 1518–1520.

[122] R. D. Peccei, "Why PQ?," *AIP Conf. Proc.* **1274** (2010) 7, `arXiv:1005.0643 [hep-ph]`.

[123] C. Bonati, M. D'Elia, H. Panagopoulos, and E. Vicari, "Change of θ dependence in 4d SU(n) gauge theories across the deconfinement transition," *Phys. Rev. Lett.* **110** (Jun, 2013) 252003.

[124] C. Bonati, M. D'Elia, M. Mariti, G. Martinelli, M. Mesiti, F. Negro, F. Sanfilippo, and G. Villadoro, "Axion phenomenology and θ-dependence from $N_f = 2 + 1$ lattice QCD," *JHEP* **03** (2016) 155, `arXiv:1512.06746 [hep-lat]`.

[125] P. Petreczky, H.-P. Schadler, and S. Sharma, "The topological susceptibility in finite temperature QCD and axion cosmology," *Phys. Lett.* **B762** (2016) 498, `arXiv:1606.03145 [hep-lat]`.

[126] S. Borsanyi *et al.*, "Calculation of the axion mass based on high-temperature lattice quantum chromodynamics," *Nature* **539** no. 7627, (2016) 69, `arXiv:1606.07494 [hep-lat]`.

[127] V. Azcoiti, "Topology in the SU(Nf) chiral symmetry restored phase of unquenched QCD and axion cosmology," *Phys. Rev.* **D94** no. 9, (2016) 094505, `arXiv:1609.01230 [hep-lat]`.

[128] W. Bietenholz, K. Cichy, P. de Forcrand, A. Dromard, and U. Gerber, "The Slab Method to Measure the Topological Susceptibility," *PoS* **LATTICE2016** (2016) 321, `arXiv:1610.00685 [hep-lat]`.

[129] V. Azcoiti, "Topology in the SU(N_f) chiral symmetry restored phase of unquenched QCD and axion cosmology. II.," *Phys. Rev.* **D96** no. 1, (2017) 014505, `arXiv:1704.04906 [hep-lat]`.

[130] V. Azcoiti, G. Cortese, E. Follana, and M. Giordano, "A geometric Monte Carlo algorithm for the antiferromagnetic Ising model with "topological"

term at $\Theta = \pi$," *Nucl. Phys.* **B883** (2014) 656, arXiv:1312.6416 [hep-lat].

[131] A. Casher, J. B. Kogut, and L. Susskind, "Vacuum polarization and the absence of free quarks," *Phys. Rev.* **D10** (1974) 732.

[132] J. B. Kogut and L. Susskind, "How to Solve the eta –¿ 3 pi Problem by Seizing the Vacuum," *Phys. Rev.* **D11** (1975) 3594.

[133] C. J. Hamer, J. B. Kogut, D. P. Crewther, and M. M. Mazzolini, "The Massive Schwinger Model on a Lattice: Background Field, Chiral Symmetry and the String Tension," *Nucl. Phys.* **B208** (1982) 413.

[134] T. Byrnes, P. Sriganesh, R. J. Bursill, and C. J. Hamer, "Density matrix renormalization group approach to the massive Schwinger model," *Phys. Rev.* **D66** (2002) 013002, arXiv:hep-lat/0202014 [hep-lat].

[135] B. Buyens, S. Montangero, J. Haegeman, F. Verstraete, and K. Van Acoleyen, "Finite-representation approximation of lattice gauge theories at the continuum limit with tensor networks," *Phys. Rev.* **D95** no. 9, (2017) 094509, arXiv:1702.08838 [hep-lat].

[136] Y. Shimizu and Y. Kuramashi, "Critical behavior of the lattice Schwinger model with a topological term at $\theta = \pi$ using the Grassmann tensor renormalization group," *Phys. Rev.* **D90** no. 7, (2014) 074503, arXiv:1408.0897 [hep-lat].

[137] J. Schwinger, "Gauge invariance and mass. ii," *Phys. Rev.* **128** (Dec, 1962) 2425.

[138] N. Seiberg, "Topology in strong coupling," *Phys. Rev. Lett.* **53** (Aug, 1984) 637–640.

[139] U. J. Wiese, "Numerical Simulation of Lattice θ Vacua: The 2-d U(1) Gauge Theory as a Test Case," *Nucl. Phys.* **B318** (1989) 153.

[140] H. Leutwyler and A. V. Smilga, "Spectrum of Dirac operator and role of winding number in QCD," *Phys. Rev.* **D46** (1992) 5607.

[141] F. D. M. Haldane, "Continuum dynamics of the 1-D Heisenberg antiferromagnetic identification with the O(3) nonlinear sigma model," *Phys. Lett.* **A93** (1983) 464–468.

[142] D. Göschl, C. Gattringer, A. Lehmann, and C. Weis, "Simulation strategies for the massless lattice Schwinger model in the dual formulation," *Nucl. Phys.* **B924** (2017) 63, arXiv:1708.00649 [hep-lat].

[143] V. Azcoiti, G. di Carlo, and A. F. Grillo, "A New proposal for including dynamical fermions in lattice gauge theories: The Compact QED case," *Phys. Rev. Lett.* **65** (1990) 2239.

[144] V. Azcoiti, G. Di Carlo, A. Galante, A. F. Grillo, and V. Laliena, "The Schwinger model on the lattice in the microcanonical fermionic average approach," *Phys. Rev.* **D50** (1994) 6994, arXiv:hep-lat/9401032 [hep-lat].

[145] S. Dürr, "Physics of η' with rooted staggered quarks," *Phys. Rev. D* **85** (Jun, 2012) 114503.

[146] S. Dürr and C. Hoelbling, "Staggered versus overlap fermions: A study in the schwinger model with $N_f = 0, 1, 2$," *Phys. Rev. D* **69** (Feb, 2004) 034503.

[147] S. R. Coleman, "There are no Goldstone bosons in two-dimensions," *Commun. Math. Phys.* **31** (1973) 259–264.

[148] N. Mermin and H. Wagner, "Absence of ferromagnetism or antiferromagnetism in one-dimensional or two-dimensional isotropic Heisenberg models," *Phys. Rev. Lett.* **17** (1966) 1133–1136.

[149] V. Azcoiti, "Interplay between $SU(N_f)$ chiral symmetry, $U(1)_A$ axial anomaly, and massless bosons," *Phys. Rev. D* **100** no. 7, (2019) 074511, arXiv:1907.01872 [hep-lat].

[150] H. Georgi, "Automatic fine-tuning in the 2-flavor schwinger model," arXiv:2007.15965 [hep-th].

[151] **HPQCD Collaboration**, C. McNeile, C. T. H. Davies, E. Follana, K. Hornbostel, and G. P. Lepage, "High-precision c and b masses, and qcd coupling from current-current correlators in lattice and continuum qcd," *Phys. Rev. D* **82** (Aug, 2010) 034512, arXiv:1004.4285.

[152] **HPQCD Collaboration**, B. Chakraborty, C. T. H. Davies, B. Galloway, P. Knecht, J. Koponen, G. C. Donald, R. J. Dowdall, G. P. Lepage, and C. McNeile, "High-precision quark masses and qcd coupling from $n_f = 4$ lattice qcd," *Phys. Rev. D* **91** (Mar, 2015) 054508, arXiv:1408.4169 [hep-lat].

[153] **PACS-CS**, S. Aoki *et al.*, "Precise determination of the strong coupling constant in $N_f = 2{+}1$ lattice QCD with the Schrodinger functional scheme," *JHEP* **10** (2009) 053, arXiv:0906.3906 [hep-lat].

[154] **ETM**, B. Blossier, P. Boucaud, M. Brinet, F. De Soto, V. Morenas, O. Pene, K. Petrov, and J. Rodriguez-Quintero, "High statistics determination of the strong coupling constant in Taylor scheme and its OPE Wilson coefficient from lattice QCD with a dynamical charm," *Phys. Rev. D* **89** no. 1, (2014) 014507, arXiv:1310.3763 [hep-ph].

[155] K. Maltman, D. Leinweber, P. Moran, and A. Sternbeck, "The Realistic Lattice Determination of alpha(s)(M(Z)) Revisited," *Phys. Rev. D* **78** (2008) 114504, arXiv:0807.2020 [hep-lat].

[156] A. Bazavov, N. Brambilla, I. Tormo, Xavier Garcia, P. Petreczky, J. Soto, and A. Vairo, "Determination of α_s from the QCD static energy: An update," *Phys. Rev. D* **90** no. 7, (2014) 074038, arXiv:1407.8437 [hep-ph]. [Erratum: Phys.Rev.D 101, 119902 (2020)].

[157] **MILC Collaboration**, A. Bazavov, C. Bernard, N. Brown, J. Komijani, C. DeTar, J. Foley, L. Levkova, S. Gottlieb, U. M. Heller, J. Laiho, R. L. Sugar, D. Toussaint, and R. S. Van de Water, "Gradient flow and scale setting on milc hisq ensembles," *Phys. Rev. D* **93** (May, 2016) 094510, arXiv:1503.02769 [hep-lat].

[158] A. Sternbeck, *The Infrared behavior of lattice QCD Green's functions*. PhD thesis, 9, 2006. arXiv:hep-lat/0609016.

[159] R. Aouane, F. Burger, E.-M. Ilgenfritz, M. Müller-Preussker, and A. Sternbeck, "Landau gauge gluon and ghost propagators from lattice QCD with N_f=2 twisted mass fermions at finite temperature," *Phys. Rev. D* **87** no. 11, (2013) 114502, arXiv:1212.1102 [hep-lat].

[160] C. T. H. Davies, G. G. Batrouni, G. R. Katz, A. S. Kronfeld, G. P. Lepage, K. G. Wilson, P. Rossi, and B. Svetitsky, "Fourier acceleration in lattice gauge theories. i. landau gauge fixing," *Phys. Rev. D* **37** (Mar, 1988) 1581–1588.